

Study on naturally ventilated double-skin façade
in hot and humid climate

Rosady Mulyadi

Study on naturally ventilated double-skin façade in hot and humid climate
(高温多湿の気候での自然換気ダブルスキンファサードに関する研究)

MULYADI, Rosady

A dissertation for the degree of Doctor of Engineering
Department of Environmental Engineering and Architecture
Graduate School of Environmental Studies, Nagoya University

2012

ABSTRACT

This research aims to study the possibility of the application, to analyze the thermal performance, and to figuring the energy performance of naturally ventilated double-skin façade in the hot and humid climate region with Indonesia's climate as a case study. Ventilated double-skin façade can be defined as a façade construction, which comprises of the outer glass, the shading device, and the inner glass. The outer glass and the inner glass form a cavity air space as a channel for the air flow to pass from the lower air inlet to the upper air outlet.

The research runs firstly by numerical simulation to predict the solar heat gain and the thermal performance of the cases. The cases were based on the combination of the thickness of the glass skin and the distance between the outer and inner glasses, including the orientation of double-skin façade. The result of the numerical simulation hereafter was used to calculate the U-value and the Shading Coefficient (SC) of the double-skin façades. After determining the U-value and the SC of double-skin façade, the next step of the research was to calculate the heat load of the double-skin façade model building using MicroHASP/TES. The heat load resulted from the calculation tool was used to designing the air-conditioning system of the double-skin façade building model and then simulated it using LCEM Tool afterward to evaluate the energy performance of the building model.

The results of the numerical calculation show that the naturally ventilated double-skin façade was effective to minimize the solar heat gain and the thermal transmittance. Proper combination of the thickness of the outer and the inner glasses can significantly reduce the solar heat gain as well as the proper arrangement of the distance between the outer and the inner glasses can reduce the thermal transmittance. In comparison to the single-skin façade, naturally ventilated double-skin façade was perform better in reducing heat load with no condensation occurred on the surface of the inner glass during building operation time from 08:00-17:00, even at rainy season. Moreover, reflectance, absorptance, and transmittance of solar radiation in double-skin façade are varying based on the angle incidence of solar radiation. When the angle incidence is lower than 70° , the percentage of transmittance, reflectance and absorptance of the solar radiation is low and relatively constant. The percentage of reflected solar radiation will increase rapidly and the percentage of absorbed and transmitted solar radiation will decrease when the solar incidence angle is higher than 70° .

Furthermore, the simulation on the energy performance of ventilated double-skin façade showed the advantages in reducing primary energy consumption. The annual total energy consumption of the double-skin façade window system was 12% lower than other window systems (8mm single-glass and 6mm pair glass window types). Moreover, the system COP for both 8mm glass single-skin façade and 6mm pair glass was 3.21, and double-skin façade window system is 3.32. The system COP can be improved by installing double-skin façade obviously. Consequently, the ventilated double-skin façade is efficient and useful in reducing energy consumption in buildings in the hot and humid climate area.

Keywords: naturally ventilated double-skin façade, hot and humid climate, solar heat gain, thermal transmittance, energy efficient, and energy consumption.

ACKNOWLEDGEMENT

First and foremost, I would like to express a greatest gratitude to my supervisor Professor Masaya OKUMIYA for the valuable guidance and advice. A deepest gratitude is also due to the supervisory from Assoc. Prof. Gyuyoung YOON, without his assistance, this study would not have been successful. I also thanks to the members of referee committee for their guidance and suggestions, Professor Satoru KUNO and Assoc. Prof. Satoru IIZUKA.

I would like to acknowledge the Hasanuddin University Engineering Faculty Development Project – JICA IP-541 for their financial support and scholarship, and to the Ministry of Education and Culture of the Republic of Indonesia.

Special thanks also to all my graduate friends, especially to all laboratory members in the Department of Environmental Engineering and Architectural Design – Graduate School of Environmental Studies – Nagoya University.

Finally, an honorable mention goes to my families, especially my lovely wife Anni, my son Fiqran, and my daughter Rani for their understanding & endless love, through the duration of my study.

No one walks alone on the journey of live...

Rosady Mulyadi

TABLE OF CONTENTS

ABSTRACT	i
ACKNOWLEDGEMENT	i
TABLE OF CONTENTS	i
LIST OF TABLES	v
LIST OF FIGURES	vii
NOMENCLATURE	xiii
CHAPTER 1. INTRODUCTION.....	1
1.1. Background	3
1.2. Problem Identification and Proposed Solution	5
1.2.1. Problem identification.....	5
1.2.2. Proposed solution.....	6
1.3. Research Aims	7
1.4. Research Significance	8
1.5. Dissertation Structure.....	9
CHAPTER 2. LITERATURE REVIEW.....	11
2.1. Short History of Double-skin Façade	13
2.2. Definitions of Ventilated Double-skin Façade	16
2.3. Classification of Ventilated Double-skin Façade	17
2.4. Types of Naturally Ventilated Double-skin Façade.....	18
2.4.1. Shaft-box ventilated double-skin façade.....	18
2.4.2. Corridor type ventilated double-skin façade partitioned by storey	20
2.4.3. Multi-storey ventilated double-skin façade.....	20
2.4.4. Multi-storey louver ventilated double-skin façade	21

2.5. Ventilation Modes.....	22
2.6. Components of Ventilated Double-skin Façade	24
2.6.1. Outer and inner glass.....	24
2.6.2. Cavity	25
2.6.3. Shading device	25
2.6.4. Apertures	26
2.7. The Physics of Double-skin Façade.....	26
2.7.1. Airflows	26
2.7.2. Thermal performances	28
2.7.3. Energy performances	30
CHAPTER 3. NUMERICAL MODEL.....	33
3.1. Numerical Model	35
3.2. Calculation Flow	37
3.3. Heat-transfer coefficient	38
3.4. Solar Radiation Properties in Double-skin	40
3.5. Heat Balance at Double-skin Façade	43
3.6. Calculation of Standardized Solar Heat Gain on 3mm Standard Glass.....	45
3.7. Calculation of U-value and Shading Coefficient (SC)	46
3.8. Validation of the Numerical Model	51
CHAPTER 4. THERMAL PERFORMANCE OF DOUBLE-SKIN FAÇADE.....	53
4.1. Climate Overview	55
4.1.1. Hot and Humid Climate	55
4.1.2. Climate Condition of Indonesia	56
4.2. The Cases	58

Outer and inner glass distance (width of double-skin) [cm]	59
4.3. Design and Operational Condition.....	60
Azimuth angle of South-facing double-skin [°]	60
Azimuth angle of West-facing double-skin [°]	60
4.4. Comparing the Thermal Transmittance and the Solar Heat Gain.....	62
4.5. Thermal Transmittance and Solar Heat Gain of Double-skin Façade in Dry Season	68
4.6. Thermal Transmittance and Solar Heat Gain of Double-skin Façade in Rainy Season	73
4.7. Possibility of Condensation	77
4.8. Comparison of Thermal Transmittance and Solar Heat Gain among Double-skin and Single-skin Façades.....	79
4.9. Effect of Solar Inclination Angle to the Solar Heat Gain of Double-skin Façade	83
4.10. Summary	91
CHAPTER 5. ENERGY PERFORMANCE OF VENTILATED DOUBLE-SKIN FAÇADE	93
5.1. Overview of the Building Model	95
5.2. U-value and SC of Double-skin Façade.....	98
5.3. Heat Load of Model Building	101
5.4. Simulation of the Energy Consumption.....	106
5.4.1. Design of air-conditioning system	106
5.4.2. Simulation condition	110
5.5. Energy Performance of Ventilated Double-skin Façade	111
5.6. Summary	114
CHAPTER 6. CONCLUSION	117

REFERENCES	123
APPENDICES	129

LIST OF TABLES

Table 4.2-1. Simulation cases.....	59
Table 4.3-1. Design and operational condition of the numerical model	60
Table 5.1-1. Floor function and are	96
Table 5.1-2. Zone properties	98
Table 5.3-1. U-value and SC of window systems	101
Table 5.3-2. Wall properties	101
Table 5.4-1. List of equipments used	107

LIST OF FIGURES

Figure 2.1-1. Steiff Factory in Giengen-Germany ^[7]	13
Figure 2.1-2. The South façade of the Cité de Refuge building right after completion in 1933 (left) and as it is now (right) ^[12]	14
Figure 2.1-3. The Occidental Chemical Center	15
Figure 2.4-1. Shaft-box ventilated double-skin façade ^{[15] [19]}	19
Figure 2.4-2. Corridor type naturally ventilated double-skin façade partitioned by storey ^[15]	20
Figure 2.4-3. Multi-storey naturally ventilated double-skin façade ^{[14] [18]}	21
Figure 2.4-4. Multi-storey louver naturally ventilated double-skin façade ^{[16] [18]}	22
Figure 2.5-1. The ventilation modes ^{[15] [20]}	23
Figure 3.1-1. Model of double-skin façade	35
Figure 3.1-2. Heat balance at each segments	36
Figure 3.2-1. Numerical calculation flowchart.....	38
Figure 3.3-1. Setting of the heat-transfer coefficient in ventilated double-skin.....	39
Figure 3.5-1. Outline of numerical calculation.....	43
Figure 3.7-2. Flow calculation of U-value and SC.....	50
Figure 4.1-1. Asia Köppen-Geiger climate classification system ^[38]	55
Figure 4.1-2. Map of Indonesia	56
Figure 4.1-3. Weather condition of Makassar	58

Figure 4.3-1. Simulation flow chart	61
Figure 4.4-1. Solar heat gain and thermal transmittance of north-facing double-skin façade.....	62
Figure 4.4-2. Solar heat gain and thermal transmittance of east-facing double-skin façade.....	63
Figure 4.4-3. Solar heat gain and thermal transmittance of south-facing double-skin façade.....	64
Figure 4.4-4. Solar heat gain and thermal transmittance of west-facing double-skin façade.....	64
Figure 4.4-5. Hourly solar heat gain and thermal transmittance of north-facing double-skin façade	66
Figure 4.4-6. Hourly solar heat gain and thermal transmittance of east-facing double-skin façade	66
Figure 4.4-7. Hourly solar heat gain and thermal transmittance of south-facing double-skin façade	67
Figure 4.4-8. Hourly solar heat gain and thermal transmittance of west-facing double-skin façade	67
Figure 4.5-1. Solar heat gain at north-facing double-skin façade at June 30	69
Figure 4.5-2. Thermal transmittance of north-facing double-skin façade at June 30.....	69
Figure 4.5-3. Heat transfer of north-facing double-skin façade at 12:00 of June 30.....	70
Figure 4.5-4. Solar heat gain of west-facing double-skin façade at September 22	71
Figure 4.5-5. Thermal transmittance of west-facing double-skin façade at September 22	72

Figure 4.5-6. Heat transfer of west-facing double-skin façade 14:00 of September 22.	72
Figure 4.6-1. Solar heat gain of south-facing double-skin façade at December 30	73
Figure 4.6-2. Thermal transmittance of south-facing double-skin façade at December 30	74
Figure 4.6-3. Heat transfer of south-facing double-skin façade at 13:00 of December 30	74
Figure 4.6-4. Solar heat gain of east-facing double-skin façade at March 22.....	75
Figure 4.6-5. Thermal transmittance of east-facing double-skin façade at March 22....	76
Figure 4.6-6. Heat transfer of east-facing double-skin façade at 12:00 of March 22.....	76
Figure 4.7-1. Possibility of condensation at rainy season	78
Figure 4.7-2. Detail of possibility of condensation	78
Figure 4.8-1. Comparison of hourly thermal transmittance and solar heat gain among north-facing double-skin and single-skin façades	80
Figure 4.8-2. Comparison of hourly thermal transmittance and solar heat gain among east-facing double-skin and single-skin façades	81
Figure 4.8-3. Comparison of hourly thermal transmittance and solar heat gain among south-facing double-skin and single-skin façades	81
Figure 4.8-4. Comparison of hourly thermal transmittance and solar heat gain among west-facing double-skin and single-skin façades	82
Figure 4.9-1. Sun-pat diagram at 5° south latitude.....	83
Figure 4.9-2. Variation of reflection, absorption and transmission of solar radiation by a single glass according the incidence angles ^[41]	84

Figure 4.9-3. Percentage of solar radiation reflected, absorbed, and transmitted on a single-glass ^[42]	84
Figure 4.9-4. Percentage of solar radiation reflected, absorbed, and transmitted on a pair-glass ^[42]	85
Figure 4.9-5. Variation of reflection, absorption and transmission of solar radiation on the outer glass of a double-skin façade at March 8 according the incidence angles	86
Figure 4.9-6. Variation of reflection, absorption and transmission of solar radiation on the shading device of a double-skin façade at March 8 according the incidence angles	86
Figure 4.9-7. Variation of reflection, absorption and transmission of solar radiation on the inner glass of a double-skin façade at March 8 according the incidence angles	87
Figure 4.9-8. Variation of reflection, absorption and transmission of solar radiation on the outer glass of a double-skin façade at October 9 according the incidence angles....	87
Figure 4.9-9. Variation of reflection, absorption and transmission of solar radiation on the shading device of a double-skin façade at October 9 according the incidence angles	88
Figure 4.9-10. Variation of reflection, absorption and transmission of solar radiation on the inner glass of a double-skin façade at October 9 according the incidence angles....	88
Figure 4.9-11. Percentage of reflection, absorption, and transmission in relation to the time and the angle of incidence of solar radiation on double-skin façade at March 8 ...	89
Figure 4.9-12. Percentage of reflection, absorption, and transmission in relation to angle of incidence of solar radiation on double-skin façade at October 9	90
Figure 5.1-2. Plan view of typical floor 10 th ~ 19 th and its zoning.....	97
Figure 5.2-1. The relationship between U-value and the standardized solar radiation	100
Figure 5.2-2. The relationship between SC and the standardized solar radiation	100

Figure 5.3-1. Occupants schedule on workdays	103
Figure 5.3-2. Lights and OA machines schedule on workdays	103
Figure 5.3-3. Air-conditioning operation schedule on workdays	104
Figure 5.3-4. Peak load of perimeter zones	104
Figure 5.3-5. Cooling load comparison among window type	105
Figure 5.4-2. Air-conditioning system diagram	109
Figure 5.4-3. Load characteristic of heat source	109
Figure 5.4-5. Secondary subsystem of LCEM	111

NOMENCLATURE

Greek symbols

γ	tilt angle of the window surface [$^{\circ}$]
v	wind speed or air velocity [m/s] or amount of ventilation per-unit width of double-skin [$\text{m}^3/(\text{s} \cdot \text{m})$]
α	absorption rate [-] or coefficient of flow [-] or azimuth angle [$^{\circ}$]
β	inclination angle [$^{\circ}$]
ε	emissivity of glass [-]
ρ	reflectance rate [-] or density of air [kg/m^3]
τ	transmittance rate [-]

Roman symbols

A	solar azimuth [$^{\circ}$]
c	specific heat of air [$\text{kJ}/(\text{kg} \cdot \text{K})$]
DN	direct normal radiation [W/m^2]
G	absorption coefficient of emission [-]
g_D	direct solar radiation rate on 3mm standard glass [-]
g_S	diffuse solar radiation rate on 3mm standard glass [-]
h	heat-transfer coefficient [$\text{W}/\text{m}^2 \cdot \text{K}$] or solar altitude [$^{\circ}$]
h^*	solar altitude as seen from the surface [$^{\circ}$]
i	incident angle of the window surface [$^{\circ}$]
I	solar radiation [W/m^2]
I_{0D}	direct solar radiation to the surface [W/m^2]
I_{0S}	diffuse solar radiation to the horizontal surface [W/m^2]
I_D	direct solar radiation [W/m^2]
I_G	solar heat gain at standard glass 3mm [-]
I_S	diffuse solar radiation [W/m^2]
n	number of segment
Q_{in}	heat flow due to temperature difference between the outdoor and indoor [$\text{W}/\text{m}^2 \cdot \text{K}$]
Q_r	convective heat flow due to temperature difference between the outdoor and indoor [$\text{W}/\text{m}^2 \cdot \text{K}$]
Q_r	radiative heat flow due to temperature difference between the outdoor and indoor [$\text{W}/\text{m}^2 \cdot \text{K}$]
SC	shading coefficient [-]
SG	glass surface area ratio to the sunshine [-]
SH	sky horizontal radiation [W/m^2]
TH	total horizontal radiation [W/m^2]

Subscripts

a	absorption
air	air layer of double-skin

<i>b</i>	black body surface
<i>c</i>	convective
<i>D</i>	direct
<i>gr</i>	ground
<i>ig</i>	inner glass
<i>in</i>	indoor
<i>og</i>	outer glass
<i>r</i>	radiative
<i>ref</i>	reflected
<i>S</i>	diffuse or sky
<i>sd</i>	shading device
<i>tran</i>	transmitted
<i>z</i>	high of segment of double-skin

Abbreviation

ACH	Air Change per Hour
AFN	Airflow Network
AHU	Air Handling Unit
BEB	Building Energy Balance
CFD	Computations Fluid Dynamics
COP	Coefficient of Performance
CT	Cooling Tower
CWC	Constant Water Volume
EPZ	East Perimeter Zone
FCU	Fan Coil Unit
IZ	Interior Zone
LCEM	Life Cycle Energy Management
NPZ	North Perimeter Zone
OA	Operating Appliances
SPZ	South Perimeter Zone
TT	Thermal Transmittance
VWV	Variable Water Volume
WPZ	West Perimeter Zone

CHAPTER 1. INTRODUCTION

1.1. Background

Since the end of World War II, modern architecture building is growing rapidly with attractive high storey glass façade. International style, modern style, and postmodern style are characterized most commonly by the glass façade providing an aesthetical view.

Essentially, the building façade has to separate the outdoor and the indoor environment. It should act like a barrier from the outdoor environment and control the indoor environment. It has the important roles in solar heat gain management, heating and cooling load control, air ventilation control, acoustical control, and aesthetical view. Therefore, the façade should be designed carefully to achieve its goals and the particular contexts of the purpose of it build ^[1]^[2].

Indonesia is an archipelago that located along the equator. Because of its location, Indonesia has tropical climate. The weather is hot and humid and divided with two distinct seasons; dry and rainy seasons. The dry season is from May to September and the rainy season is from December to April. Between these seasons, there are seasonal transition periods, which are the transition period between dry season to rainy season from October to December, and the transition period between rainy season to dry season from April to May. Since there is no distinct temperature difference between these two seasons, only cooling session is needed along the year.

There are many kinds of strategies that have been being developed to explore the potential of façade, which is varying in their design, performance, and characteristic according to their location. Building in cold and temperate region essentially has a different façade characteristic compared to building in hot and humid region and vice

versa. The difference in climatic condition would lead to the difference in the appearance, façade, material, and construction technology.

The façade design of many building in Indonesia, especially high-rise building is unfortunately looked like “western style” with fully covered glass façade with little concern for designing to the climate condition and passive design strategies to reduce the energy consumption in building. This situation leads to high-energy consumption in providing comfortable indoor environment.

Since the primary goal of the façade design in hot and humid climate is to reduce the solar heat gain, there are numbers of strategies that can be applied such as external or internal shading devices, advanced glazing technology, and double-skin façade systems. In particular, double-skin façades represents the evolution of façade technology to addressing the issue of the heat gain through largely transparent façades. One of the types of double-skin façade that can be addressed to the hot and humid climate region is a ventilated double-skin façade, which is characterized by having at least two glass panes between the outdoor and the indoor, the air spaces (cavity) between the glass panes, the blinds that act as a shading device, and the air passes through the cavity^[3].

However, there are special awareness has to be put in attention when applying double-skin façade in hot and humid climate. High humidity during all year round, especially in rainy season could cause high moisture in the cavity of double-skin, which could cause the occurrence of the condensation on the outer surface of the inner-glass.

Moreover, the solar position of the location near the equator may reach the higher position at certain month and day. For example, the solar altitude at latitude 5° South will reach the higher position at 88.7° on October 9 at 12:00 o'clock, and at 89.1°

on March 8 at 12:30 o'clock. This will affect to the amount of solar radiation reflected and transmitted into the indoor. Consequently, the higher position of solar altitude is the higher reflection and the lower transmission of solar radiation into the indoor.

Furthermore, since the high temperature and humidity all year long, the double-skin façade in hot and humid climate shall be operated by opening the lower air inlet and upper air outlet. By opening air inlet and outlet, the fresh air can be introduced into double-skin's cavity which then the hot air could be driven out through the air outlet to mitigate the hot air in the cavity and to prevent condensation to occur.

1.2. Problem Identification and Proposed Solution

1.2.1. Problem identification

Double-skin façades have proven to be efficient at reducing building energy consumption particularly heating loads in winter and cooling loads in summer, and they have been successfully applied in cold and temperate climates. However, there is currently insufficient information for designing a double-skin façade that can be used in a hot and humid climate such as Indonesia's.

There are some problems that have to be paid more attention in applying double-skin façade in Indonesia. The hot and humid weather condition may become a problem in double-skin façade. In rainy season, the ambient air will more humid and the condensation may occur in the double-skin façade.

Since the location of Indonesia is in the tropic-equator, the application of double-skin façade shall be benefit in reducing solar heat gain. Solar altitude in the equatorial lane may reach the higher position up to 90°. As the result, the solar

incidence may also reach the higher degree. Higher degree of solar incidence would be benefit for the building façade since large amount solar radiation could be reflected.

1.2.2. Proposed solution

Double-skin façade is a concept for reducing energy consumption in building, this applies the façade technology to reduce cooling and heating load. It comprises of outer glass and inner glasses, which form a cavity space. Between outer and inner glasses, there are a shading device and air space. At the bottom of the cavity, there is a lower aperture, as well as upper aperture on the top of the cavity. These apertures are operable for open and close to allow natural ventilation applied to the cavity.

The performance of double-skin façade in reducing cooling load in summer and heating load in winter has been widely discussed and proved in several European countries, which climate is moderate. In the other word, the double-skin façade has the advantages in reducing energy consumption due to summer and winter condition.

Therefore, since the double-skin façade has the advantage in reducing cooling load in summer, it can be assumed that it could also be benefited if it applied in the hot and humid climate. The double-skin façade for hot and humid climate area has to be ventilated, which allow the fresh air to be introduced into the cavity to decrease the heat over the cavity. However, there are several things to be considered including the thickness of glasses, the width and depth of cavity, the shading device, and the operation of apertures.

In this research, double-skin façade is proposed to be applied in the office building located in Makassar, Indonesia. Currently, the office building is tending to grow rapidly as a consequence of the economic growth. The lack and the high price of

the land also make the office building growth up in Indonesia. However, the accretion of office building linearly causes the increase of energy consumption for air conditioning. Furthermore, the use of fully glassed façade may increase the sensible cooling load of the building and cause the high energy consumption. Therefore, the double-skin façade is proposed as a solution to reduce energy consumption for cooling session in office building in hot and humid climate likes Indonesia.

However, in order to reach optimal result of the usage of double-skin façade in hot and humid climate, the specific design and operation of double-skin façade should be put in attention. The design of the cavity air space of double-skin façade in hot and humid climate has to be ventilated. To ventilate the cavity, the air inlet and outlet shall be opened which then allow the fresh air to be introduced into the cavity, and to allow warm air to be exhausted through the air outlet. The design and operational condition of double-skin façade are supposed to mitigate the overheated of the cavity and to prevent condensation to occur in double-skin façade.

1.3. Research Aims

The aims of this study are:

- a. To find out the possibility of the application of double-skin façade in hot and humid climate area especially in Indonesia
- b. To evaluate the thermal performance of double-skin façade under hot and humid climate condition. The thermal performance of double-skin façade takes an account of the solar heat gain the thermal transmittance of double-skin façade. The evaluation of solar heat gain and thermal transmittance of double-skin façade would lead to the information of the performance of

double-skin façade related to the solar heat gain and thermal transmittance of double-skin façade.

- c. To evaluate the energy efficient performance of double-skin façade compared to single-skin façade under hot and humid climate condition. The evaluation of energy efficient of double-skin façade in this research was focused on the energy consumption used for air conditioning only. The energy consumption of double-skin façade was compared with energy consumption of single-skin façade of the same model building. Evaluation of energy consumption takes an account of the power consumption of the air conditioning component such as heat source, cooling tower, heat pump, air handling unit, and fan coil unit.

1.4. Research Significance

The façade of building in hot and humid climate like in Indonesia should be able to minimize the effect of the solar heat gain. Naturally ventilated double-skin façade is one of the solutions to anticipate the effect of solar radiation to the building.

The significance contributions of this research are:

- 1) Analyze the thermal performance of naturally ventilated double-skin façade during dry and rainy seasons.
 - a. It tests the applicability of ventilated double-skin façade in hot and humid climate.
 - b. Analyze the effect of the thickness of the outer and inner glass, and the distance between them.

- c. Analyze the effect of solar incident angle to the reflection, absorption, and transmission of solar radiation.
 - d. Assessing the possibility of condensation to occurs in the cavity of double-skin façade.
- 2) Evaluate the energy performance of ventilated double-skin façade in hot and humid climate.

1.5. Dissertation Structure

The first chapter describes the background to the aims, and the significance of the research.

The second chapter is a review of literatures, which contains the short history of double-skin façade and the definition, which focused on ventilated double-skin façade. It also describes the classification of double-skin façade, which are based on the types of ventilation in the cavity, partitions of the cavity, and the airflow driven types. The main components that construct the ventilated double-skin façade and physical properties, including the airflows, the thermal performance, and the energy performance of double-skin façade are also described within this chapter.

The third chapter is a part that discusses the numerical model of naturally ventilated double-skin façade, including the numerical calculation, calculation flow of the numerical simulation, and the calculation of U-value and Shading Coefficient. The heat-transfer coefficients of the outer-inner glass and the shading device are described following the solar radiation properties, and the heat balance of double-skin façade.

The fourth chapter started by describing the overview of the hot and humid climate and more profound the characteristic of the Indonesia climate. It also presents

the simulation result of the solar heat gain and the thermal transmittance of ventilated double-skin façade, which based on the cases related to the outer and inner glass thickness and distance and the orientation of the double-skin, including the possibility of the occurrence of the condensation at the inner glass pane of double-skin.

The fifth chapter discusses the energy performance of double-skin façade. This chapter presents the overview of the building model used to evaluate the performance of double-skin façade, and the calculation of the heat load of the building model using MicroHASP/TES. The chapter also describes the simulation of energy-efficient performance of double-skin façade using LCEM and the result of the simulation process.

Chapter sixth is the conclusion of the study.

CHAPTER 2. LITERATURE REVIEW

2.1. Short History of Double-skin Façade

Jean Baptiste Jobard, director of the industrial museum in Brussel, introduced the early concept of double-skin façade in 1849. According to Jean Baptiste Jobard as mentioned by Saelens ^{[4][5][6]}, in winter hot air should be circulated between two glazing, while in summer it should be cold air. This concept is still in remains about 54 years until Steiff Factory was built in Giengen-Germany in 1903.



Figure 2.1-1. Steiff Factory in Giengen-Germany ^[7]

Steiff Factory as can be seen at Figure 2.1-1 is the first ever double-skin façade building was built, which intended to minimize the effect of the cold weather and the strong winds over the region. It allows exterior ventilation of the cavity and can be regarded as an early example of a naturally ventilated multiple-skin façade ^[4]. The

building consisted of three storeys with a storage in the first floor, the second and the third floor used as a working areas ^{[8] [7] [9]}.

Le Corbusier in 1916 used second skin glazing system, which is very large windows (one of them two storeys high) that designed in two layers, with heating pipes between them, to prevent down draughts in his Villa Schwob in his home town of La Chaux de Fonds in Switzerland. Later on, he designed a multiple glass layer wall called “Mur Neutralisant”, which means neutralizing walls are made of glass or stone or both of them, for the Cite de Refuge (see Figure 2.1-2), the Salvation Army Hostel in Paris ^[10], which is acts as an air duct to neutralize the effect of the cold or sun. Unfortunately, this idea was never implemented due to the high initial cost ^[11].



Figure 2.1-2. The South façade of the Cité de Refuge building right after completion in 1933 (left) and as it is now (right) ^[12]

The Occidental Chemical Center (built in 1980's) known as the first double-skin façade in North America (Figure 2.1-3), which is represent fundamental importance in

the recent history of the glass in architecture. The skin system used by Occidental is sometimes termed “dynamic” owing to its ability to change as a function of the time of year and time of day. The louver system was designed to automatically rotate to control daylight entering the building. There were solar cells on the back of each bank of the aerofoil louvers. If sunlight fell on the cell, the louver would rotate, tilting the bank and blocking out the sun^[13].



Image source: http://www.architecture.uwaterloo.ca/faculty_projects/terri/images/hooker1.jpg

Figure 2.1-3. The Occidental Chemical Center

Until the recent decade, many double-skin façade have been built. Apparently, the building façade is not just an ornamental cladding but more is a responsive skin, which is integrated to the entire building. Building skins is now becoming a major focus on the goal of reducing a building’s energy load, and this is the role of the double skin façade in transforming the way of building designs. The double skin façade can provide

a visual symbol of energy-efficiency ^[14] . For both aesthetic and performative reasons, this innovation in façade engineering should be seen as an opportunity for efficiency and whole building integration ^[8].

2.2. Definitions of Ventilated Double-skin Façade

The ventilated double-skin façade is different from conventional double and triple glazed façades, and it is characterized by the passage of air through the cavity air space between the inner and the outer glass.

Ventilated double-skin façades are further differentiated from conventional double or triple glazed façades by the passage of air through the cavity between the inner and outer skins. The movement of air is an important departure from more standard glazing systems such as double and triple glazed insulating units. The thermal mechanisms are different as are the impacts on energy and comfort. The façade can no longer be envisioned as a static object. Air moves through it modifying and at times dominating its performance characteristics ^[15].

A ventilated double skin façade can be defined as a traditional single façade doubled inside or outside by a second, essentially glazed façade. A ventilated cavity – with a depth from about 10 centimeters at the narrowest to 2 meters for the deepest accessible cavities – is located between these two skins. The cavity can be ventilated with natural, mechanical or hybrid ventilation ^[16].

The double-skin façade is ventilated with outside air and allows the ventilation of outside air through openable windows - even in high-rise buildings without causing any nuisance ^[17].

2.3. Classification of Ventilated Double-skin Façade

The Belgian Research Institute gives a useful classification of ventilated double-skin façade. The ventilated double-skin façade can be classified based upon three criteria ^[15]:

1. The type of ventilation
2. The partitioning of the façade
3. The modes of ventilation of the cavity

The type of ventilation refers to the driving forces at the origin of the ventilation of the cavity located between the two glazed façades. Only a single type of ventilation characterizes each ventilated double skin façade concept. One must distinguish between the three following types of ventilation ^{[18] [15]}:

1. Natural ventilation, which relies on pressure differences without the aid of powered air movement components.
2. Mechanical ventilation employs the aid of powered air movement components.
3. Hybrid ventilation (mix between natural and mechanical ventilation), lies in a control compromise between natural ventilation and mechanical ventilation. In general, natural ventilation is used as far as possible. The mechanical ventilation is only triggered when the driving forces of natural ventilation become inadequate and no longer make it possible to achieve the desired performances. A control system permits the shift from one type of ventilation to other in an automatic and controlled manner based on a control algorithm. It should be noted that few ventilated double façades use this type of ventilation.

Further, in this research, the natural ventilation type was used to investigate the performance of ventilated double-skin façade under the hot and humid climate condition. The reason takes into account the availability of natural ventilation as well as the simplicity of the operation of double-skin façade.

2.4. Types of Naturally Ventilated Double-skin Façade

Some types of naturally ventilated double-skin façade are ^[15]:

1. Shaft-box naturally ventilated double-skin façade
2. Corridor type naturally ventilated double-skin façade partitioned by storey
3. Multi-storey naturally ventilated double-skin façade
4. Multi-storey louver naturally ventilated double-skin façade

2.4.1. Shaft-box ventilated double-skin façade

The module of the façade, which imposes its dimensions on the cavity, physically delimits this type of façade, the cavity horizontally and vertically. The façade module has a height limited to one storey ^[15] (see Figure 2.4-1). The air is naturally drawn through the ventilation duct and then evacuated via the outlet located in several floors ^[19].

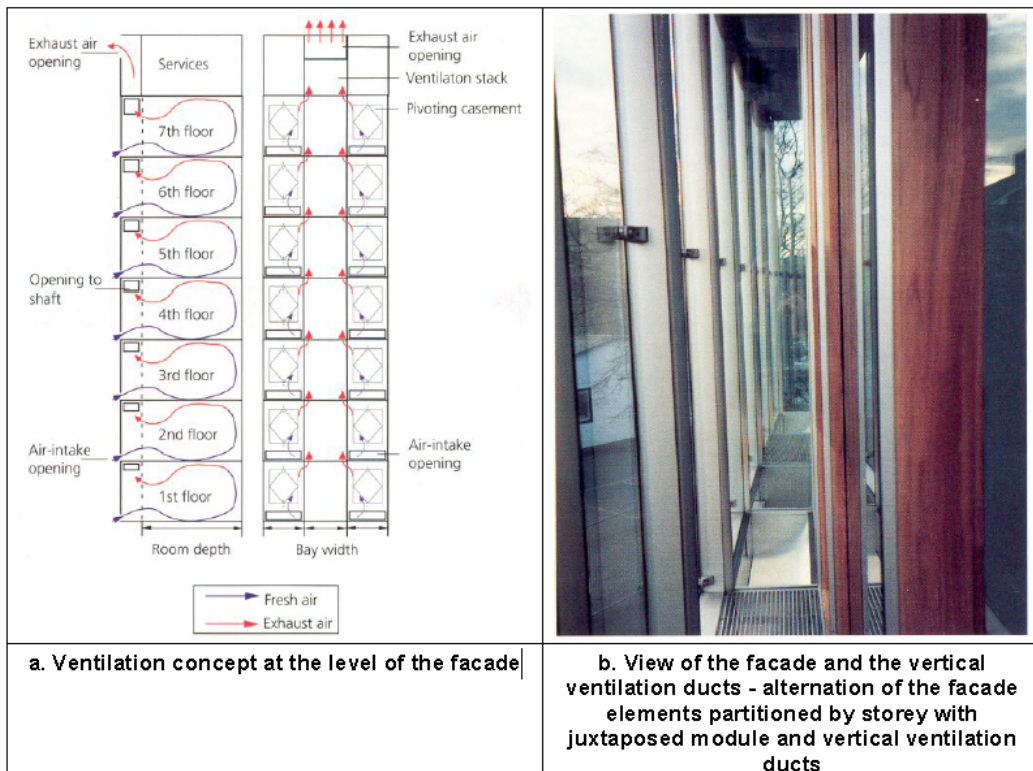
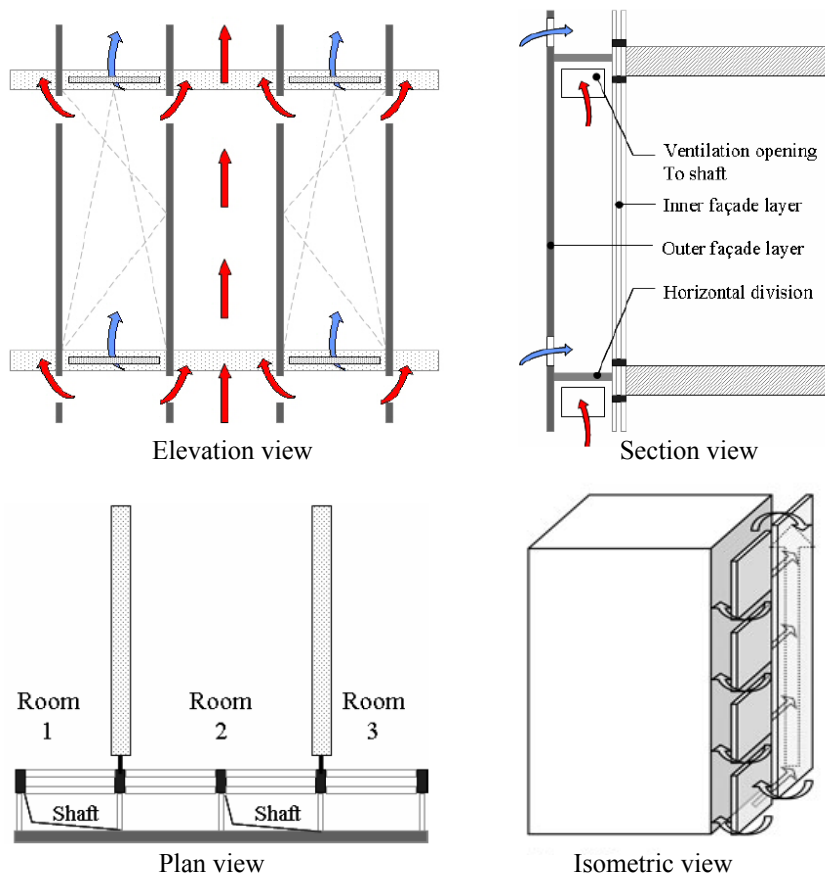


Figure 2.4-1. Shaft-box ventilated double-skin façade ^[15] ^[19]

2.4.2. Corridor type ventilated double-skin façade partitioned by storey

The corridor type ventilated double-skin (Figure 2.4-2) façades partitioned per storey are characterized by a large cavity in which it is generally possible to walk. While the cavity is physically partitioned at the level of each storey (the cavities of each storey are independent of one another), it is not limited vertically, and generally extends across several offices or even an entire floor [19].

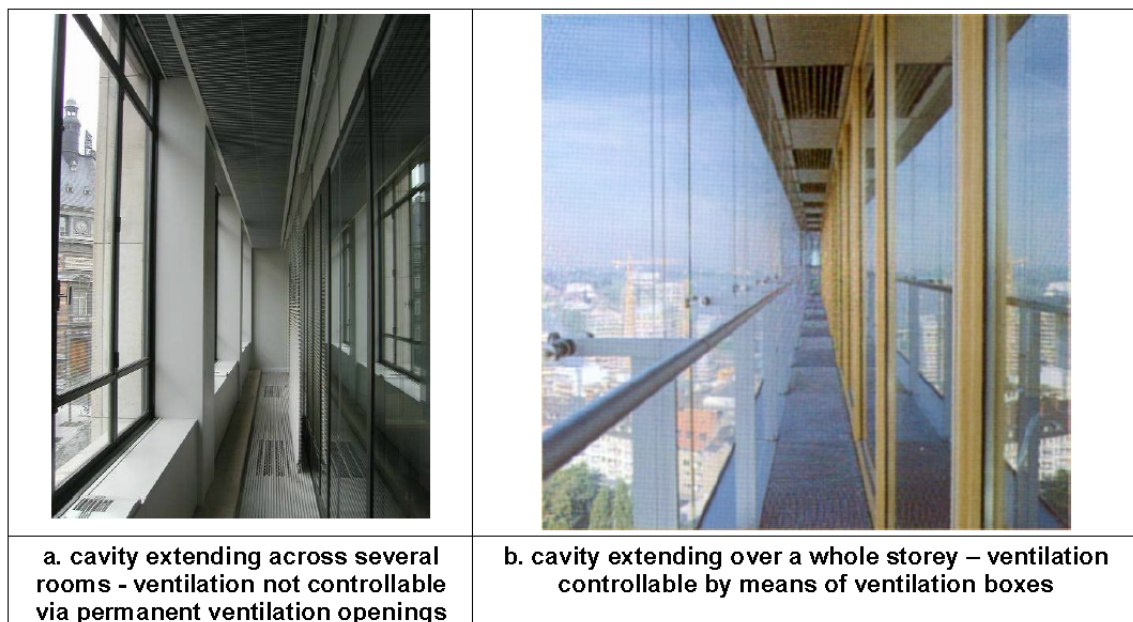


Figure 2.4-2. Corridor type naturally ventilated double-skin façade partitioned by storey [15]

2.4.3. Multi-storey ventilated double-skin façade

This kind of naturally ventilated double-skin façade is not partitioned nor vertically nor horizontally [20] with large volume of cavity. The cavity is high enough to permit access to individuals (cleaning service, etc.) and floors, which can be walked on are installed at the level of each storey in order to make it possible to access the cavity,

primarily for reasons of cleaning and maintenance ^[19]. It has at least two ventilation modes, the outdoor air curtain and buffer zone. Very good acoustical performance with fully glazed from bottom to top ^[15] (Figure 2.4-3).

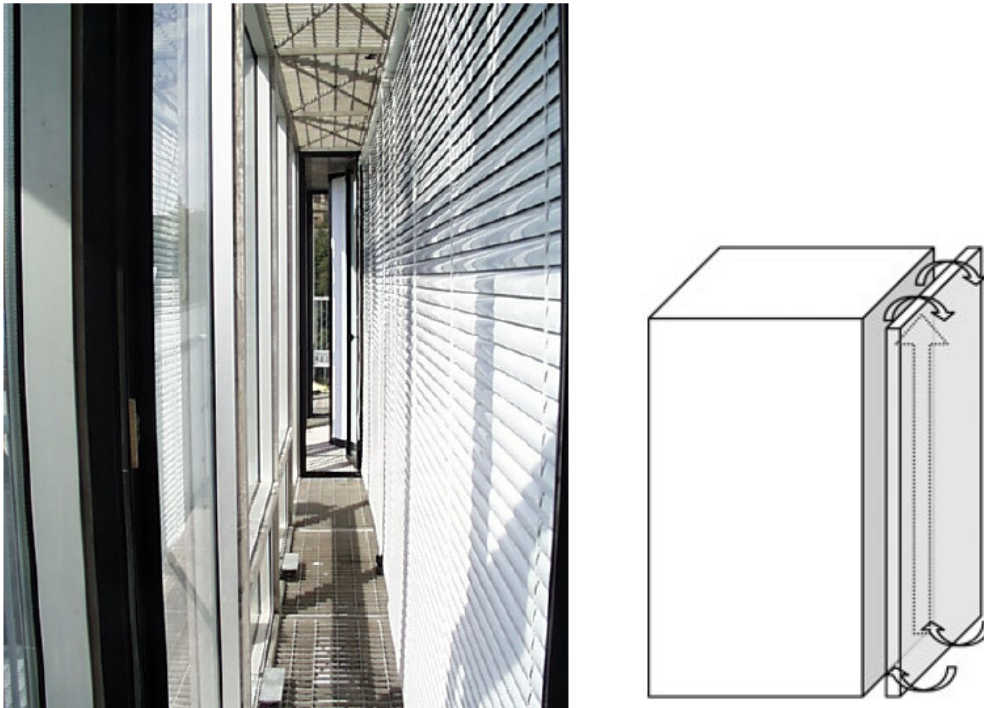


Figure 2.4-3. Multi-storey naturally ventilated double-skin façade ^[14] ^[18]

2.4.4. Multi-storey louver ventilated double-skin façade

The multi-storey louver naturally ventilated double façade is very similar to a multi-storey ventilated double façade. Its cavity is not partitioned either horizontally or vertically and therefore, forms one large volume. Metal floors are installed at the level of each storey in order to allow access to it, mainly for cleaning and maintenance. The outer glass is composed exclusively of pivoting louvers and not airtight, even when the louvers have all been put in closed position ^[19] (Figure 2.4-4).

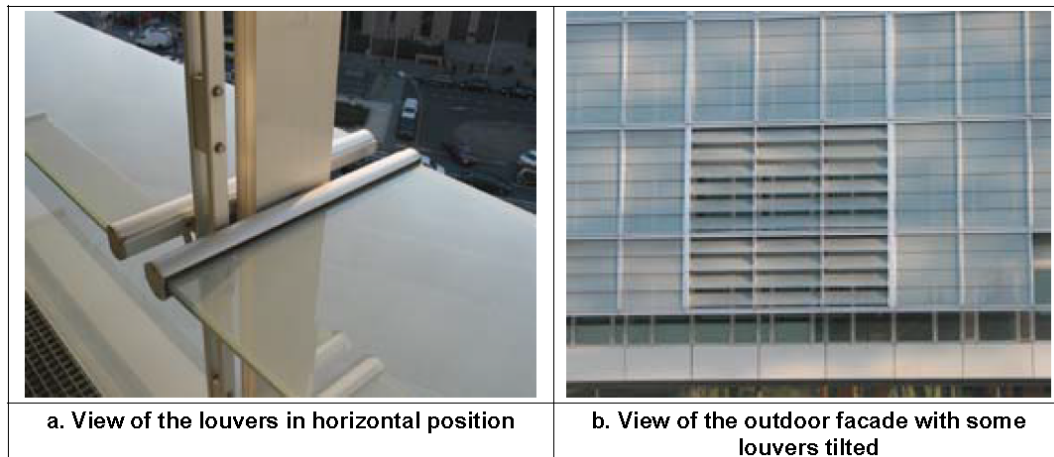


Figure 2.4-4. Multi-storey louver naturally ventilated double-skin façade ^{[16][18]}

2.5. Ventilation Modes

The ventilated double-skin façade can also be classified according to its ventilation mode. The origin of the airflow is an important characteristic because it largely influences the eventual average cavity temperature ^[4]. The ventilation mode refers to the mechanism of the air circulating in the cavity as can be seen at Figure 2.5-1 that is ^[15]:

1. Outdoor air curtain.

This ventilation mode allows the outdoor air introduced into the cavity through the bottom of the cavity and immediately rejected toward the outside through the top of cavity. Therefore, ventilation of the cavity forms an air curtain enveloping the outside.

2. Indoor air curtain.

In this ventilation mode, the air introduced from the inside of the room into the cavity and then returned into the room through the ventilation system. This

mode allows the cavity to form an air curtain which enveloping the indoor façade.

3. Air supply.

The air supply mode allows the outdoor air introduced into the cavity through the bottom of the cavity and then ventilated into the indoor through the ventilation system, creating air supply into the building.

4. Air exhaust.

The purpose of this ventilation mode is to bring the indoor air to the outdoor through the cavity. It evacuates the air from the building toward the outside.

5. Buffer zone.

The buffer zone mode makes the skin act like an airtight. No ventilation allowed, and it functioned as a buffer zone between the indoor and the outdoor.

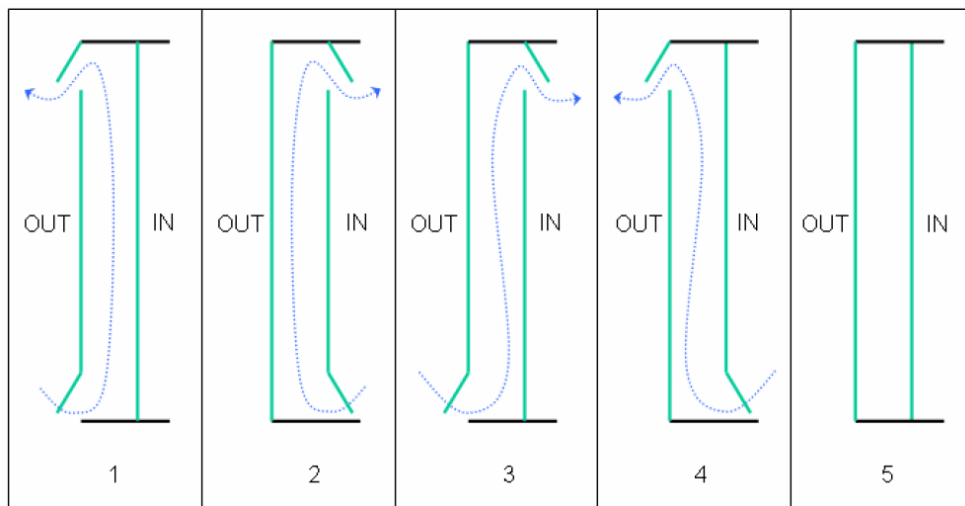


Figure 2.5-1. The ventilation modes ^{[15] [20]}

According to Shan-Shiou Li ^[11], natural ventilation can provide an environmental friendly atmosphere and reduce the requirement for mechanical

ventilation. On the other hand, natural ventilation is not without risk. It may create a door-opening problem due to pressurization. Besides, if the air path is not appropriately designed, the solar heat gain within the façade cavity will not be removed efficiently and will increase the temperature in the cavity. In the naturally ventilated double façade system, the air is brought into the cavity and exhausted by two means: wind pressure and/or the stack effect. Wind pressure typically dominates the airflow rate. If properly designed, wind flowing over the façade can create pressure differences between the inlet and outlet inducing air movement. Without wind, the cavity can still be ventilated due to the stack effect. As the air flows into the lower inlet, it is heated and becomes less dense and thermally buoyant. As a result, the air will flow into the inlet and out to the outlet while removing heat. Because there are the potentials for stack-driven and wind-driven pressures to be counteractive, the air path and exterior openings need to be correctly sized and configured to ensure the stack effect pressures and wind-driven forces are additive. Otherwise, the preheated airflow in the cavity will tend to radiate to the interior, and opening the inner layer window in summer will introduce a burst of hot air.

2.6. Components of Ventilated Double-skin Façade

2.6.1. Outer and inner glass

The distance between the outer and the inner glass could be varied from 80cm to 200cm wide. In some cases, the outer glass is double-glazed. The choice regarding the glass type for the interior and exterior panes depends on the typology of the façade. In case of a façade ventilated with outdoor air, an insulating pane (sealed double-glazed unit) is usually placed as a thermal break at the interior side and a single pane at the

exterior side. In case of a façade ventilated with indoor air, the insulating pane is usually placed at the exterior side, the single pane at the interior side. For some specific types of façades, the interior window can be opened by the user to allow natural ventilation within the building ^[14].

2.6.2. Cavity

The cavity of double-skin façade is a space between the outer and the inner glass. The cavity of double-skin façade can be air tight or ventilated. Airtight cavity is function as a buffer zone, usually used in winter to maintain the indoor temperature. The ventilated cavity is referring to the cavity with opening at the lower and upper aperture of double-skin façade. It utilized usually in summer where fresh air from outdoor introduced via the lower aperture into the cavity and ventilated throughout the upper aperture. This ventilation system is utilizing the benefit of stack effect, which allows the air in the cavity to be flowed through the upper aperture. The pressure difference between lower and upper aperture can be used if the wind speed is sufficient, which possibly make the air in the cavity circulated. Both methods stack effect and pressure difference could beneficially reduce the heat in double-skin façade.

The cavity of double-skin façade may ventilate in naturally, mechanically, and hybrid. The depth of the cavity can vary as a function of the applied concept between 10cm to more than 2m. The depth influences the physical properties of the façade, and the way that the façade maintained ^{[14] [16]}.

2.6.3. Shading device

The position of shading device is between the outer and the inner glasses. The shading device is placed inside the cavity for protective reasons. Often a venetian blind

is used. The characteristics and position of the blind influence the physical behavior of the cavity because the blind absorbs and reflects radiant energy. Thus, the selection of the shading device should be made after considering the proper combination between the pane type, the cavity geometry and the ventilation strategy ^[14] ^[16].

2.6.4. Apertures

The aperture allows the air to be circulated in the cavity of double-skin. Lower aperture is the air inlet as well as upper aperture is the air outlet. The choice of pane type, shading device, geometry of the cavity, and type, size and positioning of the apertures of the cavity and ventilation strategy is crucial to the performance of a double-skin façade system ^[16]. When designing a double skin façade it is important to determine type, size and positioning the aperture of the cavity since these parameters influences the type of airflow and the air velocity and thus the temperatures in the cavity (more important in high-rise buildings) ^[14].

2.7. The Physics of Double-skin Façade

2.7.1. Airflows

According to Harris Poirazis in his literature review of double-skin façade, ^[6] airflow simulations of the double skin façade cavities are necessary if one wants to calculate the temperatures at different heights in the cavity. The approaches for calculating the airflow inside the cavity differ in the existing literature.

Djunaedy et al ^[21] categorize the main airflow modeling levels of resolution and complexity as described below:

- Building energy balance (BEB) models that rely on the estimated values of airflow. BEB is possible to do a general comfort assessment, to check a suggested solution for the problem, and to present the associated energy consequences in the same process.
- Zonal airflow network (AFN) models that are based on (macroscopic) zone mass balance and inter-zone flow-pressure relationships; typically, for a whole building.
- CFD that is based on energy, mass and momentum conservation in all (minuscule) cells that make up the flow domain; typically, a single building zone.

Building energy balance is different with heat balance calculation used in this research. The heat balance numerical calculation used in his research is based on the calculation of air temperature of double-skin, temperature of the inner glass, temperature of shading device, the amount of ventilation in double-skin, and the amount of transmitted solar radiation.

Inside a double-skin façade, the air temperature will mainly depend on heat gains and on the amount of airflow. However, in a naturally ventilated double-skin façade the airflow itself is mainly governed by the temperature difference with outside, and, possibly, also by wind induced pressure differences; the airflow is typically highly erratic ^[22].

Natural ventilation is an important aspect of double-skin façade performance, which is related to thermal transmittance and solar heat gain. Several investigations have been performed in which an integrated modeling process was used to define the relationship between natural ventilation and the thermal performance of double-skin

façades. Pappas and Zhai investigate the thermal performance and correlations of double skin façade with buoyancy-driven airflow using a numerical model ^[23]. Ding et al has investigated the performance of naturally ventilated double-skin façade with solar ^[24]. Manz and Frank have simulated the thermal performance of double-skin façade ^[25]. Most of these reports have focused on the stack effect or the solar chimney concept.

2.7.2. Thermal performances

Some research has been done related to the thermal performance of double-skin façade. Chan et al. have investigated the performance of a double-skin façade in Hong Kong in comparison with a conventional single-skin façade with absorptive glazing ^[26]. In addition, through a comparison of double-skin and single-skin façades in a hot arid climate, Hamza found that a double-skin façade with reflective glass could achieve better energy savings than a single-skin façade with reflective glazing ^[27]. Xu and Yang have researched the thermal performance of a double-skin façade that uses natural ventilation and Venetian blinds ^[28], and Hien et al. found that a double-skin façade with natural ventilation could reduce energy consumption as well as improve thermal comfort ^[29].

Kato et al ^[30] have studied the effectiveness of double-skin façade in reducing cooling load by coupling it with earth-to-air heat exchanger. Moreover, Yoon et al have proposed the prediction technique of the performance of double-skin façade during cooling season ^[31].

According to Barták et al ^[22], in general, the double-skin façade acts as a thermal buffer in front of the offices. This has two counteracting thermal effects for the offices.

1. The air temperature in the double-skin façade will be higher than outside during most of the time. This will result in lower conductive heat losses (heating season) and higher conductive heat gains (summer) depending on ambient temperatures and solar radiation levels.
2. The extra outside pane of glass of the double-skin façade will effectively reduce the amount of solar radiation on the inside façade, thus reducing the solar radiation load of the offices due to radiation transmission via the windows.

Todorovic and Maric ^[32] developed a model for the thermal performance of a double skin façade system for estimating the inter-space air temperature and the associated cooling/heating load per hour. Calculations are made for specific double-façade constructions designed for the climatic conditions of mid-latitude Europe (45° North latitude). The used outdoor air temperatures and solar radiation are typical for Belgrade. Results for each of the double façade cases are compared with those for a traditional or single façade building, and found that the inter-space temperature directly influences transmission heat gains/losses through the basic façade.

Saelens et al have investigate the performance of double-skin façade by studying and comparing conventional insulated façade with the typologies of multiple-skin façade such as airflow window, supply air window, and naturally ventilated window under Belgian weather condition ^[33].

2.7.3. Energy performances

As can be found in the literatures, double-skin façade has a potential in reducing cooling and heating energy consumption. Pappas have been investigating the energy performance of double-skin façade by analyzing the Museum of Contemporary Art in Denver ^[34]. Stribling and Stigge studied the performance of double-skin façade by reviewing the energy saving and cost payback issue of building at three different climate area, London as mild climate, Las Vegas as dry sunny climate, and Canada as cold climate ^[35]. They simulate the three dimensional model building in TAS/EDSL (Environmental Design Solutions Limited) and calculate the time based thermal loads on a building based on its fabric, solar shading and historical weather data.

According to Poirazis in his double-skin façade literature review” ^[6], a complete study of energy performance was presented by Saelens, Carmeliet and Hens in “Energy Performance Assessment of Multiple Skin Façades” in 2003. The authors focus on the energy-saving objectives of three Multi Storey Façade typologies used in a single office. They focus on one storey high solutions, which are a conventional façade with an insulated glazing unit, a naturally ventilated double skin façade, a mechanically ventilated airflow window, and a mechanically ventilated supply air window and found that it is possible to improve the building’s energy efficiency in some way by using multiple skin façades. Unfortunately, most typologies are incapable of lowering both the annual heating and cooling demand. Only by combining typologies or changing the system settings according to the particular situation, a substantial overall improvement over the traditional insulated glazing unit with exterior shading is possible. This implies that sophisticated control mechanisms are inevitable to make multiple skin façades work

efficiently throughout the year. In order to evaluate the energy efficiency, an annual energy simulation focusing on both heating and cooling load is necessary.

Furthermore, they said that the analysis shows that the energy performance strongly depends on the way the cavity air is used. In order to evaluate the energy efficiency of multiple skin façades correctly, it is imperative not only to study the transmission gains and losses but also to take into account the enthalpy change of the cavity air and to perform a whole building energy analysis.

CHAPTER 3. NUMERICAL MODEL

3.1. Numerical Model

This section discusses the model of double-skin façade as can be seen at Figure 3.1-1 below. The model consists of five storeys with single sheet glass as outer and inner glasses. Between the outer and inner glass, there are horizontal blinds attached as shading device. At the bottom of double-skin, there is a lower aperture for airflow inlet as well as upper aperture on the top of double-skin for airflow outlet.

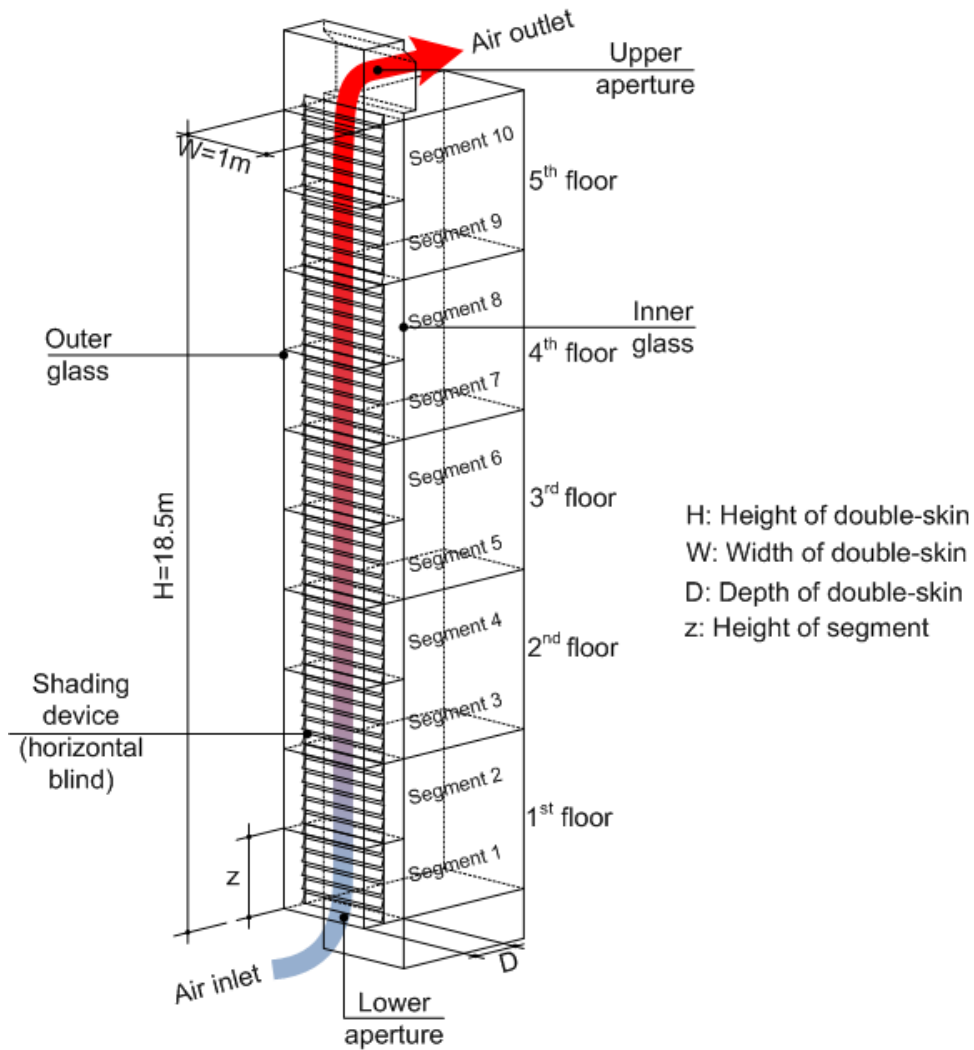


Figure 3.1-1. Model of double-skin façade

The outer glass, the inner glass, the blinds, and the layer of air (which constitute the double-skin façade) were divided into a finite number of segments height-wise. The heat-transfer in each layer was taken into account for the heat balance of each segment. Radiation, multiple reflections of solar radiation, and mutual radiation were considered. For the glass, the incident angle of direct solar radiation and the transmittance, reflectance, and absorptance ratios were taken into account. For the blinds, the variation in the absorption rate and upward and downward transmissions are changed by the profile angle of the blinds due to direct solar radiation, diffuse radiation, and ground reflection. Figure 3.1-2 show the heat balance at each segment.

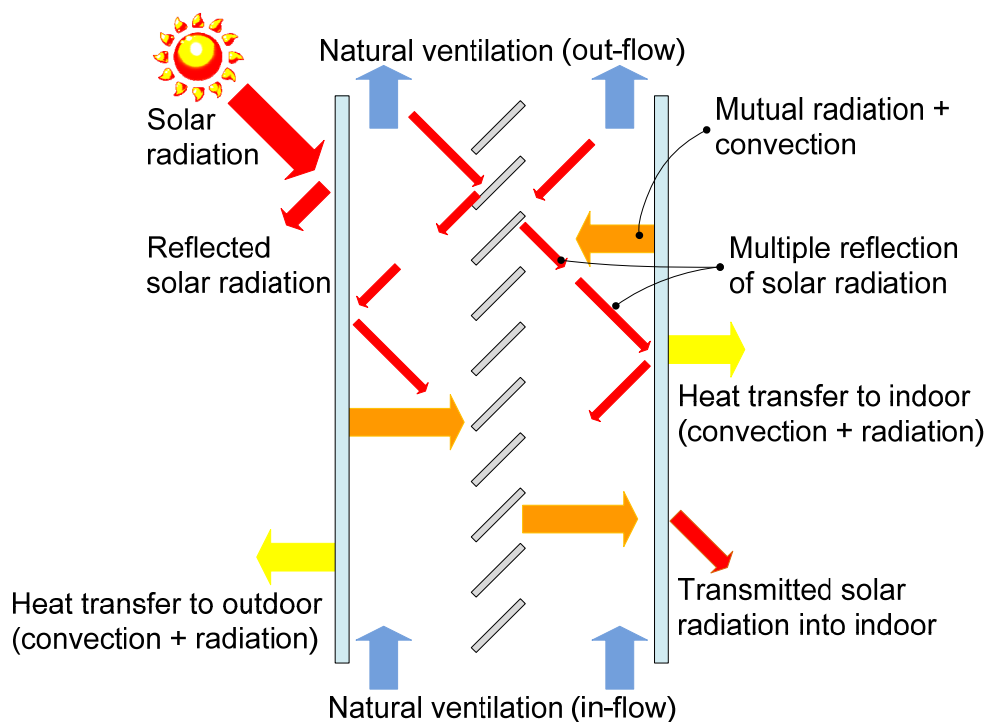


Figure 3.1-2. Heat balance at each segments

3.2. Calculation Flow

The numerical calculation flowchart can be found at Figure 3.2-1. The first step of calculation flow is the input of design condition. In this step, the thickness of the glass, emissivity, transmissivity and absorptivity of the glass and blinds, the high and width of the double-skin, the depth between the outer glass and blinds, the depth between the blinds and inner glass, the inclination and azimuth angles related to the position of the double-skin, the dimension and coefficient of the airflow rate of the lower and upper apertures, and the ground reflectance were all taken into account.

The next step is the input of weather and operational condition of double-skin. The weather components that inputted are outdoor temperature, global radiation, direct solar radiation, diffuse solar radiation, including solar altitude and solar azimuth. The inputs of operational conditions of double-skin are indoor setting temperature, air-conditioning mode (0: no air-conditioning, 1: cooling mode, 2: heating mode), and presence of shading device (0: no shading, 1: shading is used).

The simulation runs based on the design and operational parameters and the input of weather conditions. Natural ventilation through the stack effect is applied, and the temperature inside the double-skin façade was calculated according to the heat balance equations. Both the temperature distribution and ventilation volume were calculated until convergence, which is when a stationary solution condition is obtained at each time.

The results of this numerical calculation model are the air temperature in double-skin, the temperature of inner and outer glass, the temperature of shading device, the amount of ventilation in double-skin, the heat gains of room/indoor, and the amount of heat exhausted by ventilation can be obtained respectively.

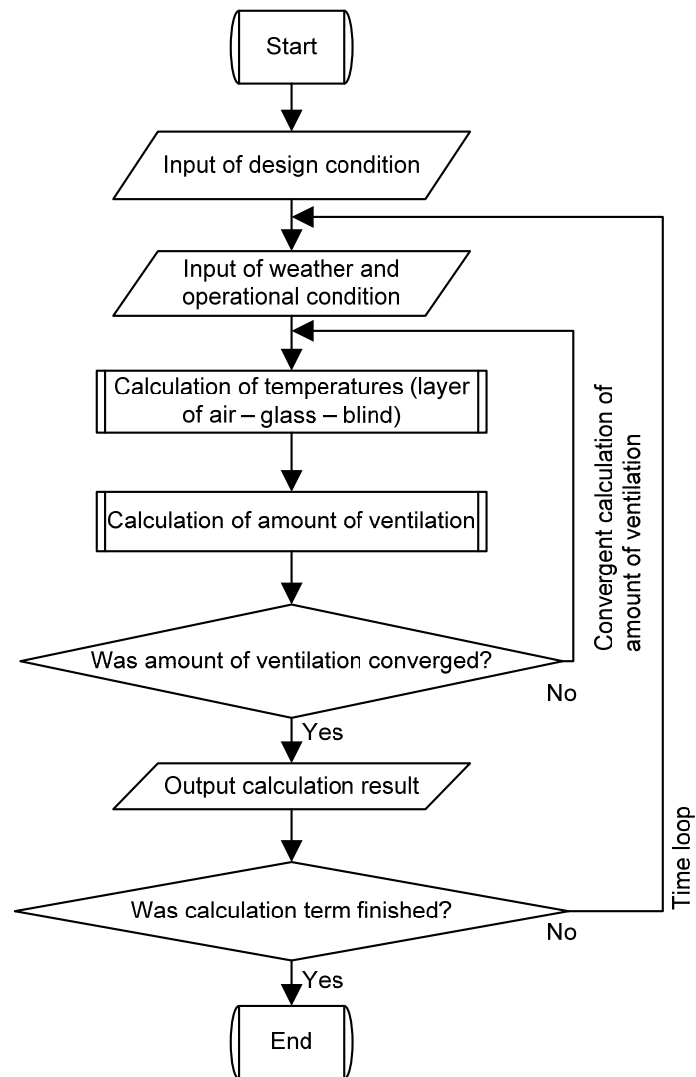


Figure 3.2-1. Numerical calculation flowchart

3.3. Heat-transfer coefficient

This sub-chapter describes the heat-transfer coefficient of double-skin façade, which are the overall heat-transfer coefficient at the outer glass (h_o), the radiative heat-transfer coefficient from the outer glass ($h_{r,og}$), the convective heat-transfer coefficient from the outer glass ($h_{c,og}$), the radiative heat-transfer coefficient from the shading

device ($h_{r,sd}$), the convective heat-transfer coefficient from the shading device ($h_{c,sd}$), the radiative heat-transfer coefficient from the inner glass ($h_{r,ig}$), the convective heat-transfer coefficient from the inner glass ($h_{c,ig}$), and the overall heat-transfer coefficient at the inner glass (h_o).

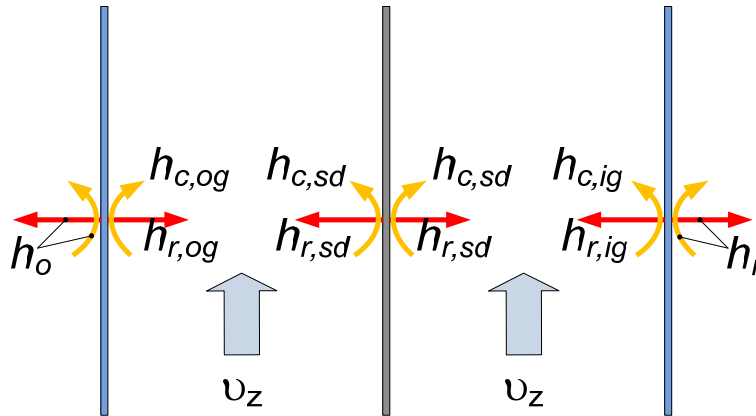


Figure 3.3-1. Setting of the heat-transfer coefficient in ventilated double-skin

The heat-transfer coefficient at the outer glass h_o [$\text{W}/\text{m}^2 \cdot \text{K}$] can be found in below equation ^{[36] [37]}:

$$h_o = 6.5 \times \varepsilon + 12.2 \dots \dots \dots \text{Eq. 3.3-1}$$

where h_o [$\text{W}/\text{m}^2 \cdot \text{K}$] is the overall heat-transfer coefficient at the outer glass and ε [-] is the emissivity of the glass.

The radiative heat-transfer coefficient in double-skin façade can be calculated using equation (3.3-2) below ^[37]

$$h_r = \varepsilon \times h_{rb} \dots \dots \dots \text{Eq. 3.3-2}$$

where h_r is the radiative heat-transfer coefficient in $[\text{W}/\text{m}^2 \cdot \text{K}]$, ε [-] is the emissivity of the glass, and h_{rb} is the radiative heat-transfer coefficient at the black body surface in $[\text{W}/\text{m}^2 \cdot \text{K}]$.

The convective heat-transfer coefficient h_c $[\text{W}/\text{m}^2 \cdot \text{K}]$ takes into account the wind speed $v \leq 5$ $[\text{m}/\text{s}]$ at each high of segments (z) of double-skin. The convective heat-transfer at the glass surface can be calculated using equation below^{[36] [37] [38] [39] [40]}

$$h_c = 5.6 + 4.0 \times v_z \dots\dots\dots \text{Eq. 3.3-3}$$

and the convective heat-transfer at the surface of shading device is^{[36] [37] [38] [39] [40]}

$$h_c = 6.2 + 4.2 \times v_z \dots\dots\dots \text{Eq. 3.3-4}$$

The heat-transfer coefficient between the inner glass to the indoor environment is presented in the equation (3.3-5) below^{[36] [37]}

$$h_i = 6.3 \times \varepsilon + 3.9 \dots\dots\dots \text{Eq. 3.3-5}$$

where h_i is the heat-transfer coefficient at the indoor glass, and ε [-] is the emissivity of glass.

3.4. Solar Radiation Properties in Double-skin

The amount of total solar radiation received at the surface of double-skin I_{DS} are depend on direct normal radiation DN $[\text{W}/\text{m}^2]$, incident angle to the window surface i $[\circ]$, glass surface area ratio to the sunshine SG [-], sky horizontal radiation SH $[\text{W}/\text{m}^2]$, tilt angle to the window surface γ $[\circ]$, global radiation TH $[\text{W}/\text{m}^2]$, and ground reflectance ρ_{gr} [-]^[37].

$$I_{DS, total} = DN \cos i \times SG + SH \cos^2 \left(\frac{\gamma}{2} \right) + TH \left[1 - \cos^2 \left(\frac{\gamma}{2} \right) \right] \times \rho_{gr} \dots\dots\dots \text{Eq. 3.4-1}$$

The amount of direct solar radiation absorbed at the outer glass $I_{a,og,D}$ is obtained from the amount of direct solar radiation I_D [W/m²] multiplied by the absorption rate of the outer glass $\bar{\alpha}_{og,D}$ and can be written as follows [37]

$$I_{a,og,D} = \bar{\alpha}_{og,D} \times I_D \dots\dots\dots \text{Eq. 3.4-2}$$

where [37]

$$\bar{\alpha}_{og,D} = \alpha_{og,D} \left[1 + \tau_{og,D} \frac{\rho_{sd} (1 - \rho_{sd} \rho_{ig,D}) + \tau_{sd}^2 \rho_{ig,D}}{(1 - \rho_{og,D} \rho_{sd})(1 - \rho_{sd} \rho_{ig,D}) - \rho_{og,D} \rho_{sd}^2 \rho_{ig,D}} \right] \dots\dots\dots \text{Eq. 3.4-3}$$

where $\bar{\alpha}_{og,D}$ absorption rate of direct solar radiation at the outer glass, $\tau_{og,D}$ is the transmittance rate of direct solar radiation at the outer glass, ρ_{sd} is the reflectance rate of the shading device, $\rho_{ig,D}$ is the reflectance rate of direct solar radiation at the inner glass, τ_{sd} is the rate of direct solar radiation transmitted by the shading device, $\rho_{og,D}$ is the reflectance rate of direct solar radiation at the outer glass.

The amount of direct solar radiation absorbed in the shading device $I_{a,sd,D}$ obtained from the amount of direct solar radiation I_D multiplied with the absorption rate of the shading device $\bar{\alpha}_{sd,D}$ as seen at the equation below [37]

$$I_{a,sd,D} = \bar{\alpha}_{sd,D} \times I_D \dots\dots\dots \text{Eq. 3.4-4}$$

where $\bar{\alpha}_{sd,D}$ is obtained from

$$\bar{\alpha}_{sd,D} = \tau_{og,D} \alpha_{sd} \frac{1 - \rho_{sd} \rho_{ig,D} + \tau_{sd} \rho_{ig,D}}{(1 - \rho_{og,D} \rho_{sd})(1 - \rho_{sd} \rho_{ig,D}) - \rho_{og,D} \tau_{sd}^2 \rho_{ig,D}} \dots\dots\dots \text{Eq. 3.4-5}$$

where $\tau_{og,D}$ is the transmittance rate of direct solar radiation at the outer glass, and α_{sd} is the absorption rate of the shading device.

The amount of direct solar radiation absorbed in the inner glass $I_{a,ig,D}$ takes into account the absorption rate of direct solar radiation at the inner glass $\bar{\alpha}_{ig,D}$ multiplied with the amount of direct solar radiation I_D as can be seen in the equation below ^[37]

$$I_{a,ig,D} = \bar{\alpha}_{ig,D} \times I_D \dots\dots\dots \text{Eq. 3.4-6}$$

where $\bar{\alpha}_{ig,D}$ is obtained from

$$\bar{\alpha}_{ig,D} = \tau_{og,D} \tau_{sd} \alpha_{ig,D} \frac{1}{(1 - \rho_{og,D} \rho_{sd})(1 - \rho_{sd} \rho_{ig,D})(\rho_{og,D} \tau_{sd}^2 \rho_{ig,D})} \dots\dots\dots \text{Eq. 3.4-7}$$

where $\alpha_{ig,D}$ is absorption rate of the inner glass.

The amount of direct solar radiation that is reflected by the double-skin $I_{ref,D}$ is taken from the amount of reflection rate $\bar{\rho}_D$ of direct solar radiation multiplied by the direct solar radiation as can be seen in below equation ^[37]

$$I_{ref,D} = \bar{\rho}_D \times I_D \dots\dots\dots \text{Eq. 3.4-8}$$

where $\bar{\rho}_D$ was taken from

$$\bar{\rho}_D = \rho_{og,D} + \tau_{og,D}^2 \frac{\rho_{sd}(1 - \rho_{sd} \rho_{ig,D}) + \tau_{sd}^2 \rho_{ig,D}}{(1 - \rho_{og,D} \rho_{sd})(1 - \rho_{sd} \rho_{ig,D}) - \rho_{og,D} \tau_{sd}^2 \rho_{ig,D}} \dots\dots\dots \text{Eq. 3.4-9}$$

The amount of direct solar radiation that is transmitted by double-skin $I_{tran,D}$ is equivalent to the amount of direct solar radiation I_D multiplied by transmittance rate $\bar{\tau}_D$ ^[37] as can be seen at the equation below

$$I_{tran,D} = \bar{\tau}_D \times I_D \dots\dots\dots \text{Eq. 3.4-10}$$

where $\bar{\tau}_D$ can be obtained from

$$\bar{\tau}_D = \tau_{og,D} \tau_{sd} \tau_{ig,D} \frac{1}{(1 - \rho_{og,D} \rho_{sd})(1 - \rho_{sd} \rho_{ig,D}) - \rho_{og,D} \tau_{sd}^2 \rho_{ig,D}} \dots \text{Eq. 3.4-11}$$

where $\tau_{ig,D}$ is the transmission rate of direct solar radiation through the inner glass.

3.5. Heat Balance at Double-skin Façade

The heat balance equation of double-skin façade takes into account the heat balance at the outer glass, the heat balance at the shading device, the heat balance at the layer of air, and the heat balance at the inner glass as can be seen at equations below.

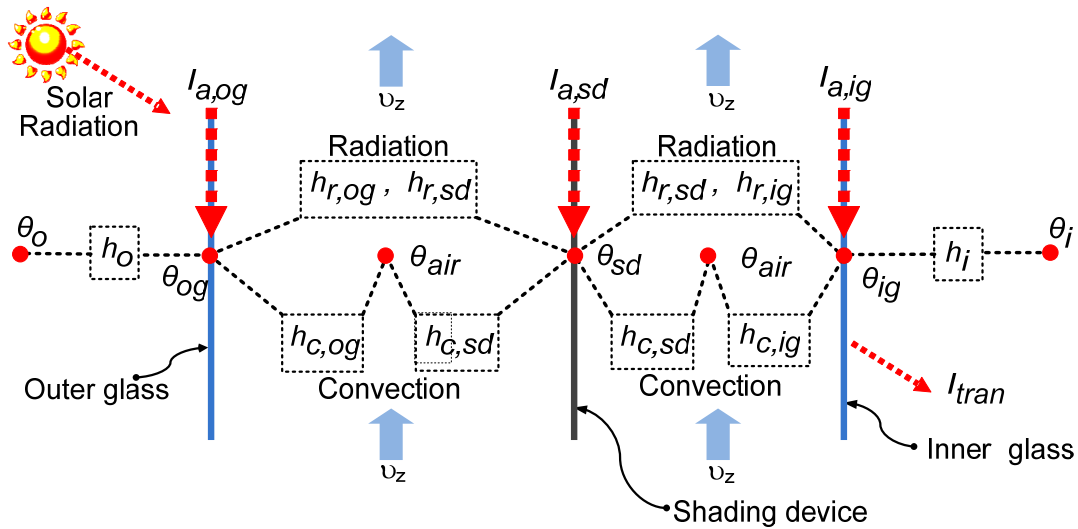


Figure 3.5-1. Outline of numerical calculation

a. Heat balance at the outer glass

$$h_o (\theta_{og} - \theta_o) + h_{r,og} \left(\theta_{og} - \sum_{n=1}^{10} G_{og_n, sd_n} \cdot \theta_{sd} \right) + h_{c,og} (\theta_{og} - \theta_{air}) = I_{a,og} \dots \text{Eq. 3.5-1}$$

b. Heat balance at the air layer of the cavity of double-skin

$$\rho_{air} c_{air} v_z \frac{\partial \theta_{air}}{\partial z} = h_{c,og} (\theta_{og} - \theta_{air}) + h_{c,ig} (\theta_{ig} - \theta_{air}) + 2h_{c,sd} (\theta_{sd} - \theta_{air}) \dots \text{Eq. 3.5-2}$$

c. Heat balance at the shading device

$$2h_{c, sd} (\theta_{sd} - \theta_{air}) + h_{r, sd} \left(\theta_{sd} - \sum_{n=1}^{10} G_{sd_n, og_n} \cdot \theta_{og} \right) + h_{r, sd} \left(\theta_{sd} - \sum_{n=1}^{10} G_{sd_n, ig_n} \cdot \theta_{ig} \right) = I_{a, sd} \dots \text{Eq. 3.5-3}$$

d. Heat balance at the inner glass

$$h_{r, ig} \left(\theta_{ig} - \sum_{n=1}^{10} G_{sd_n, ig_n} \cdot \theta_{sd} \right) + h_{c, ig} (\theta_{ig} - \theta_{air}) + h_i (\theta_{ig} - \theta_i) = I_{a, ig} \dots \text{Eq. 3.5-4}$$

where, h_o is the heat-transfer at the outer glass and the outdoor [$\text{W}/\text{m}^2 \cdot \text{K}$], θ_{og} is the temperature of the outer glass [$^\circ$], θ_o is the temperature of the outdoor [$^\circ$], $h_{r, og}$ is the radiative heat-transfer at the outer glass [$\text{W}/\text{m}^2 \cdot \text{K}$], $G_{og, sd}$ is the absorption coefficient of emission of outer glass and shading device[-], θ_{sd} is the temperature of the shading device [$^\circ$], $h_{c, og}$ is the convective heat-transfer of the outer glass [$\text{W}/\text{m}^2 \cdot \text{K}$], θ_{air} is the temperature of the air layer of double-skin [$^\circ$], $I_{a, og}$ is the solar radiation absorbed at the outer glass [W/m^2], ρ_{air} is the density of air in the cavity of double-skin [kg/m^3], c_{air} is the heat specific of the air in the cavity of double-skin [$\text{J}/\text{m}^3 \cdot \text{K}$], v_z is the velocity of the air in the cavity of double-skin [m/s], z is height if segment of double-skin [m], $h_{c, ig}$ is the convective heat-transfer at the inner glass [$\text{W}/\text{m}^2 \cdot \text{K}$], θ_{ig} is the temperature of the inner glass [$^\circ$], $h_{c, sd}$ is the convective heat-transfer at the shading device [$\text{W}/\text{m}^2 \cdot \text{K}$], $h_{r, sd}$ is radiative heat-transfer at the shading device [$\text{W}/\text{m}^2 \cdot \text{K}$], $I_{a, sd}$ is radiation absorbed at the shading device [W/m^2], $h_{r, ig}$ is radiative heat-transfer at the inner glass [$\text{W}/\text{m}^2 \cdot \text{K}$], and h_i is the heat-transfer at the inner glass and the indoor [$\text{W}/\text{m}^2 \cdot \text{K}$], and $I_{a, ig}$ is radiation absorbed at the inner glass [W/m^2], n is number of segments.

3.6. Calculation of Standardized Solar Heat Gain on 3mm Standard Glass

This section describes the calculation of standardized solar heat gain (I_G) on 3mm glass. The calculation takes into account the amount of direct solar radiation (I_D), the amount of diffuse solar radiation (I_S), the amount of direct solar radiation on 3mm standard glass (g_D), and the amount of diffuse solar radiation on 3mm standard glass (g_S) as can be seen on equation below^[37]

$$I_G = (g_D I_D + g_S I_S) \dots\dots\dots \text{Eq. 3.6-1}$$

The amount of direct solar radiation can be calculated based upon the amount of direct solar radiation to the surface (I_{0D}), diffuse horizontal radiation to the surface (I_{0S}), solar radiation area ratio SG , azimuth angle of the surface α , inclination angle of the surface β , solar altitude h , solar altitude as seen from surface h^* , and solar azimuth A as can be seen as follows

$$I_D = \begin{cases} SGI_{0D} \sin h^* = SGI_{0D} \{ \sin h \cos \beta + \cos h \sin \beta \cos (A - \alpha) \} & [\sin h^* > 0] \\ 0 & [\sin h^* < 0] \end{cases} \dots\dots\dots \text{Eq. 3.6-2}$$

Moreover, the calculation of the amount of diffuse solar radiation (I_S) can be calculated as follows

$$I_S = \frac{(1 + \cos \beta)}{2} I_{0S} + \frac{(1 - \cos \beta)}{2} \rho_{gr} (I_{0D} \sin h + I_{0S}) \dots\dots\dots \text{Eq. 3.6-3}$$

where ρ_{gr} is ground reflectance.

The amount of direct solar radiation on 3mm standard glass (g_D) then can be calculated as equation below

$$g_D = 2.3920 \sin h^* - 3.8636 \sin^3 h^* + 3.7568 \sin^5 h^* - 1.3952 \sin^7 h^* \dots \text{Eq. 3.6-4}$$

where,

$$\sin h^* = \sin h \cos \beta + \cos h \sin \beta \cos(A - \alpha) \dots \text{Eq. 3.6-5}$$

$$\cos h^* \sin A = \cos h \sin(A - \alpha) \dots \text{Eq. 3.6-6}$$

$$\cosh^* \cos A = -\sinh \sin \beta + \cosh \cos \beta \cos(A - \alpha) \dots \text{Eq. 3.6-7}$$

The amount of diffuse solar radiation is constant and expressed as follows

$$g_S = 0.808 \dots \text{Eq. 3.6-8}$$

3.7. Calculation of U-value and Shading Coefficient (SC)

There are two kinds of heat that could flow into the indoor through the window surface of double-skin. The first is the heat flow by direct transmission of solar radiation (I_{tran}); and radiative (I_r) and convective (I_c) flow of absorbed solar radiation at the windows side double-skin pane. The second is the radiative (Q_r) and convective (Q_c) heat flow due to the temperature difference between the outdoor and the indoor. Figure 3.7-1 show the heat flow through the window side pane of double-skin.

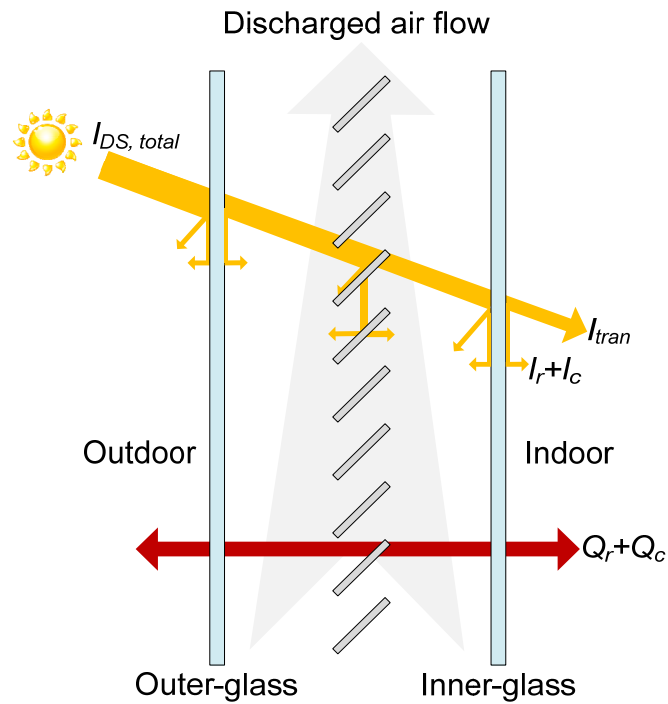


Figure 3.7-1. Heat flow to the indoor

The amount of heat flow into the indoor (I_{in}) through double-skin façade due to the transmission of direct solar radiation through the inner glass (I_{tran}), and the radiative (I_r) and convective (I_c) radiation of the absorbed solar radiation can be seen from the equation below

$$I_{in} = I_{tran} + I_r + I_c \dots\dots\dots 3.7-1$$

The heat transferred into the indoor (Q_{in}) through the double-skin façade, which is the radiative (Q_r) and convective (Q_c) heat-transfer as the temperature difference between the outdoor and the indoor is as follows

$$Q_{in} = Q_r + Q_c \dots\dots\dots \text{Eq. 3.7-2}$$

Based on above description, the U-value of double-skin façade can be calculated as a ratio of the amount of heat flow into the indoor (Q_{in}) through the inner pane of

double-skin façade to the temperature differences between the outdoor and the indoor ($\theta_o - \theta_i$), and can be written as equation below

$$U = \frac{Q_{in}}{(\theta_o - \theta_i)} \dots\dots\dots \text{Eq. 3.7-3}$$

Since the heat flow to the indoor (Q_{in}) is due to temperature difference between the outdoor and the indoor are radiative (Q_r) and convective (Q_c) heat flow, the equation then can be written as follows

$$U = \frac{Q_r + Q_c}{(\theta_o - \theta_i)} \dots\dots\dots \text{Eq. 3.7-4}$$

Furthermore, the SC of double-skin can also be determined as the ratio of the solar radiation reach the indoor (I_{in}) through the inner glass of double-skin to the solar radiation of the standard glass (I_G) (clear glass 3mm thickness) and can be calculated as follows

$$SC = \frac{I_n}{I_G} \dots\dots\dots \text{Eq. 3.7-5}$$

where I_G is taken from equation 3.6-1.

Then, from the equations 3.8-1 and 3.8-6, the SC equation can be written as follows^[41]

$$SC = \frac{(I_{tran} + I_r + I_c)}{(g_D I_D + g_S I_S)} \dots\dots\dots \text{Eq. 3.7-6}$$

From numerical calculation, we can determine the value of $I_r + I_c + Q_r + Q_c$ as follows:

$$I_r + I_c + Q_r + Q_c = h_i(\theta_{ig} - \theta_i) \dots\dots\dots \text{Eq. 3.7-7}$$

However, the heat-transfer by radiation (I_r and I_c) and the heat-transfer due to the temperature differences between indoor and outdoor (Q_r and Q_c) shall be separated

by performing additional simulation, which based on the. The simulation flow-chart can be seen at Figure 3.7-2.

In this simulation, the indoor and ambient temperature was the same and assumed as 0 differences, and the airflow in the cavity of double-skin was determined, which was taken from the previous simulation. By this additional simulation, the temperature of the inner glass (θ_{ig}') can be determined and the radiation heat-transfer can be separated as follows:

$$I_r + I_c = h_i(\theta_{ig}' - \theta_i) \dots\dots\dots \text{Eq. 3.7-8}$$

and,

$$Q_r + Q_c = h_i(\theta_{ig} - \theta_{ig}') \dots\dots\dots \text{Eq. 3.7-9}$$

Then, the SC of double-skin can be calculated as follows:

$$SC = \frac{I_{tran} + h_i(\theta_{ig}' - \theta_i)}{(g_D I_D + g_S I_S)} \dots\dots\dots \text{Eq. 3.7-10}$$

From equation 3.7-4, the U-value can be calculated also as follows:

$$U = \frac{h_i(\theta_{ig} - \theta_{ig}')}{(\theta_0 - \theta_i)} \dots\dots\dots \text{Eq. 3.7-11}$$

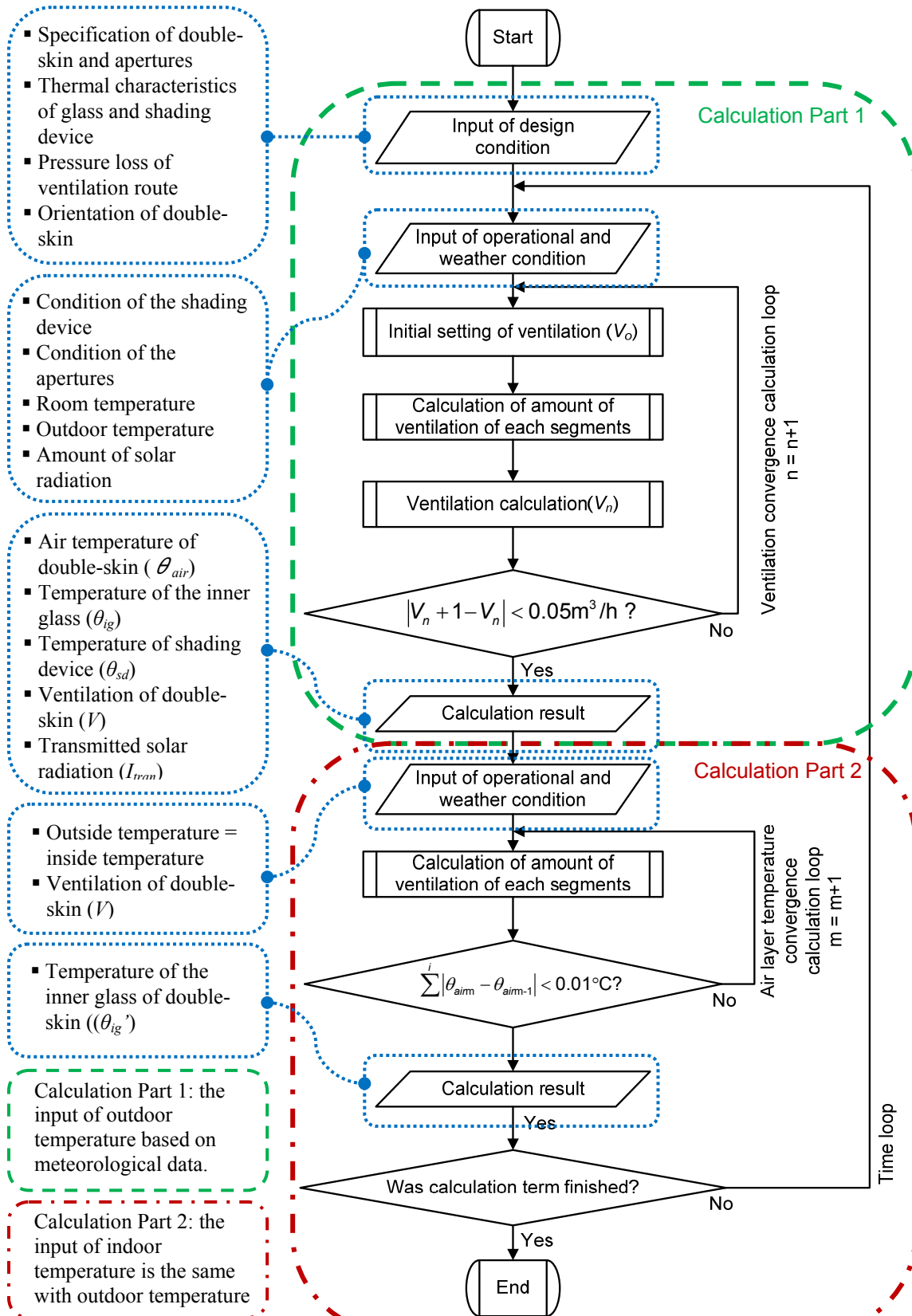


Figure 3.7-2. Flow calculation of U-value and SC

3.8. Validation of the Numerical Model

The numerical method was evaluated by the field measurement result conducted at Izumi Media Building, Meiji University Tokyo^{[30][31]}. The measurement was done in summer at 23 and 30 August with time interval between each measurement was 5 minutes. Items measured are the air temperature in double-skin, the temperature of glass surface, the room air temperature, the amount of solar radiation in double-skin, and the wind speed in double-skin.

The result shows that in summer, where the ambient temperature is relatively similar to the ambient temperature in Indonesia; the difference of both measured and simulated mean temperature in double-skin façade is 3°C. The difference between the measured and simulated amount of ventilation in double-skin façade is 1% in summer. Although the result is not exactly the same, the difference is not high enough, and it can be said that the numerical method can be used to predict the performance of double-skin façade.

CHAPTER 4. THERMAL PERFORMANCE OF DOUBLE-SKIN FAÇADE

4.1. Climate Overview

4.1.1. Hot and Humid Climate

The hot and humid climate (tropical rainforest climate) is a subtype of tropical climate denoted as *Af* in the Köppen-Geiger climate classification system. This climate is usually occurring within 5-10° latitude of equator. It characteristic is having two seasons called dry and rainy season, high humidity level, and the temperature relatively constant throughout the year. Figure show the climate classification in Asia continent.

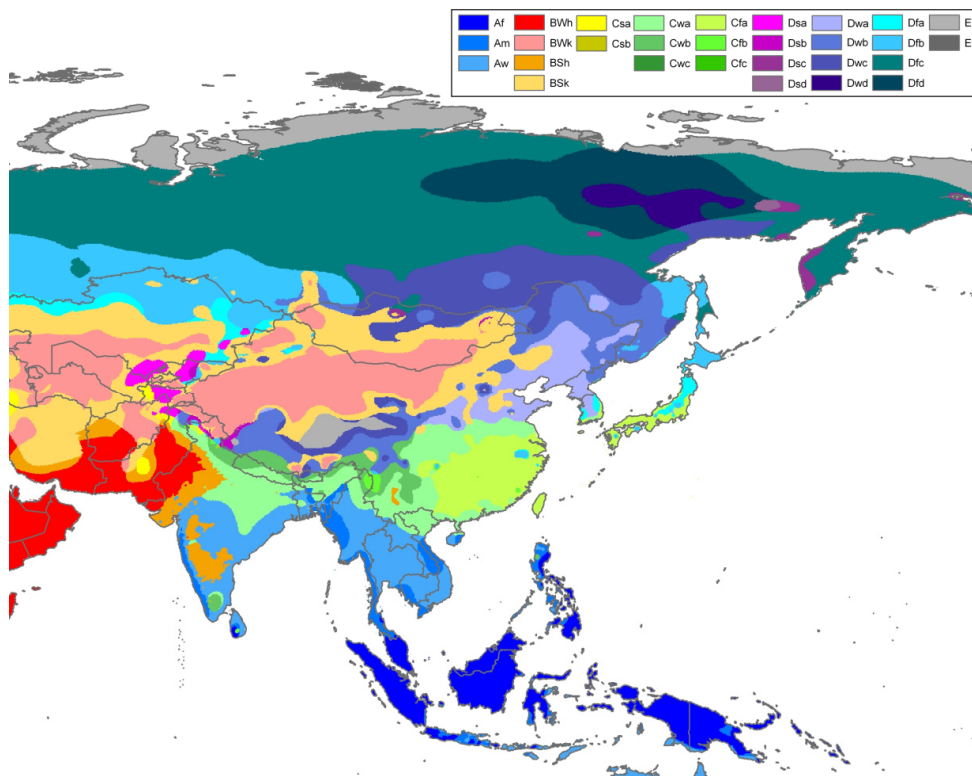


Figure 4.1-1. Asia Köppen-Geiger climate classification system ^[38]

4.1.2. Climate Condition of Indonesia

Indonesia is split by the equator; therefore, the climate condition is tropical. There is slight daily variation in temperature, with the greatest variation at inland points and at higher levels. At the coastal plain areas, the yearly average temperature is around 29°C. The inland and mountain areas averaging temperature is 26°C. At the higher mountain regions, the averaging temperature is 16°C. The relative humidity is range from 60% to 90% throughout the year.



Image source: <http://maps.nationmaster.com/country/id/1>
Figure 4.1-2. Map of Indonesia

There are only two seasons in Indonesia, the dry season and the rainy season. The dry season is from May to September and the rainy season is from December to

April. Between these seasons, there are seasonal transition periods, which are the transition period between dry season to rainy season is from October to December, and the transition period between rainy season to dry season is from April to May. Western and northern parts of Indonesia experience the most precipitation, since the north- and westward-moving monsoon clouds are heavy with moisture by the time they reach these more distant regions. Western Sumatra, Jawa, Bali, the interiors of Kalimantan, Sulawesi, and Papua are the most predictably damp regions of Indonesia, with rainfall measuring more than 2,000 millimeters per year^[39]. Rainfall in lowland areas averages 180–320 cm (70–125 in) annually, increasing with elevation to an average of 610 cm (240 in) in some mountain areas. In the lowlands of Sumatra and Kalimantan, the rainfall range is 305–370 cm (120–145 in); the amount diminishes southward, closer to the northwest Australian desert^[40]. In addition, between September and December on the transition period, Typhoon can hit the island and can cause the storm and heavy rains.

Since Indonesia is a large area country, the weather condition could vary in details among island/region. Therefore, it is necessary to specify the actual place of the weather data used in this study. The actual place is in Sulawesi Island, the place is called Makassar (see Figure 4.1-2). Makassar is formerly called Ujung Pandang, the capital of South Sulawesi Province. It is located at 5°8' South Latitude and 119°25' East Longitude, and about 1276.23 km distant from Jakarta (the capital of Indonesia) heading east. The weather condition of Makassar can be seen on Figure 4.1-3.

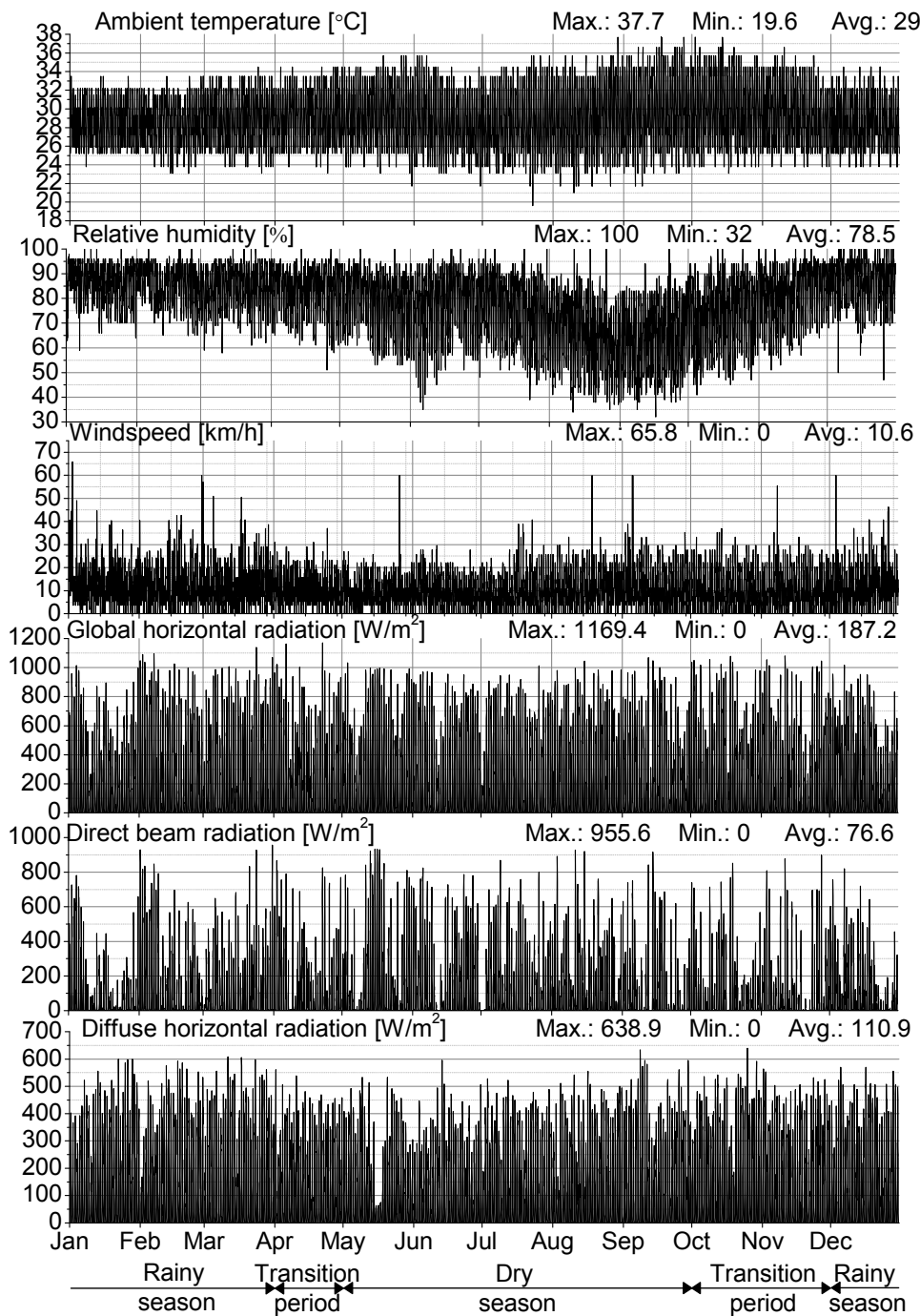


Figure 4.1-3. Weather condition of Makassar

4.2. The Cases

In order to define the performance of double-skin façade in Indonesia, some cases have been chosen according to the thickness of the glasses, the distance between

the outer and inner glasses, and the orientation of double-skin. The cases can be found at Table 4.2-1 below.

Table 4.2-1. Simulation cases

Orientation	Cases	Glass thickness		Outer and inner glass distance (width of double-skin) [cm]	Orientation	Cases	Glass thickness		Outer and inner glass distance (width of double-skin) [cm]
		Outer glass [mm]	Inner glass [mm]				Outer glass [mm]	Inner glass [mm]	
East	Case E1	10	6	80	West	Case W1	10	6	80
	Case E2	10	8	80		Case W2	10	8	80
	Case E3	10	10	80		Case W3	10	10	80
	Case E4	10	12	80		Case W4	10	12	80
	Case E5	12	12	80		Case W5	12	12	80
	Case E6	10	6	100		Case W6	10	6	100
	Case E7	10	8	100		Case W7	10	8	100
	Case E8	10	10	100		Case W8	10	10	100
	Case E9	10	12	100		Case W9	10	12	100
	Case E10	12	12	100		Case W10	12	12	100
	Case E11	10	6	150		Case W11	10	6	150
	Case E12	10	8	150		Case W12	10	8	150
	Case E13	10	10	150		Case E13	10	10	150
	Case E14	10	12	150		Case E14	10	12	150
	Case E15	12	12	150		Case E15	12	12	150
	Case E16	10	6	200		Case W16	10	6	200
	Case E17	10	8	200		Case E17	10	8	200
	Case E18	10	10	200		Case E18	10	10	200
	Case E19	10	12	200		Case E19	10	12	200
	Case E20	12	12	200		Case E20	12	12	200
North	Case N1	10	6	80	South	Case S1	10	6	80
	Case N2	10	8	80		Case S2	10	8	80
	Case N3	10	10	80		Case S3	10	10	80
	Case N4	10	12	80		Case S4	10	12	80
	Case N5	12	12	80		Case S5	12	12	80
	Case N6	10	6	100		Case S6	10	6	100
	Case N7	10	8	100		Case S7	10	8	100
	Case N8	10	10	100		Case S8	10	10	100
	Case N9	10	12	100		Case S9	10	12	100
	Case N10	12	12	100		Case S10	12	12	100
	Case N11	10	6	150		Case S11	10	6	150
	Case N12	10	8	150		Case S12	10	8	150
	Case N13	10	10	150		Case S13	10	10	150
	Case N14	10	12	150		Case S14	10	12	150
	Case N15	12	12	150		Case S15	12	12	150
	Case N16	10	6	200		Case S16	10	6	200
	Case N17	10	8	200		Case S17	10	8	200
	Case N18	10	10	200		Case S18	10	10	200
	Case N19	10	12	200		Case S19	10	12	200
	Case N20	12	12	200		Case S20	12	12	200

4.3. Design and Operational Condition

The design conditions of the double-skin, the operational scheme, and the weather conditions were considered. The thickness of glasses, the emissivity and transmissivity of the glasses, the absorptivity of the blinds, the height and width of the double-skin, the depth between the outer glass and the blinds, the depth between the blinds and the inner glass, the inclination and azimuth angles related to the position of the double-skin, the dimension and coefficient of the airflow rate of the lower and upper apertures, and the ground reflectance were all taken into account (Table 4.3-1).

Table 4.3-1. Design and operational condition of the numerical model

Physical properties	Value
Azimuth angle of North-facing double-skin [°]	0
Azimuth angle of East-facing double-skin [°]	90
Azimuth angle of South-facing double-skin [°]	180
Azimuth angle of West-facing double-skin [°]	270
Inclined angle of double-skin [°]	90
Thickness of outer glass (refer to Table 1)	
Thickness of inner glass (refer to Table 1)	
Distance between outer glass and blinds:	
▪ for 200 cm width of double-skin [cm]	190
▪ for 150 cm width of double-skin [cm]	140
▪ for 100 cm width of double-skin [cm]	90
▪ for 80 cm width of double-skin [cm]	70
Distance between blinds and inner glass [cm]	10
Slat angle of blinds [°]	45
Solar transmittance rate of blinds [-]	0.1
Solar absorption rate of blinds [-]	0.5
Emissivity of blinds [-]	0.95
Emissivity of glass [-]	0.837
Flow coefficient of lower and upper apertures [-]	0.65
Area of lower and upper apertures [m ² /m]	0.30
Ground reflectance [-]	0.14

The weather conditions take into account the ambient temperature, relative humidity, and solar radiation data. The data used is hourly data and was taken from the Meteorological, Climatological and Geophysical Agency of Indonesia.

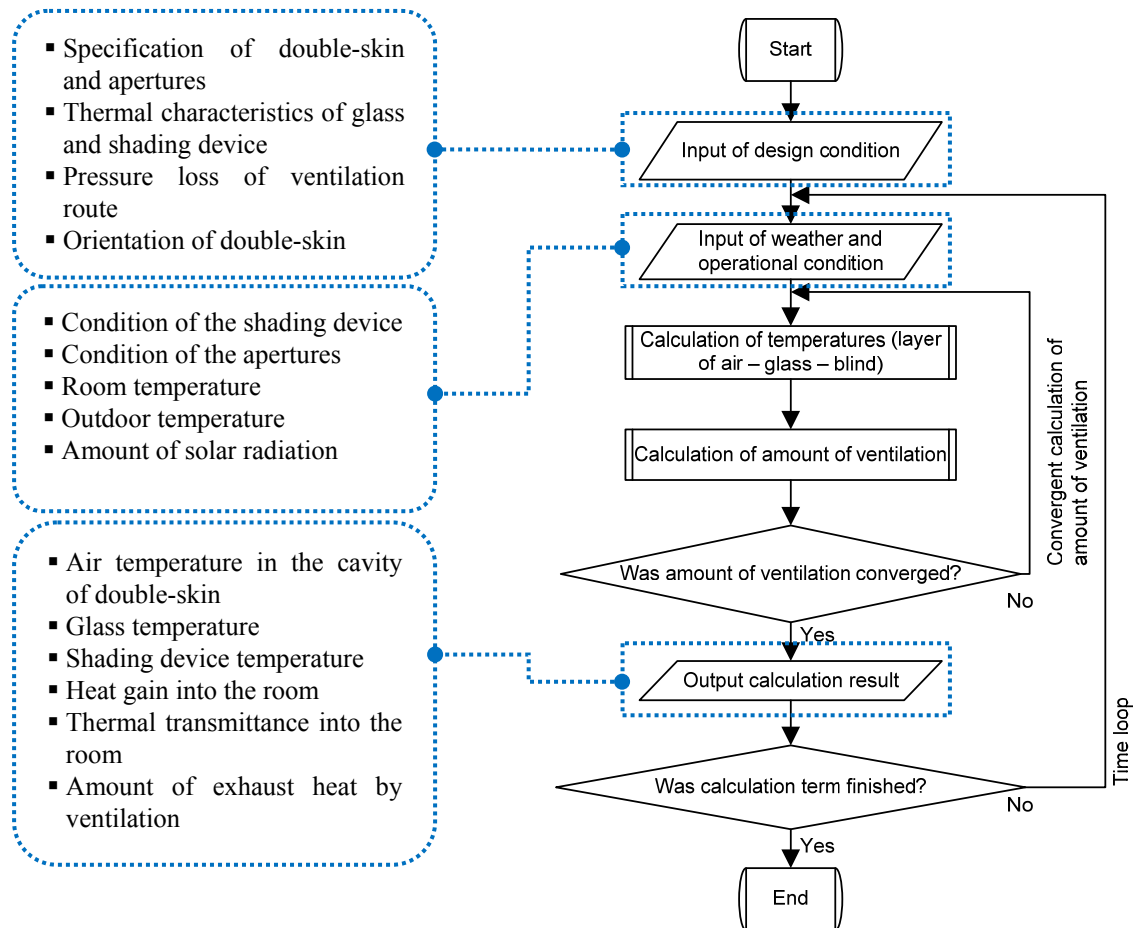


Figure 4.3-1. Simulation flow chart

The simulation runs based on the design and operational parameters (see Table 4.3-1.) and the input weather conditions for working hours from 8:00 am until 5:00 pm. The indoor temperature was set to 25 °C. Natural ventilation through the stack-effect was applied, and the temperature inside the double-skin façade was calculated according to the heat balance equations (see equation 3.5-1~3.5.4). Both the temperature

distribution and ventilation volume were calculated until convergence, which is when a stationary solution condition is obtained at each calculation time. The simulation flow chart can be found in Figure 4.3-1.

During the operational time of the double skin, the lower and upper apertures were opened. When the solar radiation reaches the outer skin, the temperature in the cavity will increase gradually. Opening the apertures allows fresh air from the outdoors to be introduced into the cavity through the lower aperture. Then, the warm air inside the double-skin façade vented out through the upper aperture.

4.4. Comparing the Thermal Transmittance and the Solar Heat Gain

The amount of thermal transmittance is higher than solar heat gain for north-, east-, south- and west-facing double-skin façade. From Figure 4.4-1 to Figure 4.4-4 represent the hourly thermal transmittance and solar heat gain of the case of 12mm outer and inner glass skin combination at the distance of 100cm.

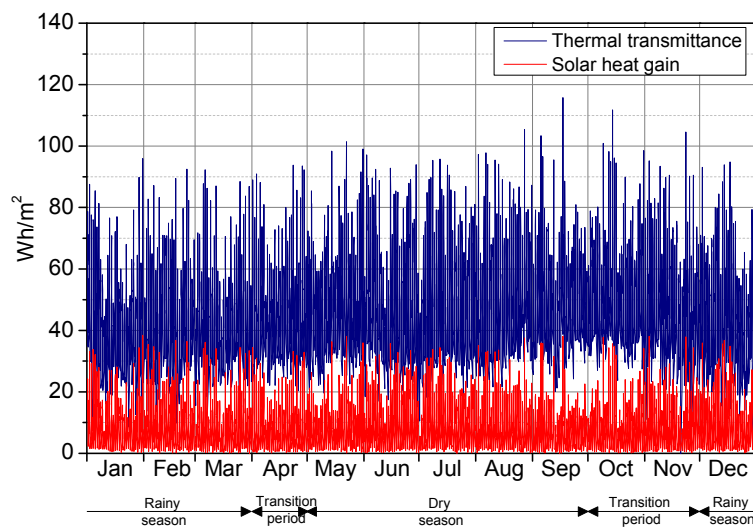


Figure 4.4-1. Solar heat gain and thermal transmittance of north-facing double-skin façade

During a year, north-facing double-skin façade has a higher value in thermal transmittance and solar heat gain performance. The thermal transmittance is up to 115.72 Wh/m² in maximum and 48.55 Wh/m² in the average. The solar heat gain maximum is 38.43 Wh/m², and the average is 10.21 Wh/m².

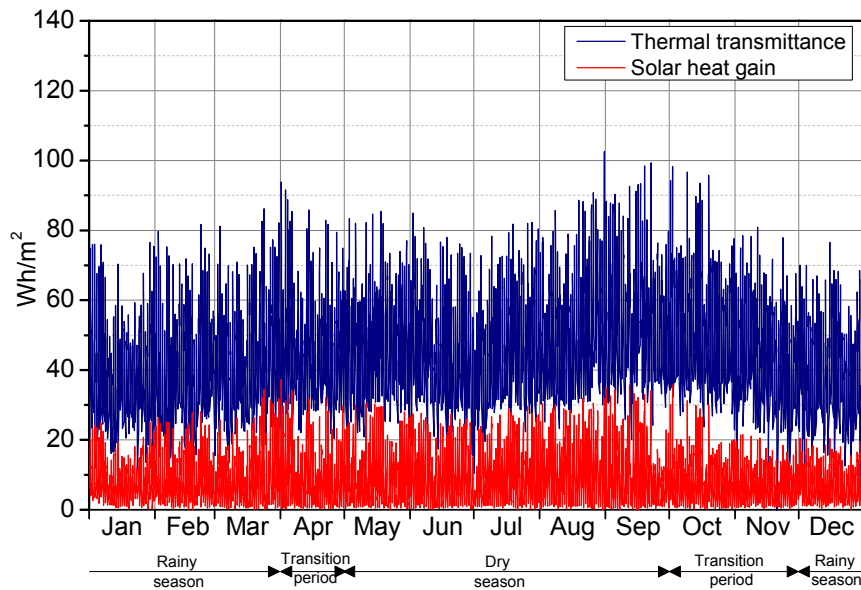


Figure 4.4-2. Solar heat gain and thermal transmittance of east-facing double-skin façade

For the east-facing double-skin façade, hourly maximum of thermal transmittance is 102.60 Wh/m² with 47.48 Wh/m² in the average. The hourly maximum of solar heat gain is 37.26 Wh/m², and the average is 10.12 Wh/m².

South-facing double-skin façade has the lowest thermal transmittance compared to the other double-skin façades orientation. The maximum thermal transmittance is 77.50 Wh/m²; and the solar heat gain is 19.27 Wh/m². Average thermal transmittance is 43.30 Wh/m², and the solar heat gain is 7.96 Wh/m².

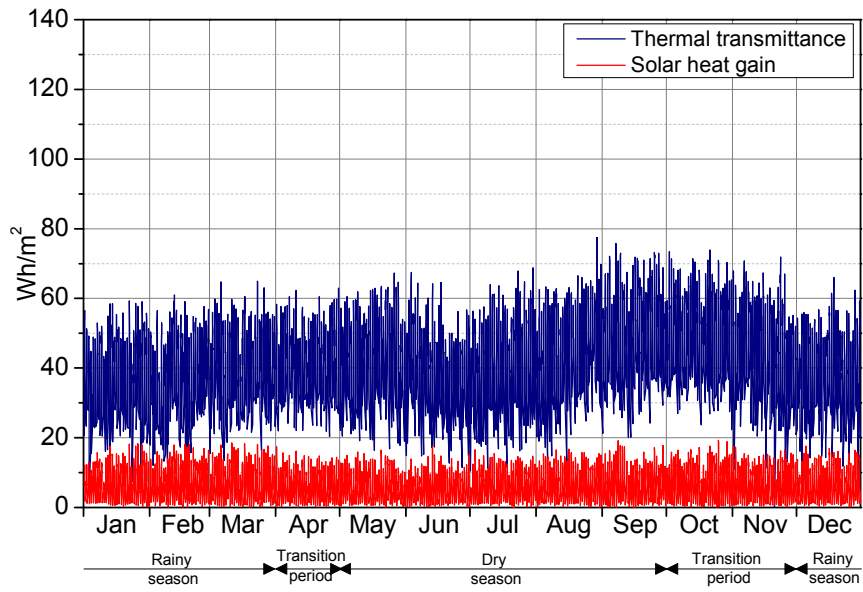


Figure 4.4-3. Solar heat gain and thermal transmittance of south-facing double-skin façade

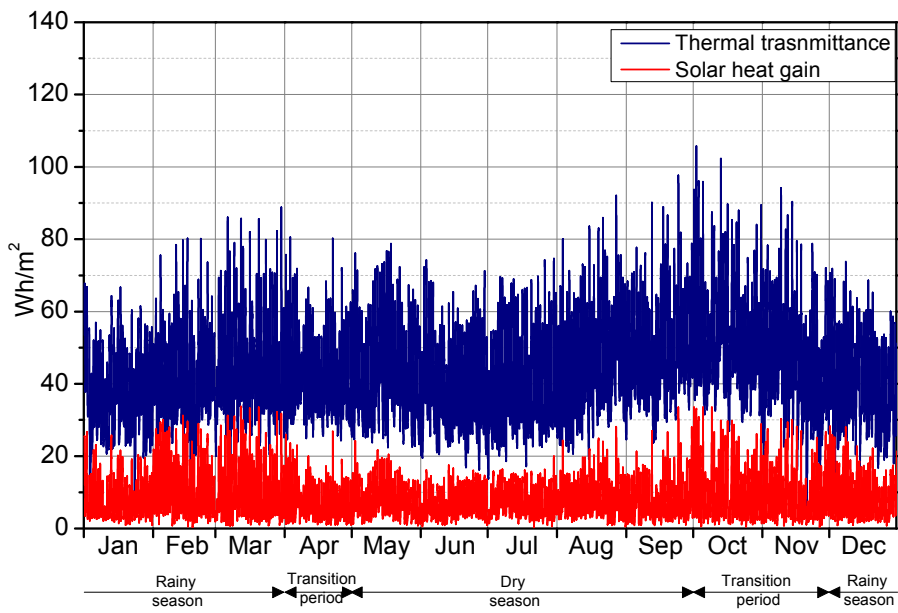


Figure 4.4-4. Solar heat gain and thermal transmittance of west-facing double-skin façade

The hourly thermal transmittance at west-facing double-skin is 109.51 Wh/m² in maximum, and 47.17W/m² in average. Solar heat gain maximum is 36.99W/m², and the average is 9.93W/m².

From the numerical simulation results, it is found that the hourly heat gain due to thermal transmittance is higher than the solar heat gain for north-, east-, south-, and west-facing double-skin façades. Figure 4.4-5 until Figure 4.4-8 show the hourly solar heat gain and thermal transmittance of east-, south-, north-, and west-facing double-skin façades, respectively. This phenomenon explains the benefit of double-skin façades in reducing the solar heat gain. Double-skin façade components such as the outer glass, shading device, and the inner glass, plays an important role in minimizing the effect of solar radiation into the indoor environment. However, since the temperature difference between the ambient temperature and the indoors is relatively high, including high absorption at the outer glass, shading device, and inner glass, causes high conduction in the double-skin.

Furthermore, the thickness of the glass plays an important role in the solar heat gain performance of double-skin façades. As can be seen in Figure 4.4-5 until Figure 4.4-8, the solar heat gain of the double-skin façade with 12mm thickness outer and inner glass skins at any designated distance between, is substantially less than that of other glass skin combinations. Otherwise, the lower glass thickness causes a higher solar heat gain at any glass skin distance combination.

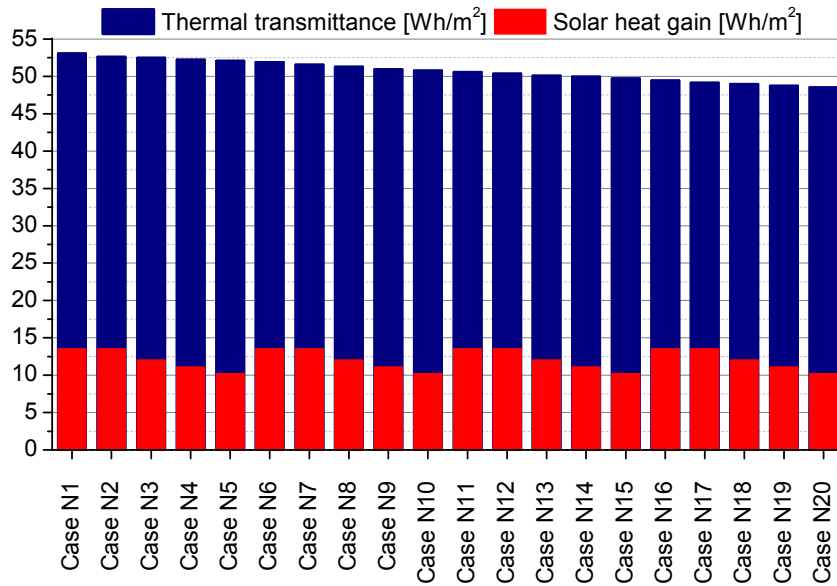


Figure 4.4-5. Hourly solar heat gain and thermal transmittance of north-facing double-skin façade

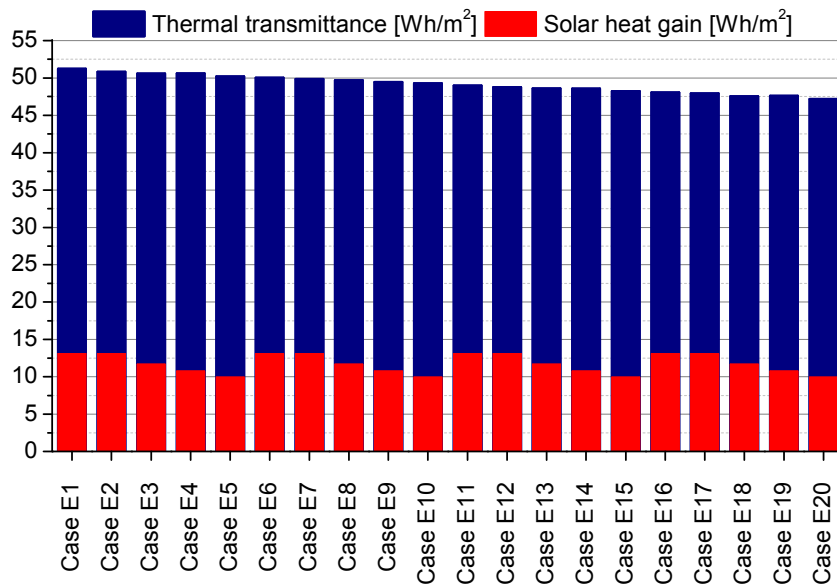


Figure 4.4-6. Hourly solar heat gain and thermal transmittance of east-facing double-skin façade

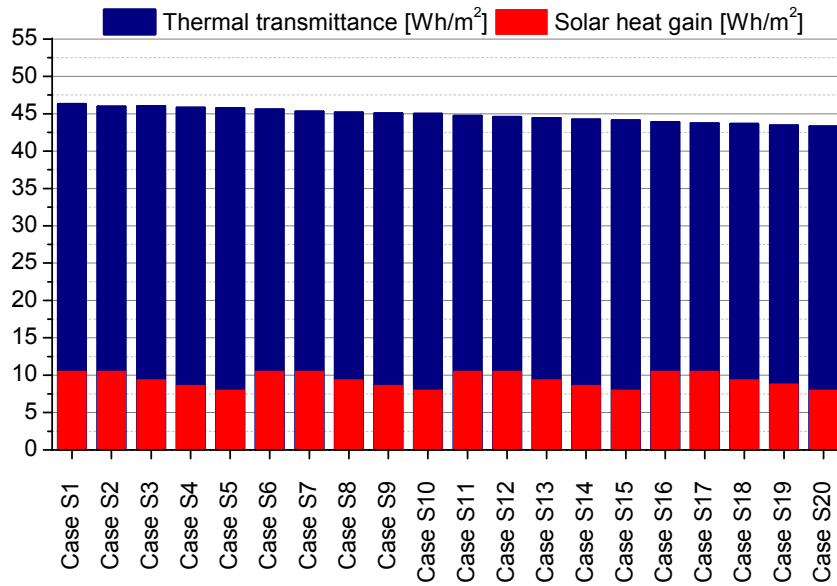


Figure 4.4-7. Hourly solar heat gain and thermal transmittance of south-facing double-skin façade

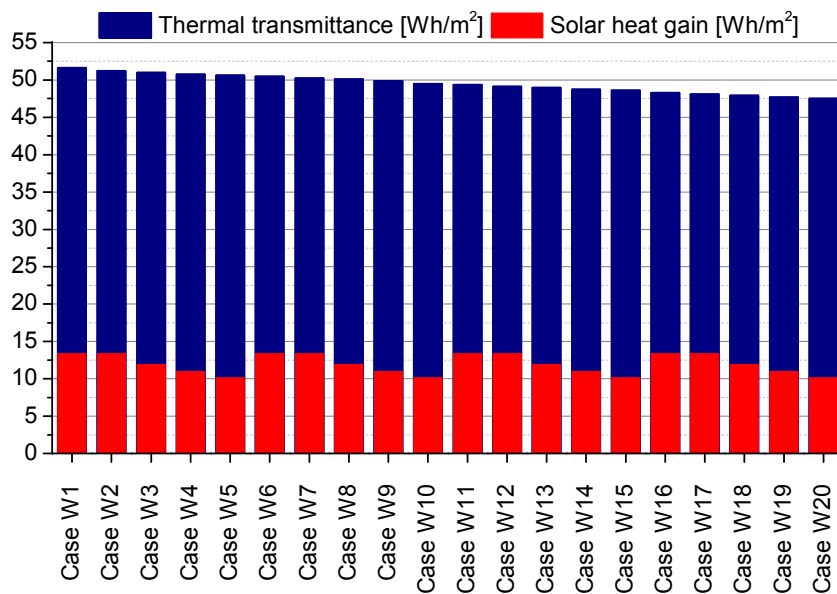


Figure 4.4-8. Hourly solar heat gain and thermal transmittance of west-facing double-skin façade

In contrast, the distance between the outer and inner glass skins of the double-skin façade strongly influences the thermal transmittance. As can be seen in Figure

4.4-5 until Figure 4.4-8, the double-skin cases with an 80 cm distance between the outer and inner glass have a higher thermal transmittance indication. A substantial reduction in thermal transmittance is achieved at a distance of 200 cm between the outer and inner glass skins, while the solar heat gain at that distance is nearly constant. Therefore, thermal transmittance appears to affect the load more strongly than the solar heat gain. Furthermore, the thermal transmittance of a double-skin façade is mostly influenced by the distance between the outer and inner glass skin, while the solar heat gain is influenced mainly by the thickness of the glass.

4.5. Thermal Transmittance and Solar Heat Gain of Double-skin Façade in Dry Season

North-facing and west-facing double-skin has been chosen as a reference orientation to examine the performance of thermal transmittance and solar heat gain of double-skin façade during dry season. June 30 has selected as the reference date for north-facing and September 22 for west facing double-skin façade.

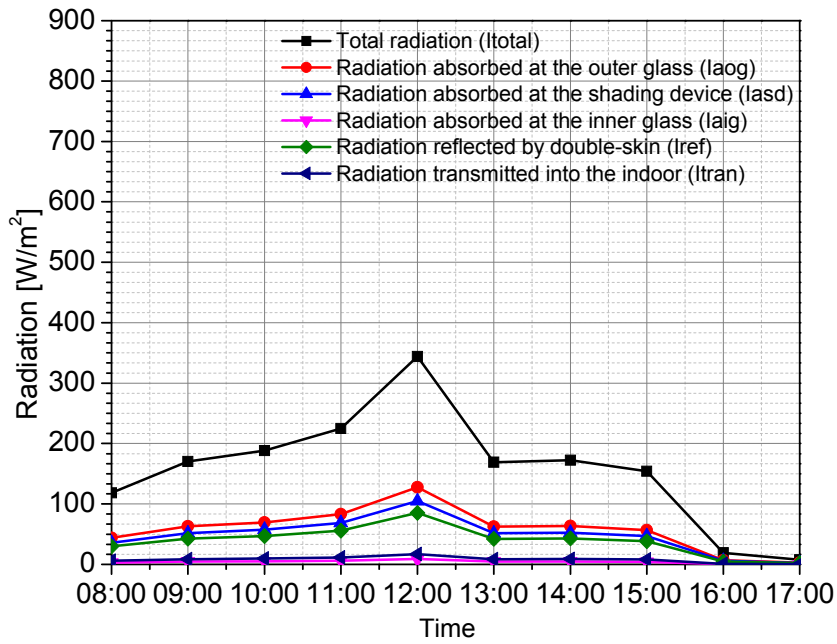


Figure 4.5-1. Solar heat gain at north-facing double-skin façade at June 30

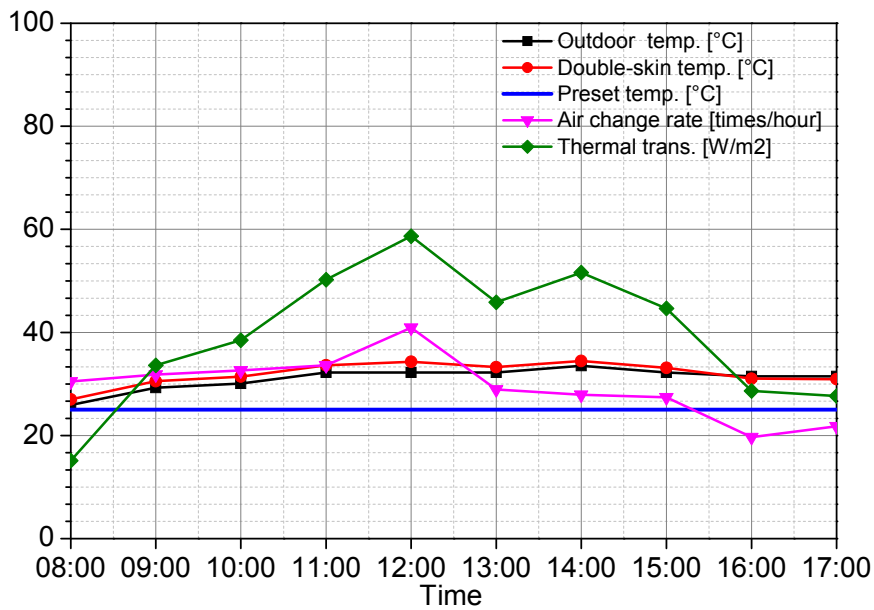


Figure 4.5-2. Thermal transmittance of north-facing double-skin façade at June 30

At June 30 (Figure 4.5-1), total radiation (I_{total}) received by the north-facing double-skin façade is high and up to 343.96W/m^2 at noon (12:00 o'clock).

Approximately, 4.94% of radiation (I_{tran}) was transmitted into the room. Amount of 24.83% of radiation was reflected (I_{ref}), 37.16% was absorbed at the outer glass (I_{aog}), 30.51% was absorbed by shading device (I_{asd}), and 2.56% was absorbed by inner glass (I_{aig}).

At the same time (Figure 4.5-2), maximum outdoor temperature reach to 32.2°C, and temperature inside double-skin was 34.9°C. With the air change rate 40.9 times per hour, the thermal transmittance was reach to 58.68W/m².

Figure 4.5-3 shows a detail of heat-transfer through double-skin. It can be seen that temperature of outer glass (θ_{og}), temperature of shading device (θ_{sd}) and temperature of inner glass (θ_{ig}) was raised and higher at the top of double-skin. Lower thermal transmittance was at 1st floor (segment 1 to segment 2) and higher thermal transmittance was at 5th floor (segment 9 to segment 10). The shading device and the inner glass could reduce heat-transfer up to 3.02 W/m² in the average.

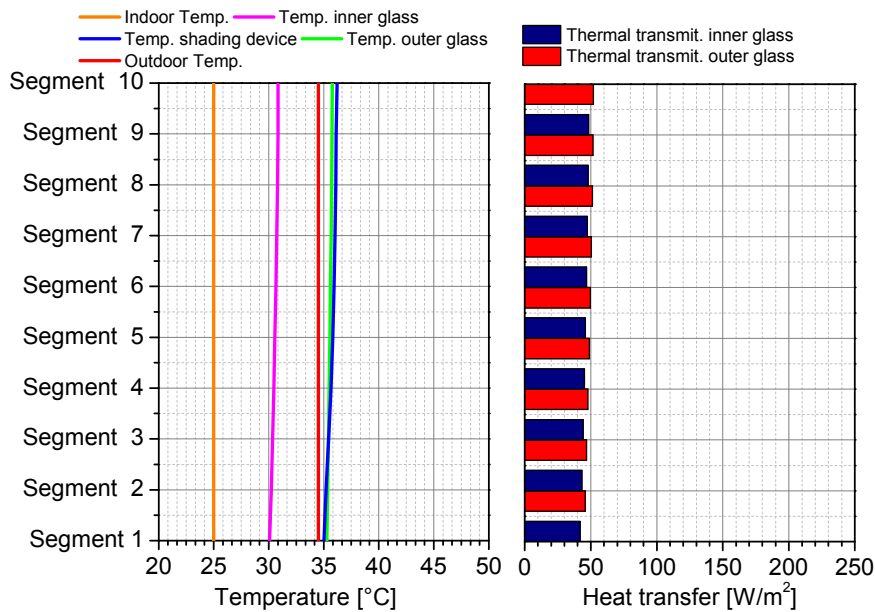


Figure 4.5-3. Heat transfer of north-facing double-skin façade at 12:00 of June 30

At September 22, when the sun position is near to the equator, as the representative date of west-facing double-skin façade, total radiation (I_{total}) received by west-facing double-skin façade is higher in the afternoon at 14:00 o'clock (540.45W/m^2). Approximately 4.30% of radiation was transferred into the room (I_{tran}). About 24.82% of radiation were reflected (I_{ref}), 37.97% were absorbed by the outer glass (I_{aog}), 30.73% was absorbed by shading device (I_{asd}), 2.17% of radiation was absorbed by the inner glass (I_{aig}) (see Figure 4.5-4).

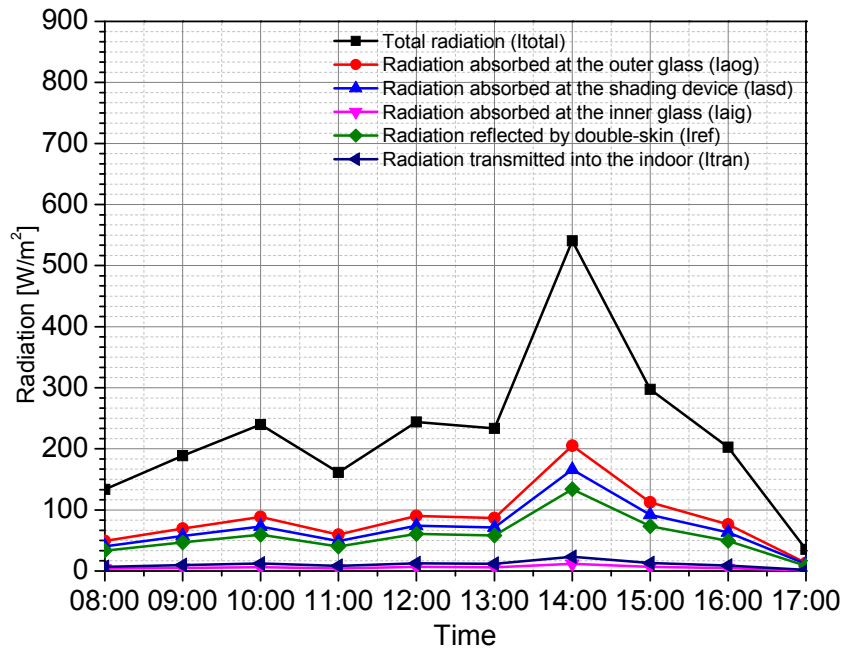


Figure 4.5-4. Solar heat gain of west-facing double-skin façade at September 22

Meanwhile, in this reference date (see Figure 4.5-5), outdoor temperature was reach to 35.7°C higher than north-facing double-skin. The temperature inside double-skin façade was reach to 38.6°C , higher than temperature outside, with the air change rate was 47.9 times per hour, the amount of thermal transmittance through double-skin at that time was 86.75W/m^2 .

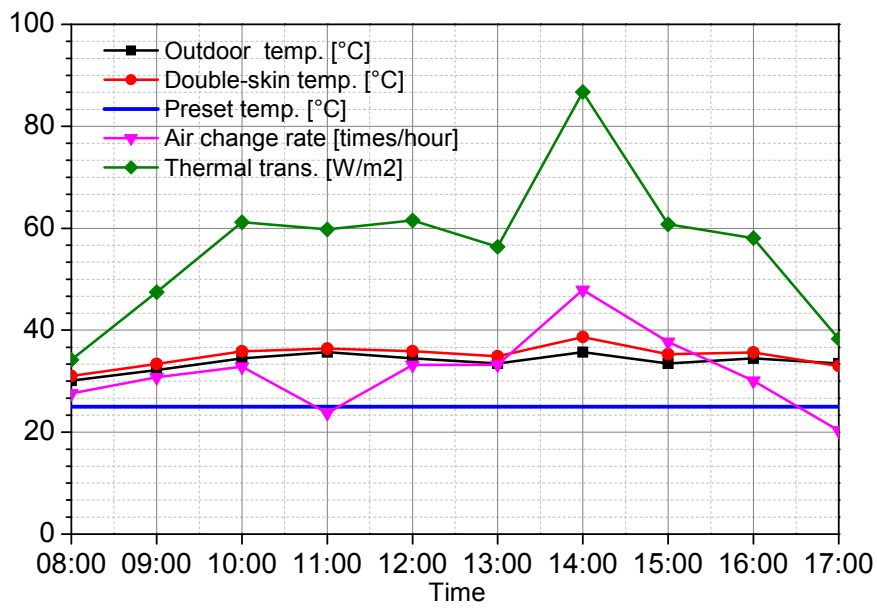


Figure 4.5-5. Thermal transmittance of west-facing double-skin façade at September 22

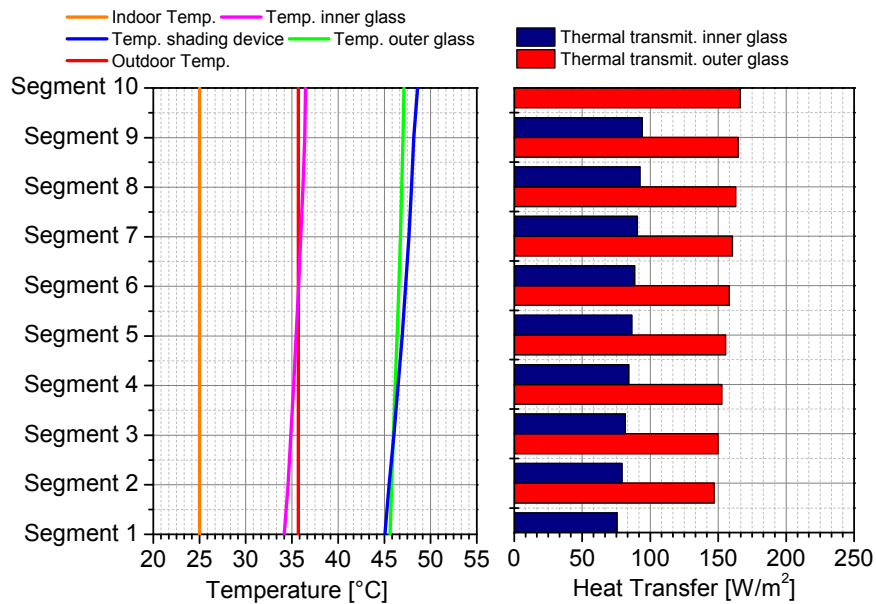


Figure 4.5-6. Heat transfer of west-facing double-skin façade 14:00 of September 22

As can be seen in Figure 4.5-6, temperature of the outer glass (θ_{og}), temperature of shading device (θ_{sd}) and temperature of inner glass (θ_{ig}) was raised and higher at the top of double-skin (segment 10). However, with the utilization of shading device and

the inner glass, the amount of heat transmitted into the room can be reduced up to 69.39W/m^2 in the average.

4.6. Thermal Transmittance and Solar Heat Gain of Double-skin Façade in Rainy Season

South-facing double-skin façade on December 30 and east-facing double-skin façade on March 22 has been chosen as reference cases for the rainy season.

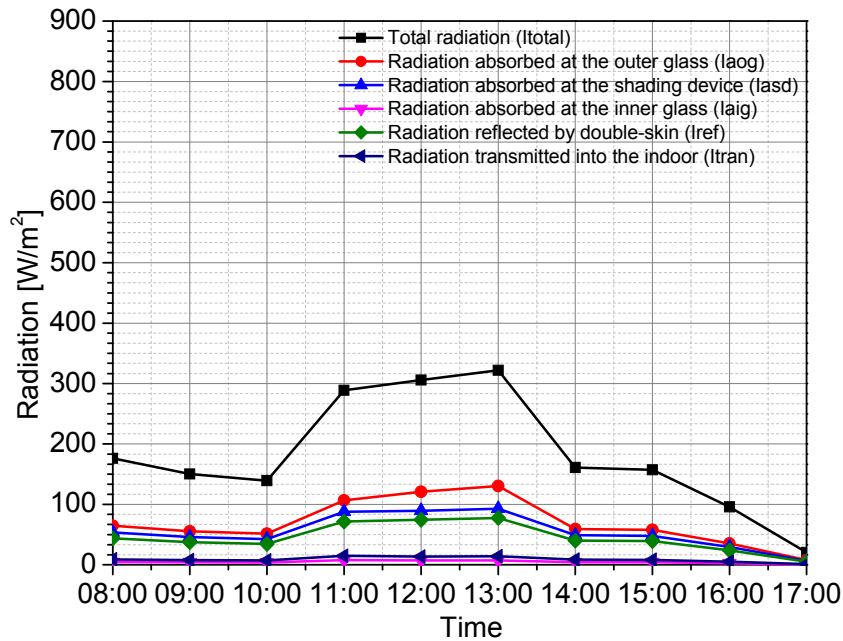


Figure 4.6-1. Solar heat gain of south-facing double-skin façade at December 30

At the south-facing double-skin façade, approximately 4.37% of radiation (I_{total}) was transmitted into the room. About 24.07% of radiation were reflected (I_{ref}), 40.45% were absorbed in the outer glass (I_{aog}), 28.82% was absorbed in the shading device (I_{asd}), and only 2.29% was absorbed in the inner glass (I_{aig}) (see Figure 4.6-1). Outside

temperature was reached 33.5°C, temperature inside double-skin was rising to 33.9°C, and air change rate was 35.9 times per hour. The amount of heat transmitted into the room was 59.32W/m² (Figure 4.6-2).

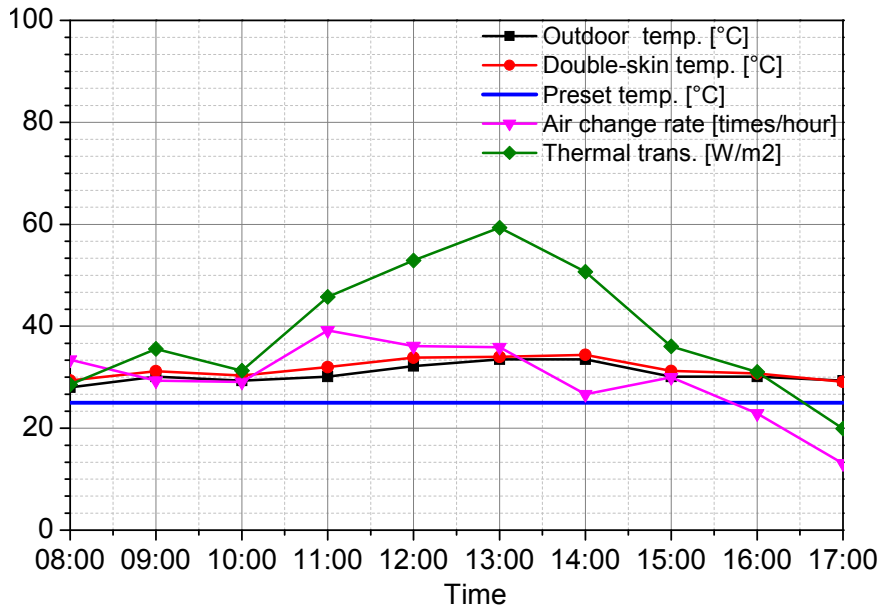


Figure 4.6-2. Thermal transmittance of south-facing double-skin façade at December 30

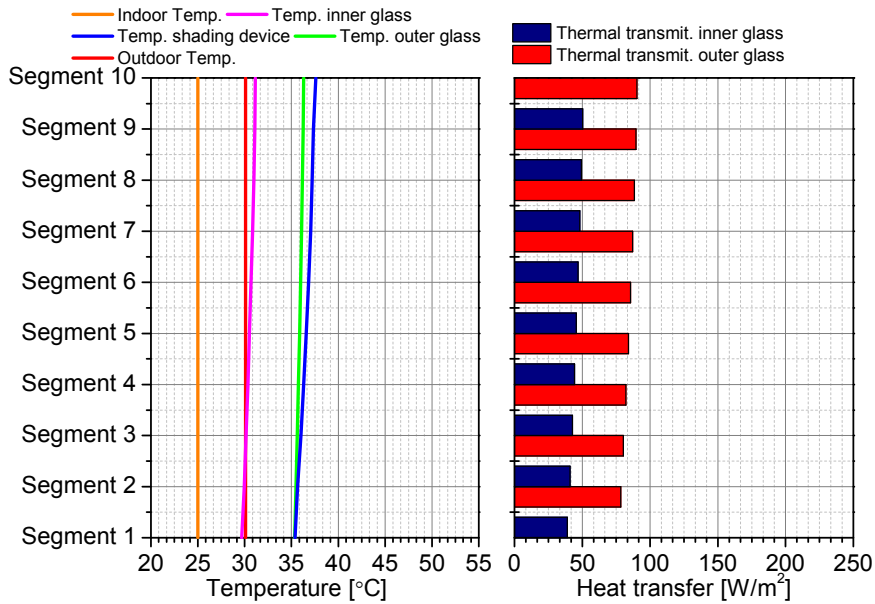


Figure 4.6-3. Heat transfer of south-facing double-skin façade at 13:00 of December 30

Figure 4.6-3 shows the heat transfer on south-facing double-skin façade at 13:00 of December 30. It is expectable that temperature inside the double-skin façade will rise to the top of double-skin. In this orientation, the amount of heat transmitted into the room can be reduced to approximately 38.46% in the average.

The amount of solar heat gain received in the east-facing double-skin seems to be higher at 12:00 of March 22. In this time, total radiation (I_{total}) was 301.55W/m². However, looks like double-skin façade was working properly in this orientation. The amount of radiation transmitted (I_{tran}) into the room was 6.07%. The amount of solar radiation reflected (I_{ref}) was 27.4%. The amount of solar radiation absorbed in the outer glass (I_{aog}) was 31.09%. Solar radiation absorbed in the shading device (I_{asd}) was 32.99%, and solar radiation absorbed in inner glass (I_{aig}) was 2.44% (see Figure 4.6-4).

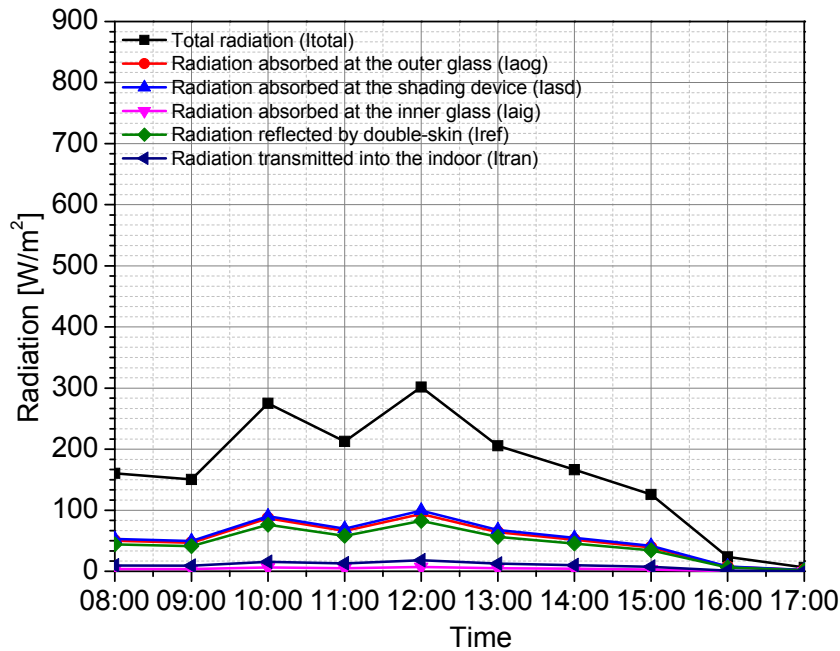


Figure 4.6-4. Solar heat gain of east-facing double-skin façade at March 22

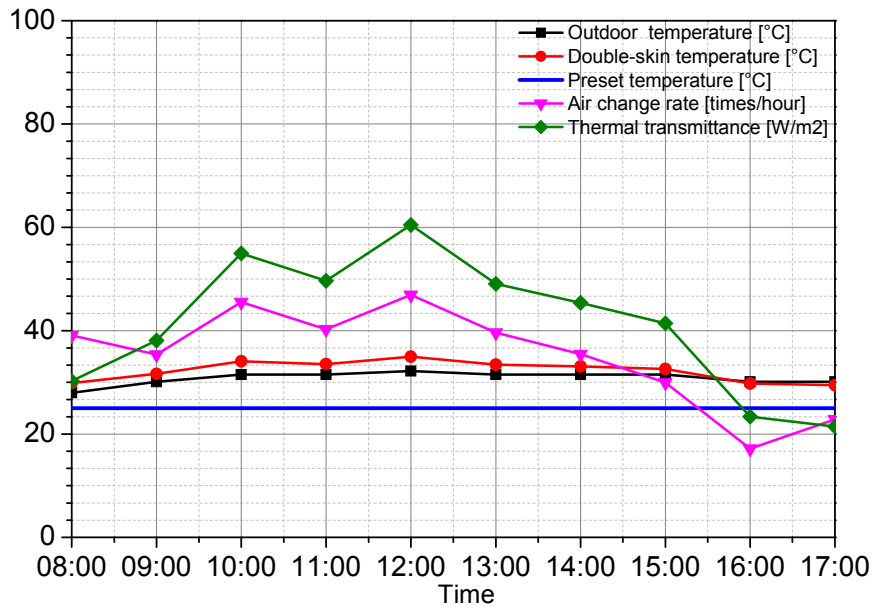


Figure 4.6-5. Thermal transmittance of east-facing double-skin façade at March 22

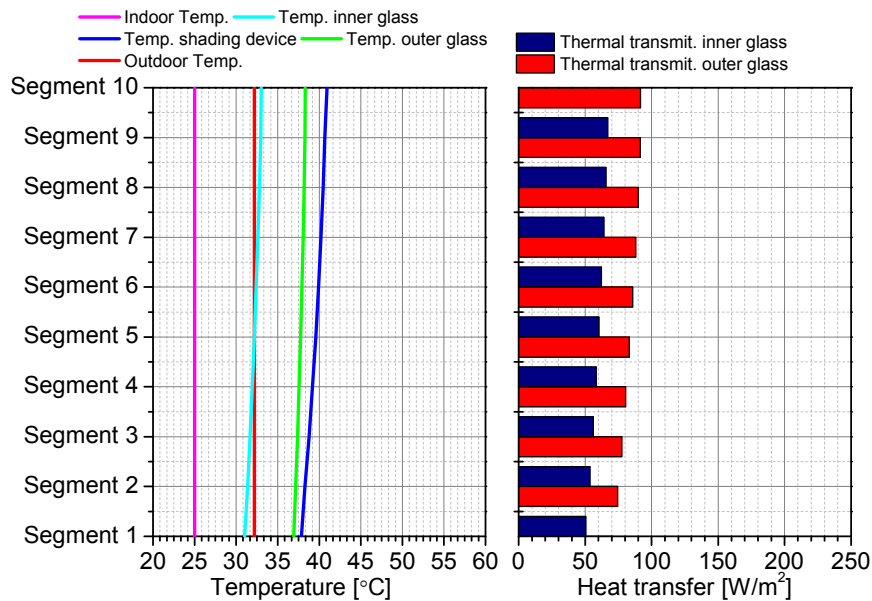


Figure 4.6-6. Heat transfer of east-facing double-skin façade at 12:00 of March 22

At the same time, thermal transmittance was also raised to 60.46W/m^2 as the consequence of the rise of outdoor temperature that also makes the temperature inside double-skin was raised (Figure 4.6-5). Temperature of outdoor was 32.2°C and

temperature of inside double-skin was 34.96°C. The amount of air change rate was 47 time per hour.

In detail (Figure 4.6-6), the maximum heat transmitted in outer glass was 91.65W/m², and in the inner glass was 67.44W/m². The amount of heat transmitted into the room could be reduced up to 23.5W/m² in the average. Since the temperature inside double-skin was raised from 1st floor to 5th floor, the amount of heat-transfer also raised from segment1 to segment 10. Approximately 1 W/m² of heat was raised on each segment.

4.7. Possibility of Condensation

Furthermore, it is important to analyze the possibility of condensation at the outer surface of inner glass of double-skin since during the rainy season the humidity is high. Calculation had been performed during operation time of building from 08:00 to 17:00 with indoor setup temperature was 25°C. The result found that there is no possibility of condensation, which can be occurred during operation time.

Figure 4.7-1 and Figure 4.7-2 shows the condition of double-skin during the rainy time on January 3. Temperature of the outer surface of the inner glass was nearly the same with the outdoor temperature in the morning and afternoon. However, at that time, temperature of the outer surface of inner glass of double-skin was not reached saturated point, since there was approximately more than 1°C difference to dew point temperature. Condensation occurs when the temperature of air is lowered to its dew point. However, since simulation time was limited to the building operation time, and also there is a tendency of the temperature of outer surface of inner glass to become decrease during the time, there is a possibility of condensation to occur at night.

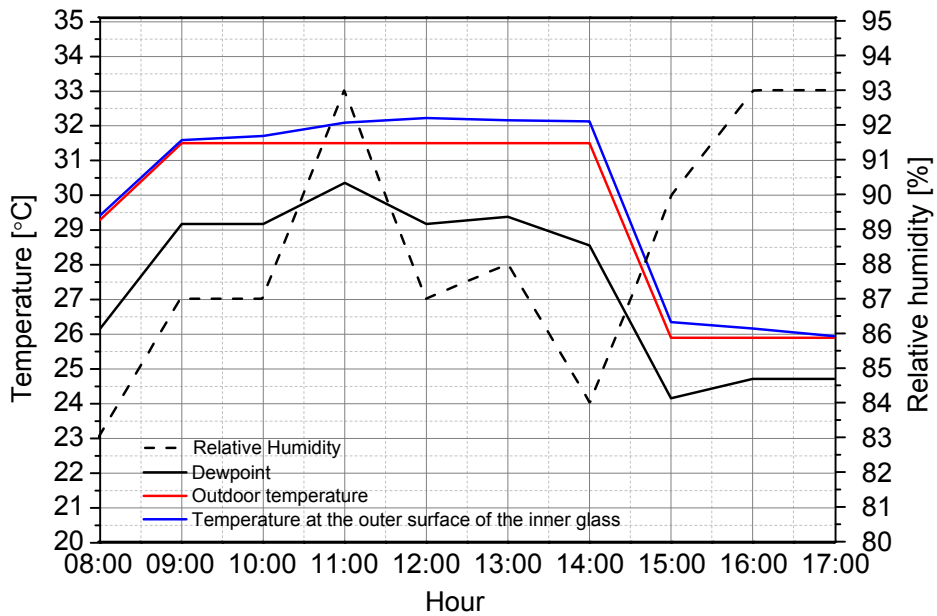


Figure 4.7-1. Possibility of condensation at rainy season

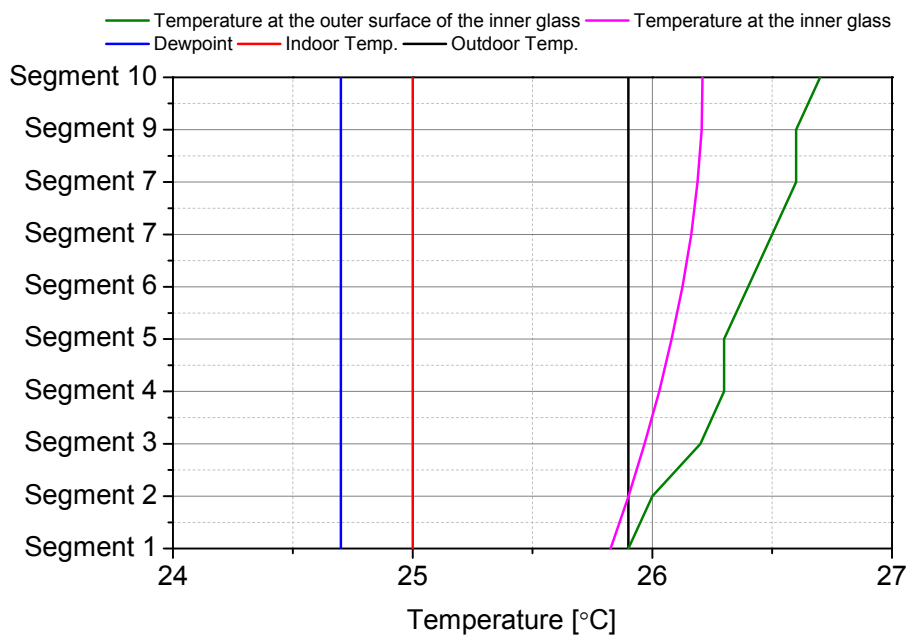


Figure 4.7-2. Detail of possibility of condensation

4.8. Comparison of Thermal Transmittance and Solar Heat Gain among Double-skin and Single-skin Façades

To find out the effectiveness of a double-skin façade in hot and humid climate, the thermal transmittance and solar heat gain were compared with those of single-skin and pair glass window system. The cases that were used to compare the double-skin façade the single-skin and pair glass window system can be seen at section 4.2. The models of the double-skin, single-skin, and pair glass façades and their orientations were the same, except for the glass properties. The properties of the single-glass and pair glass façade that were used for the comparison are based on those commonly used in buildings in Indonesia. Through this comparison, the benefits of a double-skin façade in reducing the heat gains can be identified.

The single-skin façades have the following properties:

- a. Float glass with light-colored inner blinds (FL+BD) – the shading coefficient is 0.55, and the overall heat-transfer coefficient is 4.8 [W/m²·K].
- b. Double-glazed glass with 6 mm air layer, equipped with light-colored inner blinds (ML+BD) – the shading coefficient is 0.54, and the overall heat-transfer coefficient is 3.0 [W/m²·K].
- c. Highly insulated double-glazed glass with 6 mm air layer, equipped with light-colored inner blinds (HF+BD) – the shading coefficient is 0.34, and the overall heat-transfer coefficient is 2.2 [W/m²·K].

The result can be seen at Figure 4.8-1 until Figure 4.8-4. As seen in Figure 4.8-1 until Figure 4.8-4, double-skin façades have higher thermal transmittance but lower in solar heat gain in comparison with single-skin and pair glass façades. On the other hand,

the single-skin façades have higher solar heat gain but lower thermal transmittance. Through this comparison, it can be stated clearly that the heat gain can be reduced by more than 50% through the use of a double-skin façade instead of a single-skin façade. In the case of single-skin façades, more than 80% of the heat gain is by solar radiation and less than 20% is by thermal transmittance.

This was different from the heat gain values seen in the double-skin façades. In contrast, for the double-skin façades, approximately 80% of the solar heat gain due to orientation was caused by thermal transmittance and about 20% was caused by the solar heat gains. However, since there was a large reduction in the solar heat gain, the overall heat gain of the double-skin façade was lower than that of the single-skin façade. This result indicates that the double-skin façade is applicable and can be more beneficial in reducing the façade heat gain in the hot and humid areas such as Indonesia.

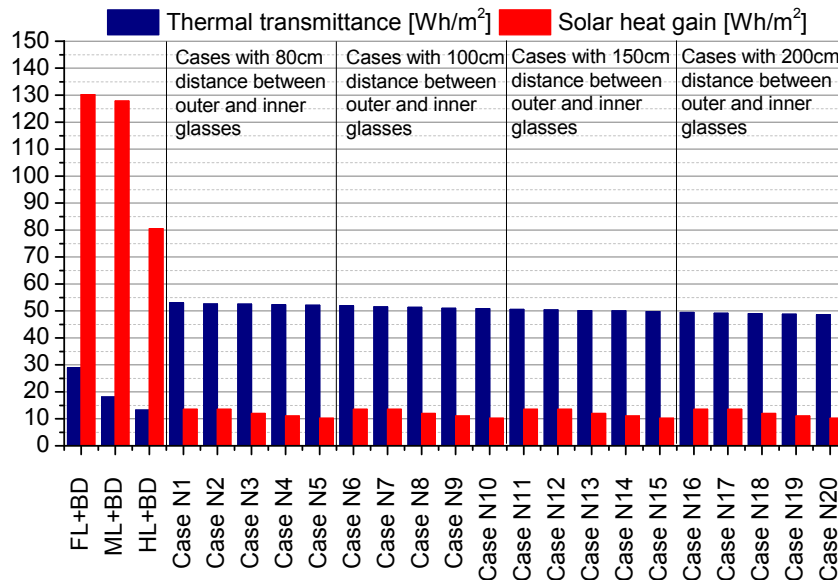


Figure 4.8-1. Comparison of hourly thermal transmittance and solar heat gain among north-facing double-skin and single-skin façades

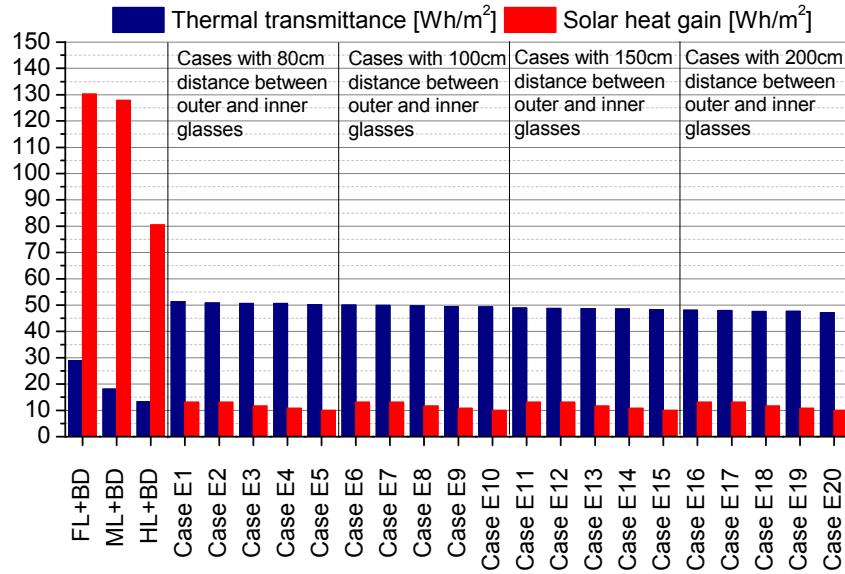


Figure 4.8-2. Comparison of hourly thermal transmittance and solar heat gain among east-facing double-skin and single-skin façades

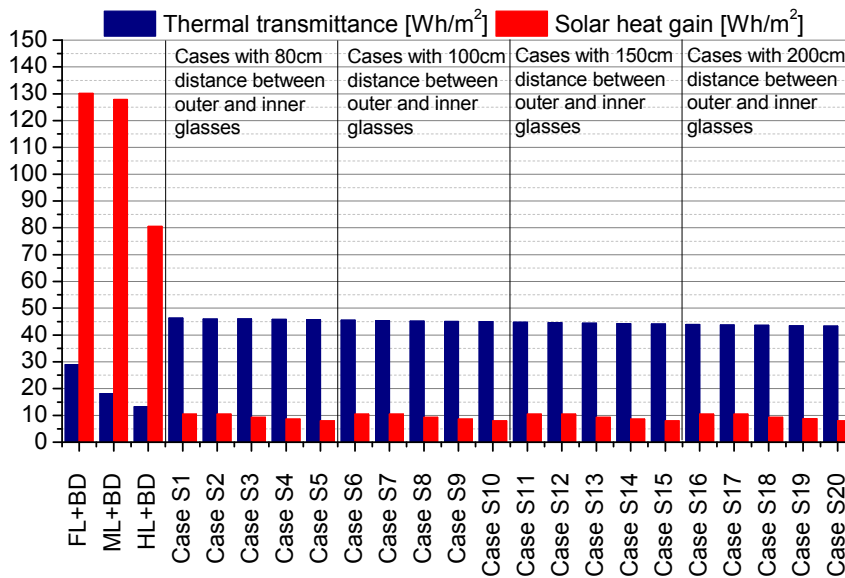


Figure 4.8-3. Comparison of hourly thermal transmittance and solar heat gain among south-facing double-skin and single-skin façades

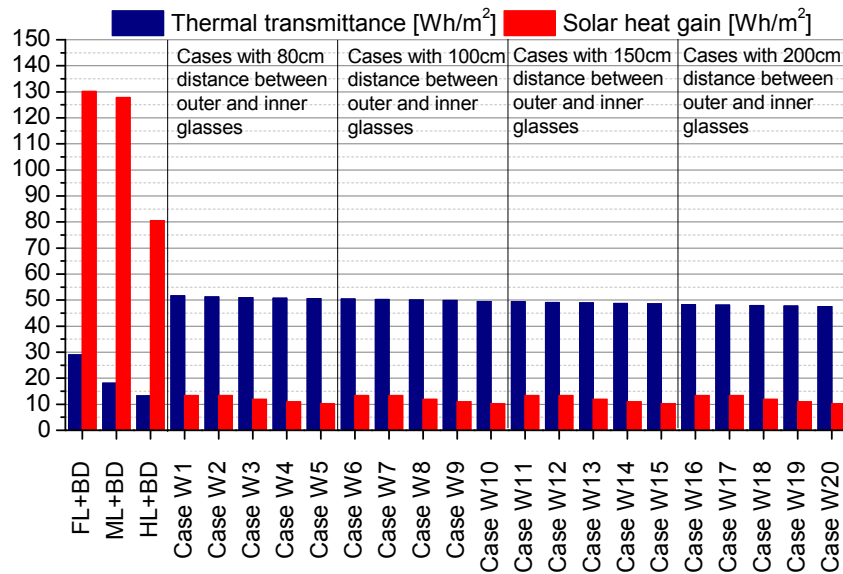


Figure 4.8-4. Comparison of hourly thermal transmittance and solar heat gain among west-facing double-skin and single-skin façades

In comparison among double-skin façade cases, the same outer and inner glasses combination has an equal heat gain value for the same outer and inner glasses distance. For example, the heat gain value of the combination of 10mm thickness of outer glass and 8mm thickness of inner glass for the 80cm distance between outer and inner glasses has the same value with other of 10mm thickness of outer glass and 8mm thickness of inner glass of the 100cm, 150cm, and 200cm glasses distances. The combination of 10mm thickness of outer glass and 6mm thickness of inner glass has the higher solar heat gain, and the combination of 12mm thickness has the lower solar heat gain among cases. It seems the higher glass thickness combination, the lower solar gain in double-skin façade.

Furthermore, among the double-skin façade cases, the thermal transmittance was slightly decreased due to the wider distance and the higher thickness between the outer and the inner glasses. The narrower distance and the smaller thickness of inner and

outer glasses resulted higher thermal transmittance. As can be seen on the cases of 10mm thickness of outer glass and 6mm thickness of the inner glass with the distance of 80cm distance of glasses has the higher thermal transmittance. The lower thermal transmittance among double-skin façade cases was found on the combination of 12mm thickness of the outer and the inner glasses with the distance of 200cm between the outer and the inner glass.

4.9. Effect of Solar Inclination Angle to the Solar Heat Gain of Double-skin Façade

Indonesia is located in the tropics and crossed by the equator. As the consequence, the solar altitude could reach higher degree of incidence angle (see Figure 4-9.1). For example, the solar altitude at latitude 5° South will reach the higher position at 88.7° on October 9 at 12:00 o'clock, and at 89.1° on March 8 at 12:00 o'clock.

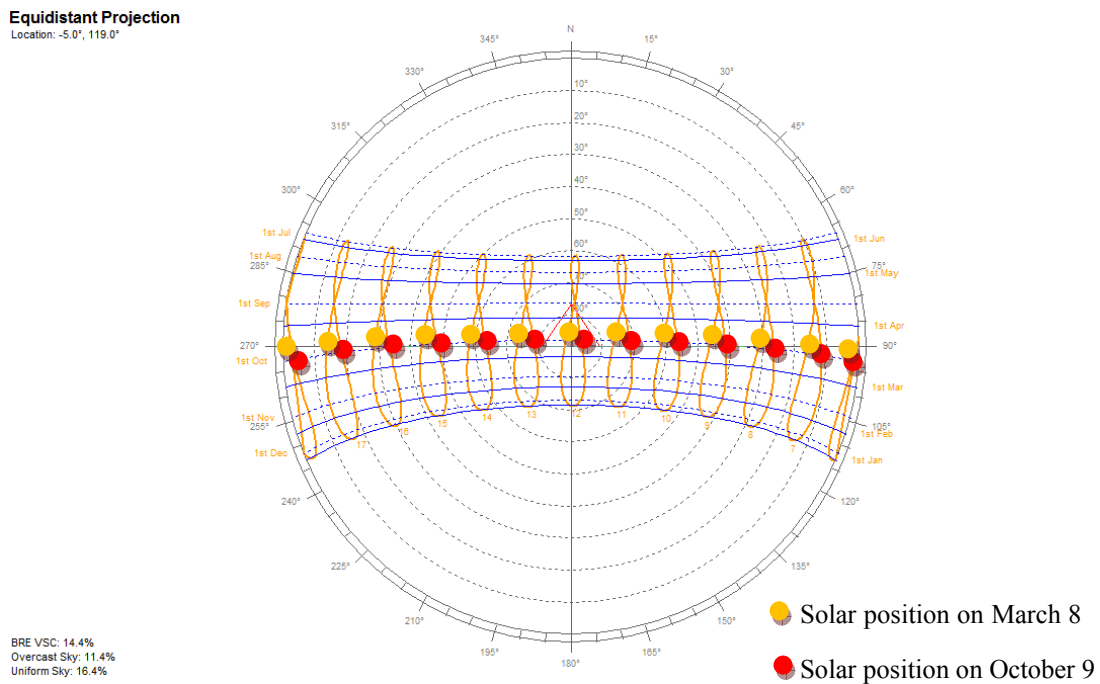


Figure 4.9-1. Sun-pat diagram at 5° south latitude

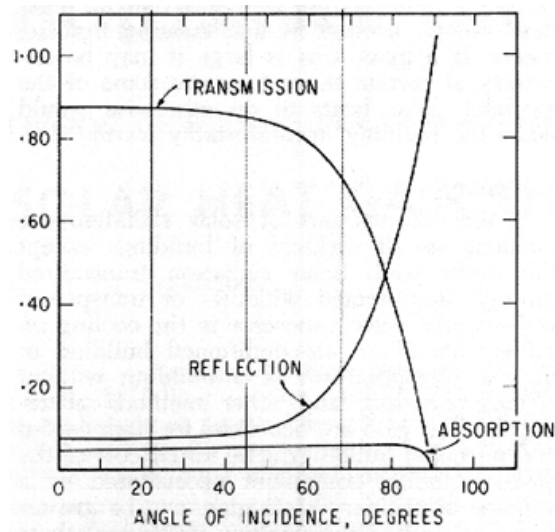


Figure 4.9-2. Variation of reflection, absorption and transmission of solar radiation by a single glass according to the incidence angles ^[41]

The angle of solar incidence affects the amount of solar radiation reflected, absorbed and transmitted by the glass into the indoor. When solar radiation falls on the glass, some of the solar radiation is reflected, some is absorbed by the glass, and some is transmitted into the indoor. Consequently, the higher position of solar altitude is the higher reflection and the lower transmission of solar radiation into the indoor (Figure 4.9-2).

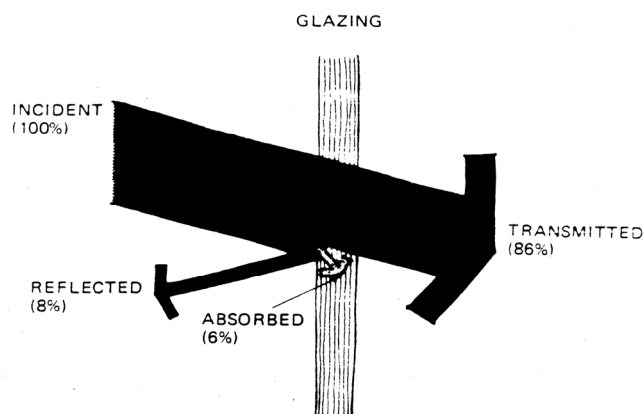


Figure 4.9-3. Percentage of solar radiation reflected, absorbed, and transmitted on a single-glass ^[42]

When solar incidence is perpendicular to the ordinary glass surface, the amount of 8% of solar radiation is reflected, 6% is absorbed and 86% is transmitted by the single glass ^[42] as can be seen at Figure 4.9-3. In pair-glass (double-glass), the outer glass could reflect 8%, and absorbs 6% of solar radiation. The inner glass could reflect 7%, and absorbs 5% of solar radiation. The rest of solar radiation is 74% transmitted into the indoor (see Figure 4.9-4).

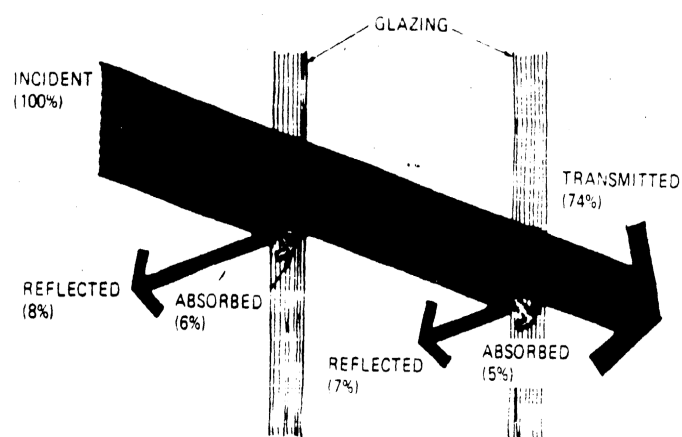


Figure 4.9-4. Percentage of solar radiation reflected, absorbed, and transmitted on a pair-glass ^[42]

The amount of reflectance, absorptance, and transmittance of solar radiation is varying according to the altitude and incident angle of the sun. In double-skin façade, the amount of solar radiation reflected, absorbed, and transmitted are different to the outer glass, shading device, and inner glass.

As can be seen at Figure 4.9-5 and Figure 4.9-8, variation of the reflectance of solar radiation is gradually increase until the angle of incidence reach to more than 70°, and increased rapidly to 100% as the solar incidence is raise when get near to 90°.

While, variation of absorptance and transmittance is decrease tend to 0% when the solar incidence is in high position.

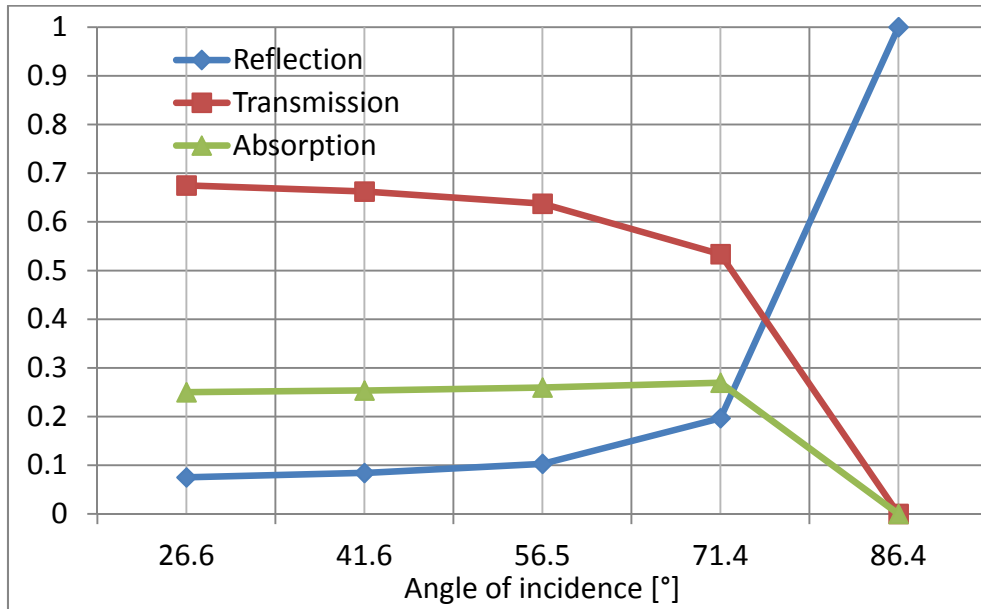


Figure 4.9-5. Variation of reflection, absorption and transmission of solar radiation on the outer glass of a double-skin façade at March 8 according the incidence angles

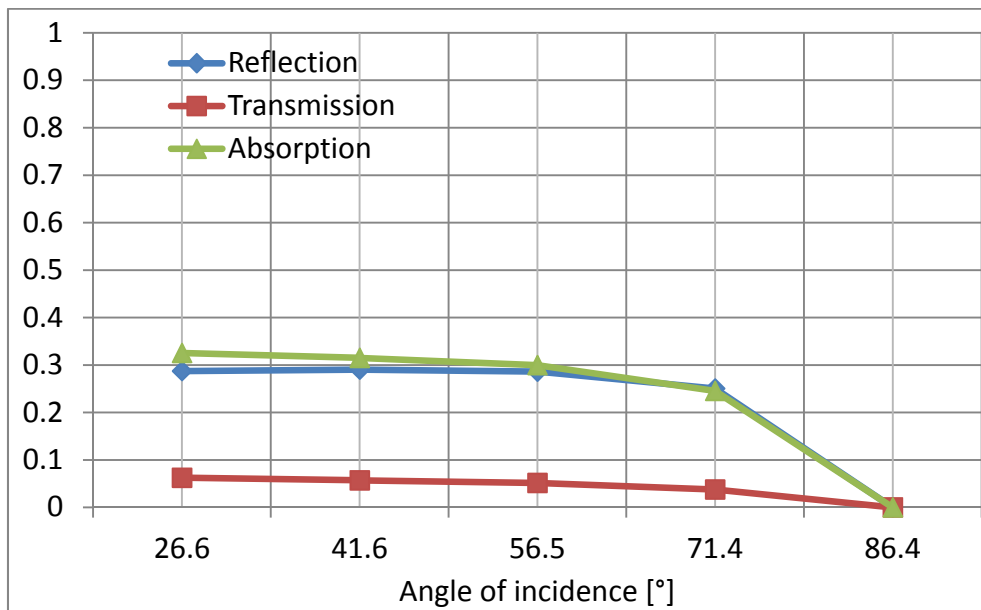


Figure 4.9-6. Variation of reflection, absorption and transmission of solar radiation on the shading device of a double-skin façade at March 8 according the incidence angles

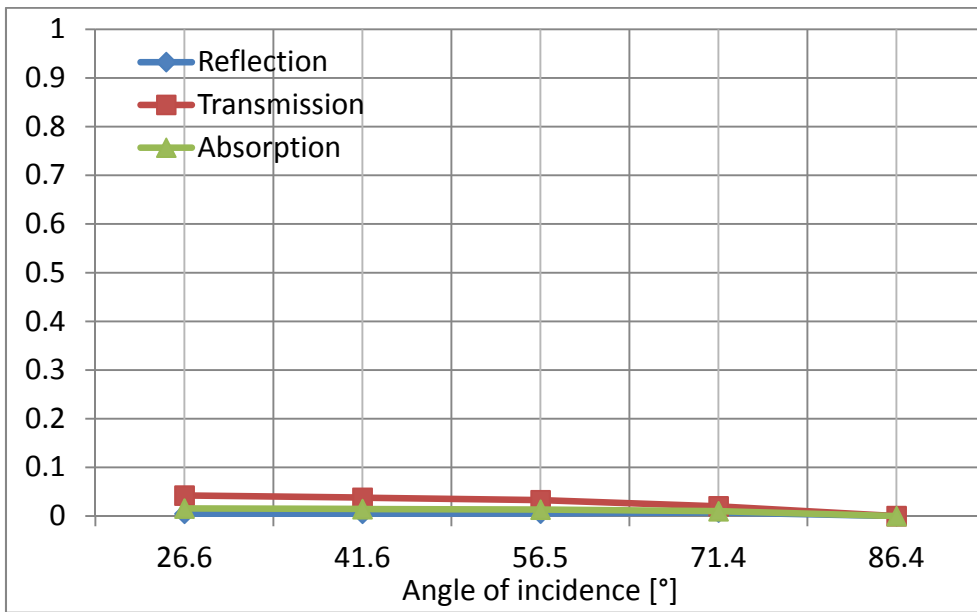


Figure 4.9-7. Variation of reflection, absorption and transmission of solar radiation on the inner glass of a double-skin façade at March 8 according the incidence angles

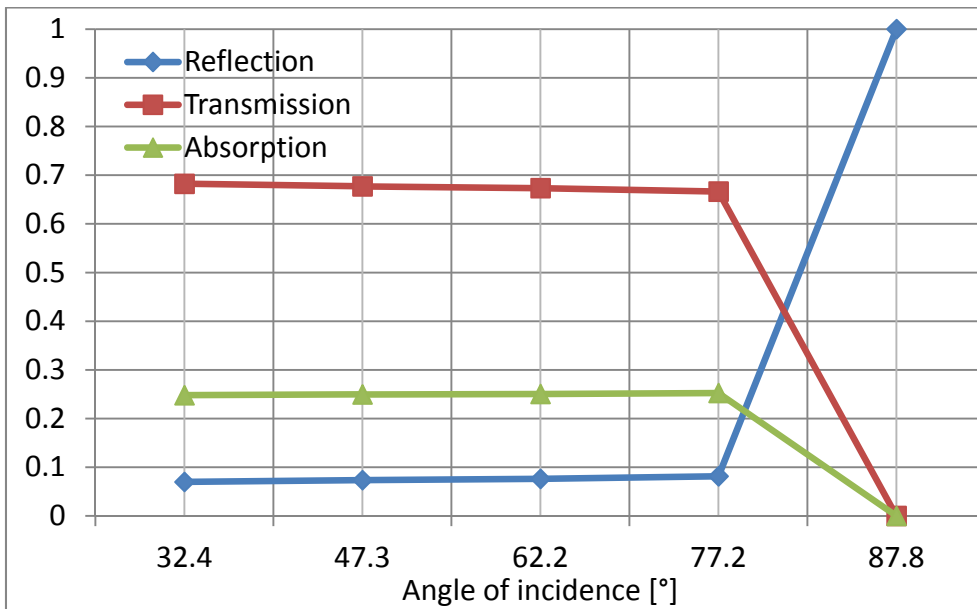


Figure 4.9-8. Variation of reflection, absorption and transmission of solar radiation on the outer glass of a double-skin façade at October 9 according the incidence angles

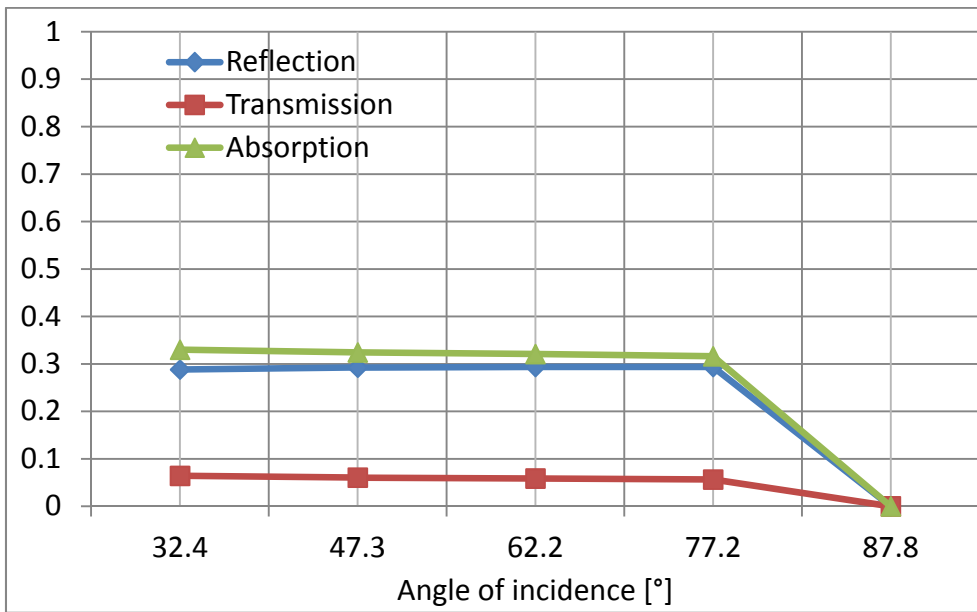


Figure 4.9-9. Variation of reflection, absorption and transmission of solar radiation on the shading device of a double-skin façade at October 9 according the incidence angles

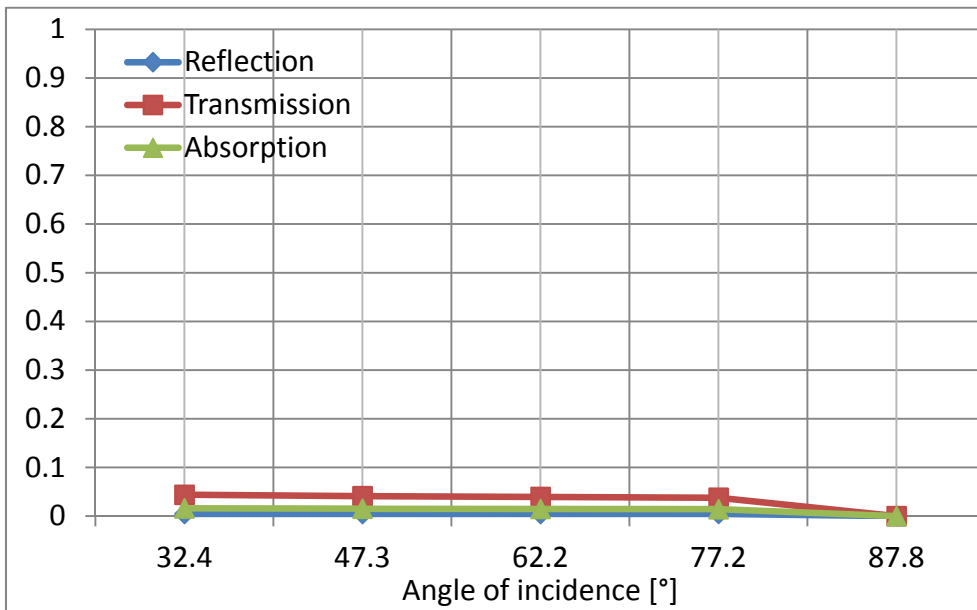


Figure 4.9-10. Variation of reflection, absorption and transmission of solar radiation on the inner glass of a double-skin façade at October 9 according the incidence angles

Variation of reflectance, absorptance, and transmittance of solar radiation on the shading device is slightly different with the outer glass. In the outer glass, large amount of solar radiation is transmitted before the solar incidence reach to more than 70°. In shading device, most of solar radiation is reflected and absorbed (see Figure 4.9-5, Figure 4.9-6, Figure 4.9-8, and Figure 4.9-9). The amount of reflection, absorption, and transmission of solar radiation on the inner glass is relatively low and reach 0% when the solar incidence higher than 80° (refer to Figure 4.9-7 and Figure 4.9-10).

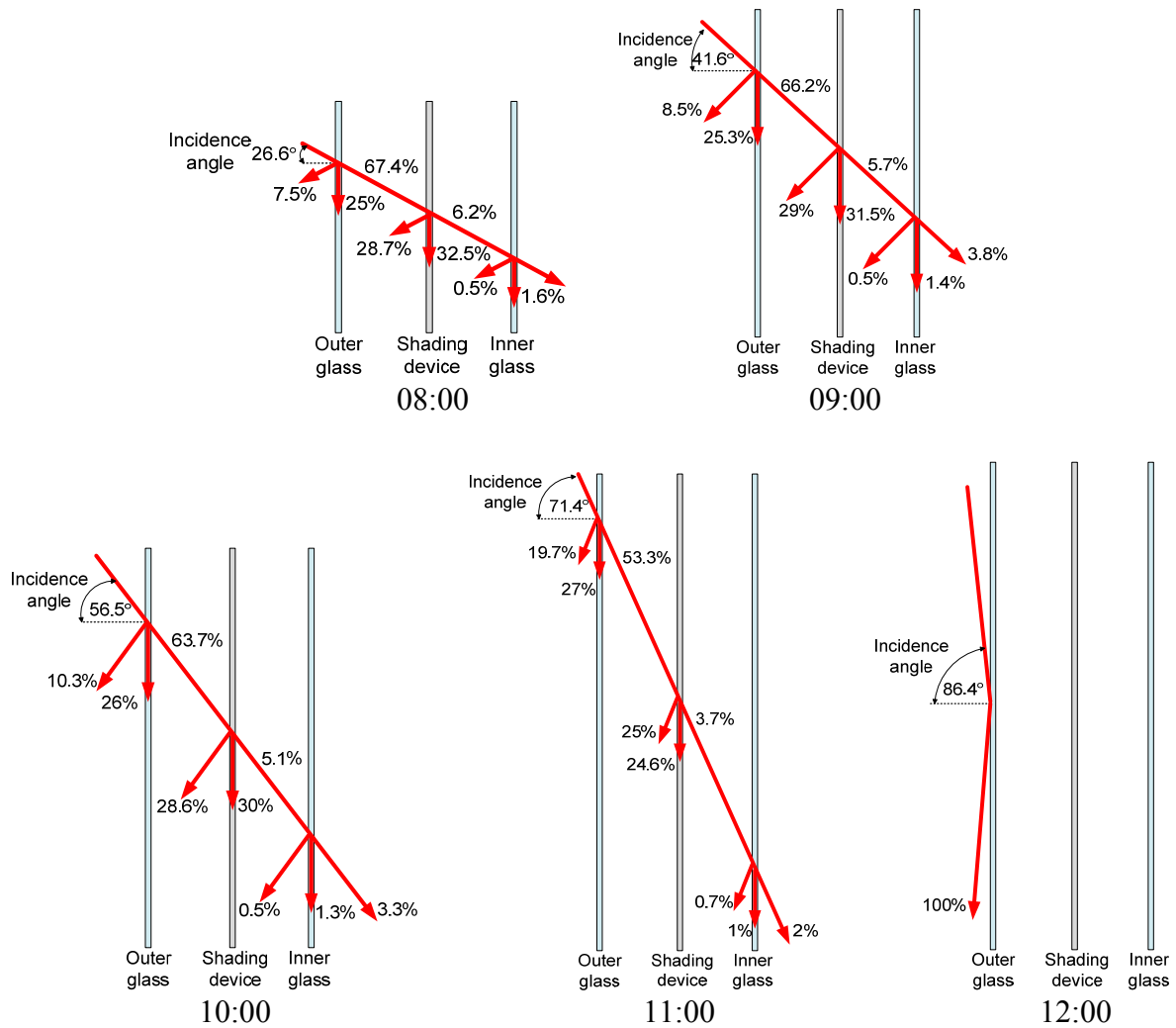


Figure 4.9-11. Percentage of reflection, absorption, and transmission in relation to the time and the angle of incidence of solar radiation on double-skin façade at March 8

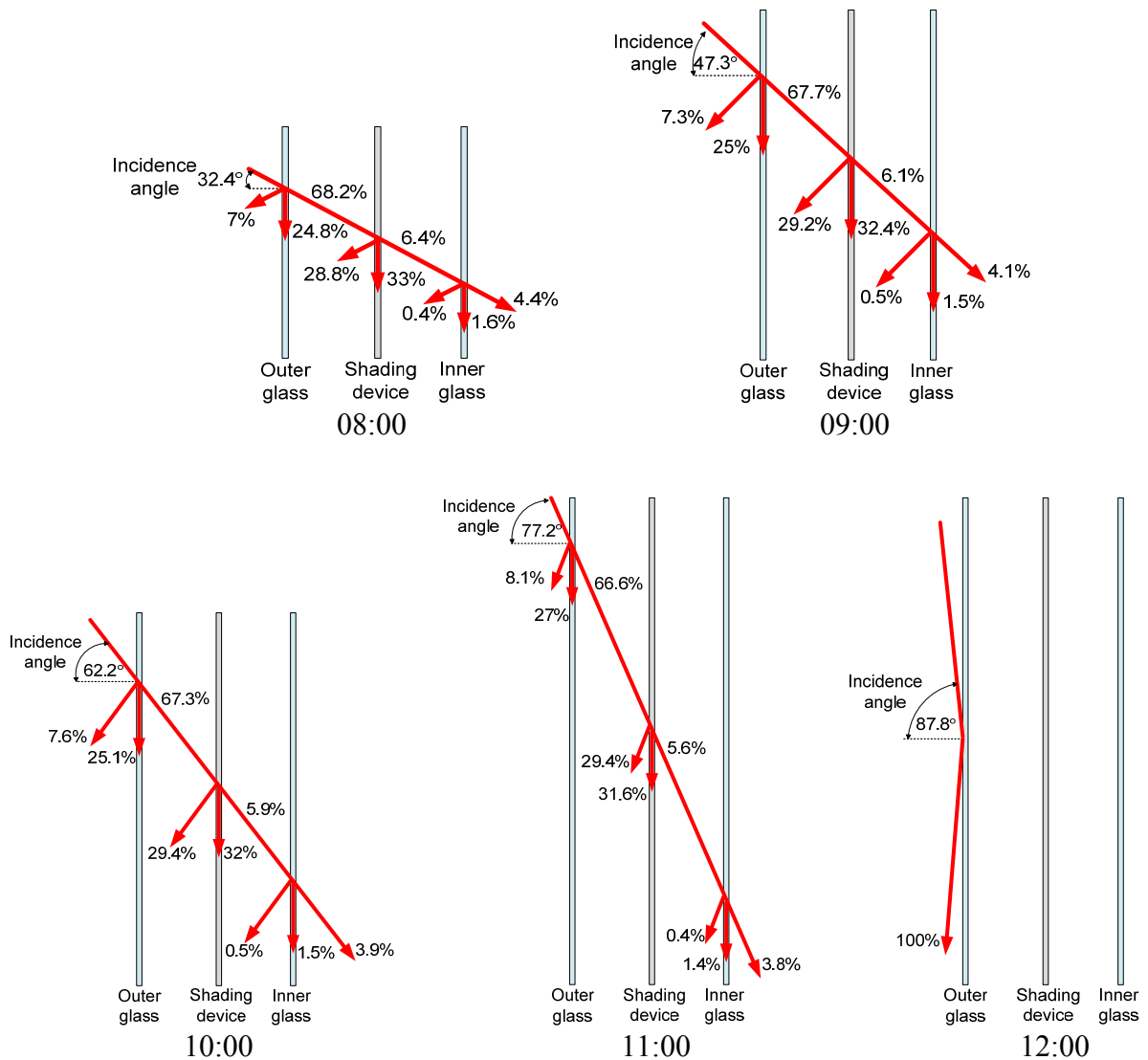


Figure 4.9-12. Percentage of reflection, absorption, and transmission in relation to angle of incidence of solar radiation on double-skin façade at October 9

The percentage of incident solar radiation reflected from the glass depends on the property of the glass and the angle of incidence. As can be seen on Figure 4.9-11 and Figure 4.9-12, percentage of reflected of solar radiation is lowest when the solar incidence at low degree of angle. At the higher degree of incidence angle of solar radiation (87.8°), the solar radiation completely reflected by the outer glass of double-

skin façade without absorbed and transmitted. Reflectance is important in term of solar heat gain because it represent the net heat loss from the indoor.

In double-skin façade, the shading device has the higher percentage of absorption of solar radiation compared to the outer and the inner glasses. Absorbed radiation warms the material (glass and blind) and transmits it by convection into the indoor. The capacity of the material to absorb solar radiation depend on the distance of the radiation has to travel in the material. The outer and the inner glasses have the thinner layer than the shading device, therefore, the outer and the inner glass is less absorption capability than the shading device. Moreover, the traveling distance of radiation in the material also determined by the direction of incident radiation. When the incident angle of radiation is higher, the absorption will increase as the result of distance factor.

Transmission of solar radiation in the outer glass of double-skin is considered higher than transmission in the shading device and the inner glass. The outer glass of double-skin façade relatively transmits more than 60% of solar radiation into the double-skin's cavity. The transmittance of solar radiation will decrease gradually as the solar incident angle increase.

4.10. Summary

The heat gain performance and the thermal transmittance of naturally ventilated double-skin façade models has been simulated, and the cases have been compared with single-skin façade for a hot and humid climate using the case study of Indonesia's climate. It was found that the thermal transmittance was higher than the solar heat gain throughout the year. The double-skin façade was also found to be effective in

minimizing the heat gain by solar radiation compared with single-skin and pair glass window system.

In comparison among double-skin façade cases, selecting a suitable combination of inner and outer glass skin thickness was useful for reducing the solar heat gain. Although there was only slight difference in thermal transmittance could be achieved, the distance between the outer and inner glass skins is an important factor for reducing thermal transmittance in a double-skin façade system.

Moreover, the double-skin façade also exhibited the best performance at reducing the solar heat gain when compared with a single-skin façade. More than 50% of heat gain can be reduced when using a double-skin façade.

In addition, during the rainy season the humidity is increase. Calculation has been performed during operation time of building from 08:00 to 17:00 with indoor setup temperature was 25°C. The result found that there is no possibility of condensation, which can occur during building operation time.

Moreover, reflectance, absorption, and transmission of solar radiation in double-skin façade are varying based on the angle incidence of solar radiation. When the angle of incidence is lower than 70°, the percentage and absorptance of the solar radiation increased gradually, while the percentage of transmission decreased gradually. The percentage of reflected solar radiation will increase rapidly and percentage of absorbed and transmitted solar radiation will decrease rapidly when the solar incidence angle higher than 70°.

In future work, it will be necessary to extend the simulation to take into account several glass properties, including glass coatings, to determine the performance of double-skin façades in reducing the heat gain.

**CHAPTER 5. ENERGY PERFORMANCE OF VENTILATED DOUBLE-SKIN
FAÇADE**

The result from previous simulation on five storey ventilated double-skin model (18.5m height, Figure 3.1-1) with various glass combinations and skin distances on four cardinal orientations confirmed the possibility of the application of double-skin façade in Indonesia with advantages in reducing the solar heat gain and thermal transmittance.

Selecting a suitable combination of inner and outer glass thicknesses is useful for reducing the solar heat gain, and the distance between the outer and inner glass is an important factor for reducing the heat gain due to thermal transmittance in a double-skin façade system. Moreover, double-skin façade also exhibited the best performance in reducing solar heat gain when compared to a single-skin façade; more than 50% of heat gain can be reduced. Furthermore, double-skin façade shows satisfactory performance in reducing the external heat gain without condensation forming on the surface of the inner glass during typical building operation hours, even during the rainy season.

5.1. Overview of the Building Model

The simulated building is located in Makassar – Indonesia. Main function of the building is a rental office and consists of 23 storeys (see Figure 5.1-1). Lower ground floor located in the basement and functioned as a parking lot. Ground floor has a function as a main hall, several large-scale office units, and 1st level parking lot. Mezzanine floor functioned as office area units and 2nd level parking lot, as same as 2nd floor. From 3rd floor to 5th floor utilized as office area units, including a parking lot at 3rd floor, cafeteria at 4th floor, and multifunction hall at 5th floor. The 6th floor's function is office area units including roof deck on the back of building. Typical floor from 7th floor to 19th floor is used as rental office units. From 20th floor to 23rd floor also functioned as rental office units. Table 5.1-1 show the list of function and the floor area.



Figure 5.1-1. Views of “Menara Bosowa”

Table 5.1-1. Floor function and area

Floor	Function	Area/floor
Lower ground	Basement, parking	2832.8m ²
Ground floor	Main hall, large office, parking	2244.4m ²
Mezzanine	office area units, 2 nd level parking lot	1923.1m ²
2 nd	Same with Mezzanine	2208.0m ²
3 rd -5 th	Office, parking, canteen, multifunction	2321.7m ²
6 th	Office	2325.1m ²
7 th -9 th	Office	1050.0m ²
10 th -19 th	Rental office	1050.0m ²
20 th -23 rd	Office	681.8m ²

Based on the result of previous simulation, typical floor from 10th to 14th floor and from 15th floor to 19th floor was chosen to be simulated with ventilated double-skin façade attached to the west and east side of the building façade. Figure 5.1-2 show the plan view of typical floor 10th ~ 19th and its zoning.

The typical floor consists of office area units as air-conditioned spaces. The corridor, which is located between the office area units and the core, the core itself, and the outdoor air-conditioning cabin, was considered as non air-conditioned spaces.

The model floor considered to consist of five air-conditioned zones, such as North perimeter zone (NPZ), East perimeter zone (EPZ), South perimeter zone (SPZ), West perimeter zone (WPZ), and Interior zone (IZ). Room temperature set condition for those zones is 25°C. Corridor and the core area are considered as non air-conditioned zones. The property of air-conditioned zones can be found on Table5.1-2.

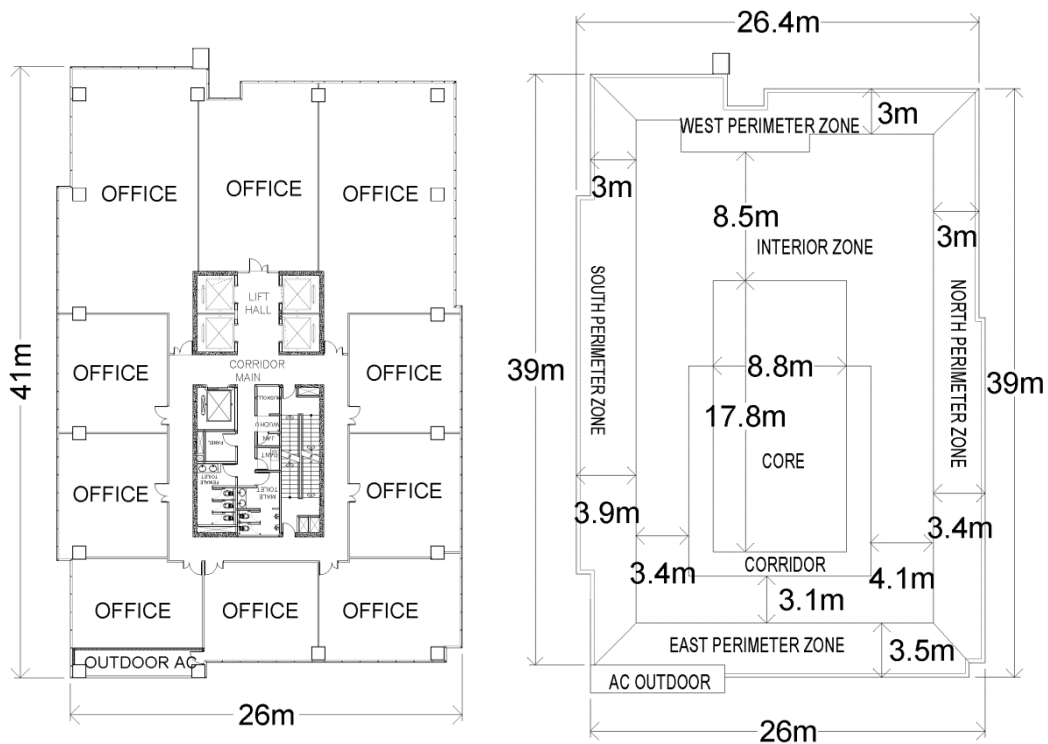


Figure 5.1-2. Plan view of typical floor 10th ~ 19th and its zoning

Table 5.1-2. Zone properties

Zone	Area [m ²]	Volume [m ³]	Occupants [person]
NPZ	104.9	388.2	16
EPZ	69.2	256.2	11
SPZ	120.6	446.2	19
WPZ	70.0	259.0	11
IZ	403.5	1492.8	61
Total	768.2	2842.3	118

5.2. U-value and SC of Double-skin Façade

This section focuses to the calculation of U-value and SC of 12mm thickness of outer and inner glass at the distance of 100cm. This combination of the thickness of the outer and inner glass, and the distance between them is considered is the most effective configuration among all cases that have been simulated in this research.

The calculation of U-value and SC is based upon the equation 3.7-11 and 3.7-12 as described in Section 3.7 of Chapter 3. From this part of calculation, a set of hourly data of U-value and SC has been obtained for one-year duration. Therefore, there is a necessity to define the regression equation in order to define the exact value among of those set of U-value and SC data in relation to the standardized solar radiation (I_G).

The least-square method was used to define the approximation formula of the U-value and SC. In this approximation, the calculated U-value and SC in relation to the standardized solar radiation (I_G) were fitted using the polynomial least-square method as can be seen as follows

$$U = aI_G^b + c \dots\dots\dots \text{Eq. 5.2-1}$$

$$SC = dI_G^e + f \dots\dots\dots \text{Eq. 5.2-2}$$

From those equations (eq. 5.2-1 and 5.2-2) we can formulate the equation of the U-value and SC as can be seen in equation below. The curve fitted polynomial least-square can be seen at Figure 5.2-1 and Figure 5.2-2.

$$U = 1.315I_G^{0.121} + 0.940 \dots\dots\dots \text{Eq. 5.2-3}$$

$$SC = 0.732I_G^{-0.389} + 0,098 \dots\dots\dots \text{Eq. 5.2-4}$$

Finally, based on the equation above the U-value of designated double-skin façade can be obtained by below equation

$$U_{period} = \frac{\sum_{k=1}^m (1.315I_{G,k}^{0.121} + 0.940)(\theta_{o,k} - \theta_{i,k})}{\sum_{k=1}^m (\theta_{o,k} - \theta_{i,k})} = 3.45 \dots\dots\dots \text{Eq. 5.2-5}$$

and the equation and result for the SC is shown in equation below

$$SC_{period} = \frac{\sum_{k=1}^m (0.732I_{G,k}^{-0.389} + 0.098)I_{G,k}}{\sum_{k=1}^m I_{G,k}} = 0.20 \dots\dots\dots \text{Eq. 5.2-6}$$

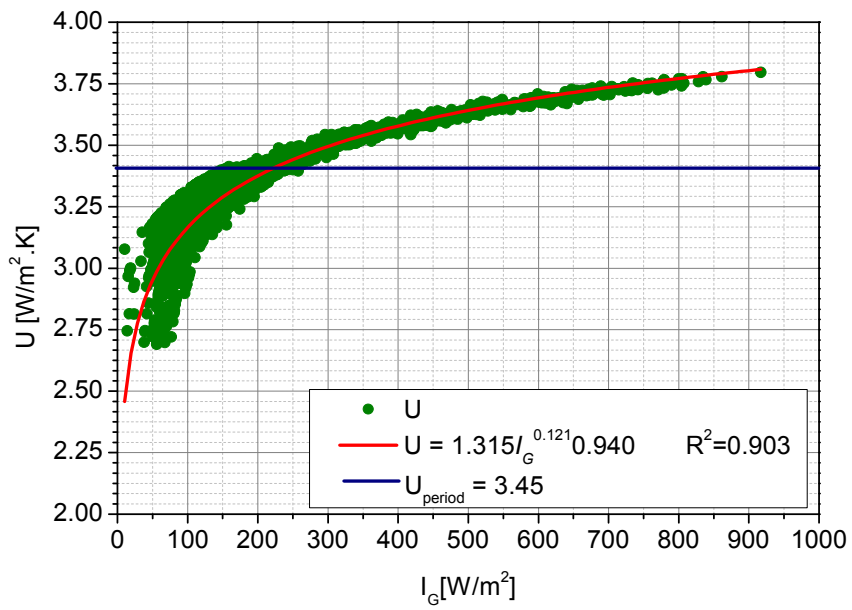


Figure 5.2-1. The relationship between U-value and the standardized solar radiation

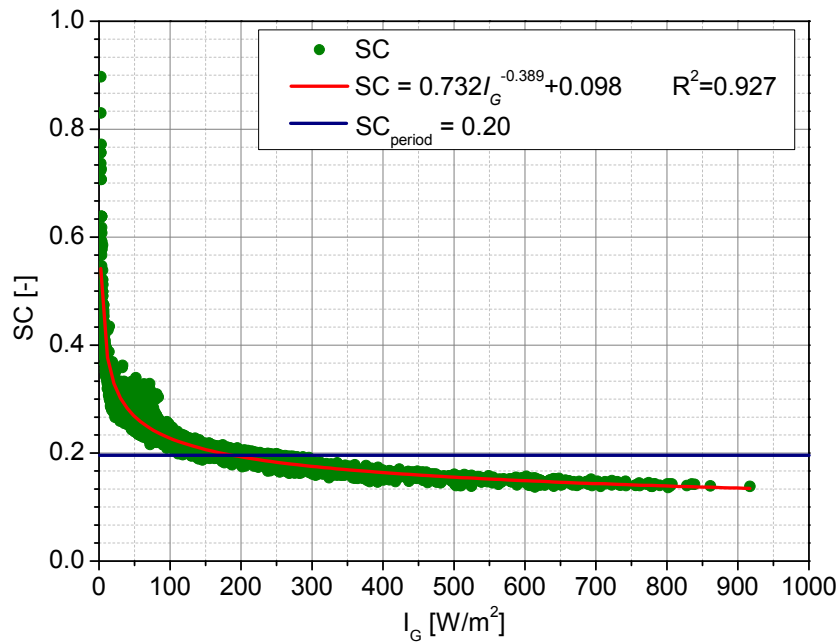


Figure 5.2-2. The relationship between SC and the standardized solar radiation

5.3. Heat Load of Model Building

Heat load of building models was obtained by using MicroHASP/TES version 2.40. The cases are; 8mm single glass, 6mm pair glass, and double-skin façade model, as described in Table 5.3-1, including their U-value and SC. The U-value and SC of double-skin façade were taken from equation 5.2-4 and 5.2-6 respectively, while 8mm single glass and 6mm pair glass was taken from the Nippon Sheet Glass Catalogue 2006-2007. The wall properties can be found at Table 5.3-2.

Table 5.3-1. U-value and SC of window systems

Window type	U-value [W/(m ² ·K)]	SC [-]
8mm single glass	3.6	0.52
6mm pair glass	2.19	0.52
Double-skin façade	3.45	0.20

Table 5.3-2. Wall properties

Wall type	Material	U-value
External wall (1)	Aluminum, Insulation, Airspace	0.43 W/(m ² ·K)
External wall (2)	Bricks, plaster	1.33 W/(m ² ·K)
Partition	Gypsum board, insulation	4.48 W/(m ² ·K)
Internal wall	Concrete, plaster, marble	1.36 W/(m ² ·K)

Moreover, though the single glass and the pair glass would be more benefit if accompanied with an external shading device such as louver or blind, this kind of cases was excluded because there is a possibility of the external shading device to be crashed by the strong wind (storm). The storm sometimes occurs when the season changes from dry season to rainy season. Furthermore, the weather condition of Indonesia is humid, especially in rainy season. Consequently, higher precipitation could cause the shading

device vulnerable to rust. Therefore, external shading device or louver is not commonly used in high-rise building in Indonesia. However, in the future works, external shading device or louver will remain studied.

The room set temperature is 25°C, relative humidity is 50%, and fresh air volume is 30m³/hour/person. All of these cases are considered to have the same indoor thermal conditions, because the heat load calculations of each case were conducted under the same set temperature and humidity. The room set condition was set based on “The guidelines on energy saving for office building” published by Ministry of Energy and Mineral Resources Republic of Indonesia ^[43]. However, their indoor surface temperature might be slightly different due to the window configuration though it would be small. This matter might be produced the different of the thermal indoor environment of radiation; it should be studied in the future.

Moreover, internal heat gains indicated by the activity at the office such as seated light work, and typing. Occupant density is 0.15 person/m² with sensible heat and latent heat produced per occupant is 75Watts. Lighting heat gain is 10 W/m², and OA machine heat gain is 21W/m².

The occupant’s schedule is started from 8:00. From 12:00 - 13:00, it is assumed that 50% of occupants have taking a rest for lunch, praying, and other activities outside office, and use of the light and OA machine reduced to 70% of usage. Workday ends at 18:00. Saturday and Sunday is assumed no activities in the offices. Figure 5.3-1 and Figure 5.3-2 shows the occupancy schedule, lighting and OA machines respectively.

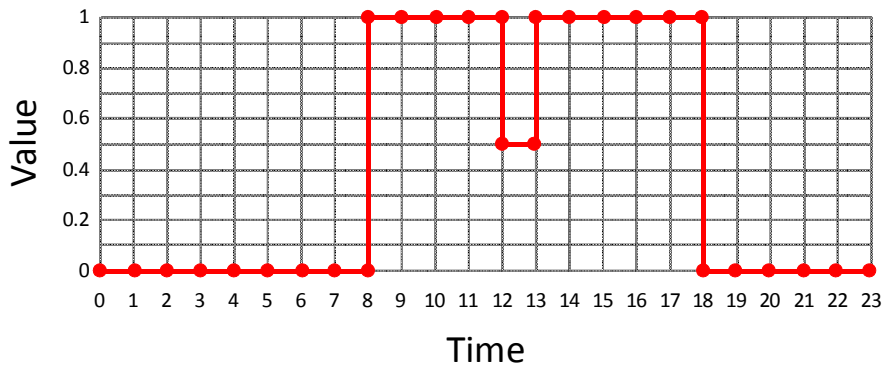


Figure 5.3-1. Occupants schedule on workdays

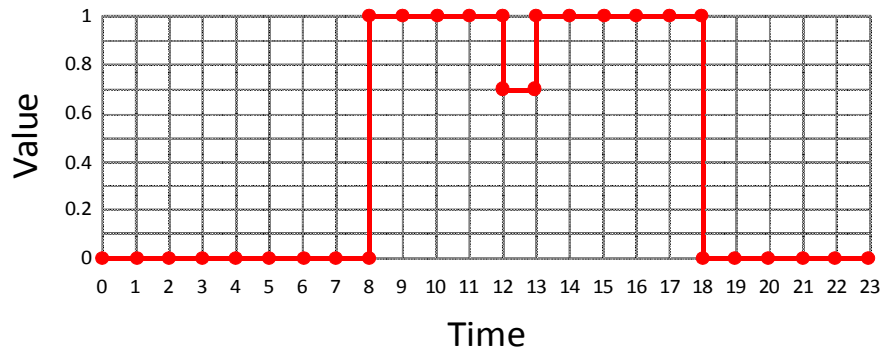


Figure 5.3-2. Lights and OA machines schedule on workdays

As it can be seen on the Figure 5.3-3, air-conditioning system was scheduled to be turned on 1 hour earlier than occupant's schedule to provide pre-cooling session. By this setting, it is expected that the room temperature will reach 25°C right-on at 08:00 as the occupant's schedule started. The air-conditioning system will be turned off as the occupant's schedule finished at 18:00.

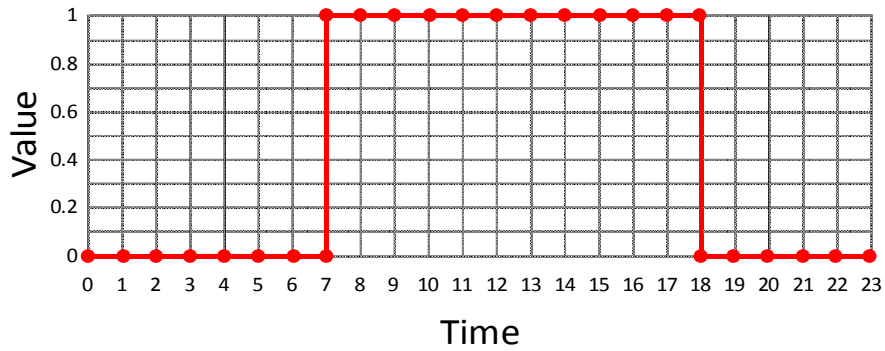


Figure 5.3-3. Air-conditioning operation schedule on workdays

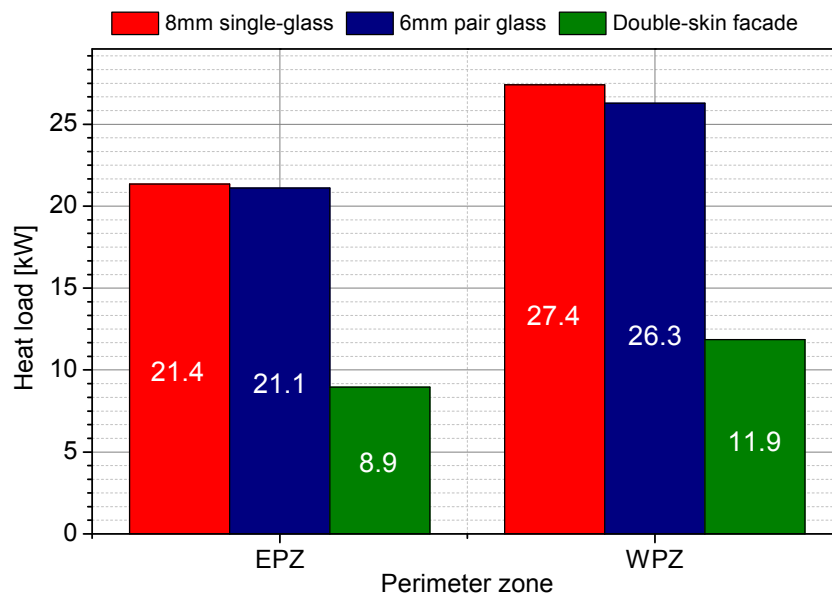


Figure 5.3-4. Peak load of perimeter zones

The simulation of heat load runs by using MicroHASP/TES for a one-year period of duration. The simulation results in the room load and the fresh air load of perimeter zones and interior zone. It was found that approximately more than 50% of heat load of perimeter zones on a peak load time can be reduced by using double-skin façade at west and east side of the building, refers to Figure 5.3-4. Peak load time for east perimeter zone is on August 18 at 9 am, while west perimeter zone is on September

28 at 4 pm. Note that those values presented on Figure 5.3-4 is a peak load value for one floor.

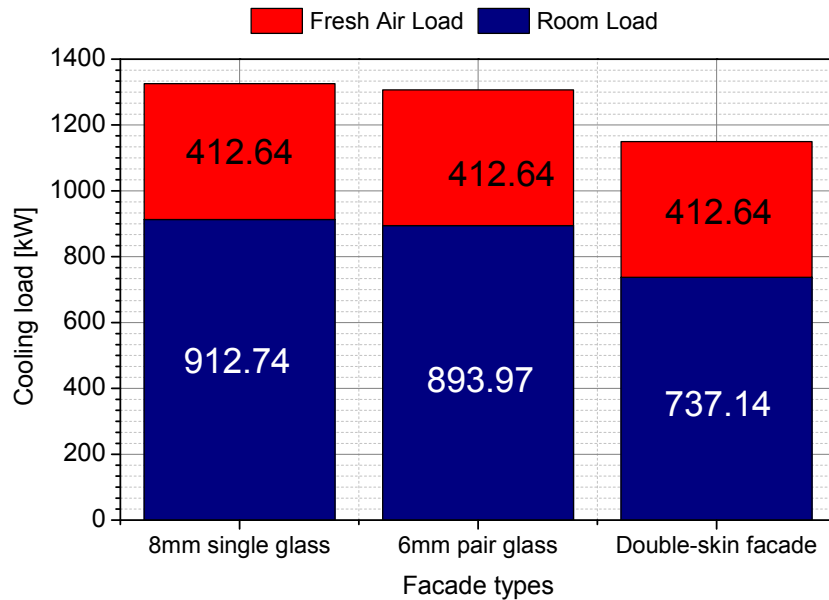


Figure 5.3-5. Cooling load comparison among window type

Refer to Figure 5.3-5, in comparison of room load of double-skin façade to other window systems, the amount of 19% of room load can be reduced if compared to 8mm single-glass window system, and amount of 18% of room load can be reduced if compared to the 6mm pair-glass window system. Totally, about 11% of total load is reduced if compared to 8mm single-glass window system, and 10% of total load can be reduced if compared to the 6mm pair glass window system.

5.4. Simulation of the Energy Consumption

5.4.1. Design of air-conditioning system

Based on the heat load calculation result from MicroHASP/TES version 2.40, we can design the air-conditioning system for building models. From Figure 5.3-5, we can see that the heat load of 8mm single-glass window system is 1325.4kW. The heat load of the 6mm pair-glass window system is 1307.6kW, and the heat load of double-skin façade is 1182.6kW respectively.

Heat load calculation using MicroHASP/TES results in the data of sensible and latent heat of room load and fresh air load of zones. The peak load taken from MicroHASP/TES calculation for the model building was issued on February 22 at 15:00. The peak load of model building was determined from the amount of sensible and latent heat of the zones at that date and time. For interior zone, the amount of 15% heat load was added for the allocation of fan and ducting. Moreover, for the total amount of peak load, there is 4% allocation for the heat from the pump. In the essence, the peak load of the model building was the sum of sensible and latent heat load of zones, including additional heat load by fans and ducts, and also pumps and pipes.

Table 5.4-1 shows configuration of the air-conditioning system for each case. The air-conditioning system designed to use 2 units screw refrigerator, which has 703kW cooling capacity. Along with this, 2 open type cooling tower, 2 primary chilled water pump, 4 secondary chilled water pump, and 2 cooling water pump also used. On each floor (totally 10 floor), an air-handling unit with 72kW cooling capacity is installed on each floor to supply cool air for interior zone. At north perimeter zone, the amount of 10 fan coil units with 1.54kW cooling capacity is installed on each floor. The amount of

10 fan coil units with 4.63kW cooling capacity is also installed at south perimeter zone on each floor.

Table 5.4-1. List of equipments used

Type		8mm single glass	Double-skin façade
		6mm pair glass	
R-1	Screw refrigerator #1	Cooling capacity: 703kW. Power consumption of main motor 129.0kW. Cold water: 2,016 L/min (7–12°C). Cooling water: 2,386 L/min (32–37°C)	
R-2	Screw refrigerator #2	Cooling capacity: 703kW Power consumption of main motor 129.0kW. Cold water: 2,016 L/min (7–12°C). Cooling water: 2,386 L/min (32–37°C)	Cooling capacity: 580kW Power consumption of main motor 103.2kW. Cold water: 1,663 L/min (7–12°C). Cooling water: 1,959 L/min (32–37°C)
CT-1	Cooling tower #1	Open type. Cooling water 2,386 L/min (32–37 °C). Power consumption 5.5kW	
CT-2	Cooling tower #2	Open type. Cooling water 2,386 L/min (32–37 °C). Power consumption 5.5kW	Open type. Cooling water 1,959 L/min (32–37 °C). Power consumption 3.7kW
PDC-1	Primary Pumps #1	2,016 L/min×120kPa×7.5kW	
PDC-2	Primary Pumps #2	2,016 L/min×120kPa×7.5kW	1,663 L/min×120kPa× 5.5kW
PC1-4	Secondary pump	1,010 L/min×280kPa× 7.5kW. 4 units.	920 L/min×280kPa× 7.5kW. 4 units.
PCC 1-2	Cooling water pump	2,386 /min×250kPa×15.0kW 2,386 min×250kPa×15.0kW. 2 units.	2,386L/min×250kPa×15.0kW 1,959 /min×250kPa×11.0kW. 2 units.
AHU	Air handling unit	Front area: 0.532 Air volume: 3,540m ³ /h. Air supply fan: 5,300m ³ /h×800Pa×3.7kW. Number of rows: 8rows. Number of tubes: 20 tubes. Cooling capacity: 72kW. Water flow rate: 205 L/min (7-12°C). 10 units (1 unit per floor).	
FCU	Return air fan	5,300 L/min×230kPa×1.5kW. 10 units (1 unit per floor)	
	Fan coil unit (NPZ)	Air supply: 280m ³ /h. Cooling capacity: 1.54kW. Water flow rate: 4.0 L/min (7-12°C). 100 units (10 units per floor)	
	Fan coil unit (SPZ)	Air supply: 840m ³ /h. Cooling capacity: 4.63kW. Water flow rate: 12.0 L/min (7-12°C). 100 units (10 units per floor)	
	Fan coil unit (WPZ)	Air supply: 840m ³ /h. Cooling capacity: 4.63kW. Water flow rate: 12.0 L/min(7-12°C). 60 units (6 unit per floor)	Air supply: 520m ³ /h. Cooling capacity: 2.45kW. Water flow rate: 7.0 L/min(7-12°C).60 units (6 unit per floor)
	Fan coil unit (EPZ)	Air supply: 840m ³ /h. Cooling capacity: 4.63kW. Water flow rate: 12.0 L/min (7-12°C). 60 units (6 unit per floor)	Air supply: 280m ³ /h Cooling capacity: 1.54kW. Water flow rate: 4.0 L/min (7-12°C). 60 units (6 unit per floor)

The same cooling capacity of the fan coil unit (4.63kW) is installed at west perimeter zone and east perimeter zone with the amount of 6 fan coil units on each floor. The layout of zoning of air handling unit and fan coil units can be found on Figure 5.4-1. Moreover, the 6mm pair-glass window type also uses the same air-conditioning system with the 8mm single-glass window type.

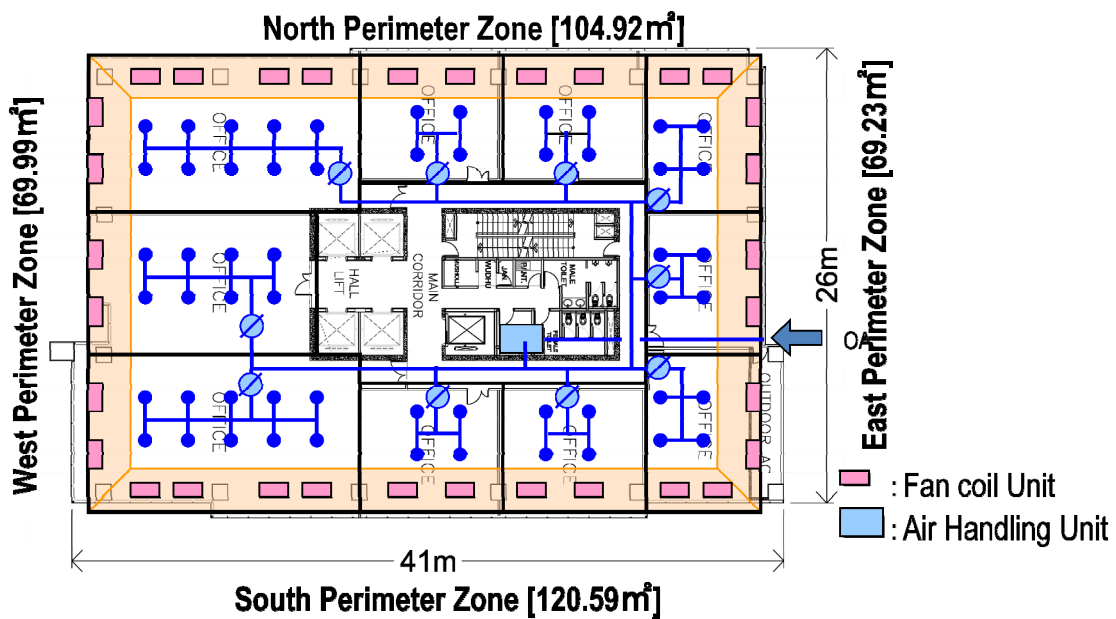


Figure 5.4-1. Zoning of air handling unit and fan coil units

The air-conditioning system design for double-skin façade window type was slightly different to both the 8mm single-glass window type and the 6mm pair glass window type. Since the amount of air-conditioning loads of double-skin façade was lower than those two window systems, we found that there is a possibility to optimize the system design for the double-skin façade case by changing several system components. Screw refrigerator (R-2) for the second unit was substituted to 580kW cooling capacity, while the first unit (R-1) was still using as same type as used at 8mm

single-glass and 6mm pair glass type. Amount of 2 cooling tower, 2 primary chilled water pumps, 2 cooling water pumps on each type, and 4 secondary pumps were used respectively. Cooling capacity of fan coil units of west and east perimeter zone was also changed to 2.45kW and 1.45kW respectively.

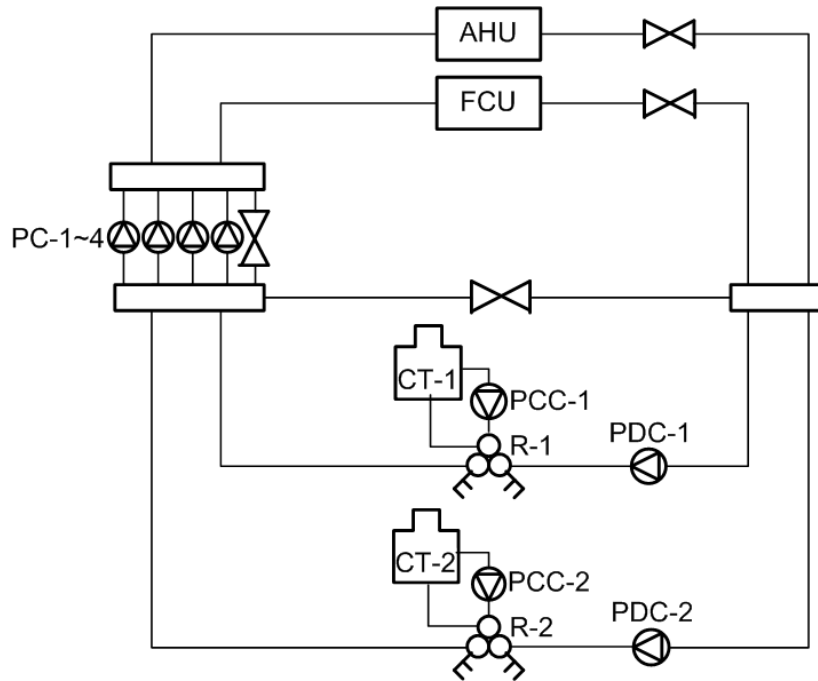


Figure 5.4-2. Air-conditioning system diagram

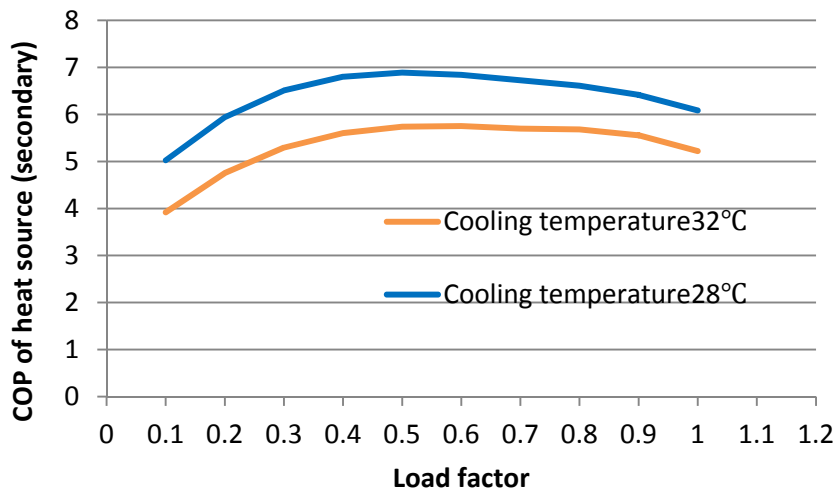


Figure 5.4-3. Load characteristic of heat source

5.4.2. Simulation condition

LCEM (Life Cycle Energy Management) Tool was used to simulate the energy consumption of air-conditioning of building models.

Since the simulation was intended to evaluate the energy consumption of the building model under Indonesia’s weather condition, the room load of interior zone and perimeter zones, which resulted from MicroHASP/TES simulation, and the setting temperature for indoor and humidity were inputted along with the outside dry-bulb temperature and relative humidity air condition of Indonesia. Simulation runs for 1 year duration for cooling session to obtain energy consumption from heat sources, cooling towers, chilled water pumps, primary pumps, secondary pump, air handling unit supply and return fan, and fan coil units.

Figure 5.4-4 shows the diagram of the skeleton of primary subsystem and as well as Figure 5.4-5 shows the diagram of the skeleton of secondary subsystem. The skeletons were built based on the equipments and the air-conditioning system diagram on Figure 5.4-4 and Figure 5.4-5.

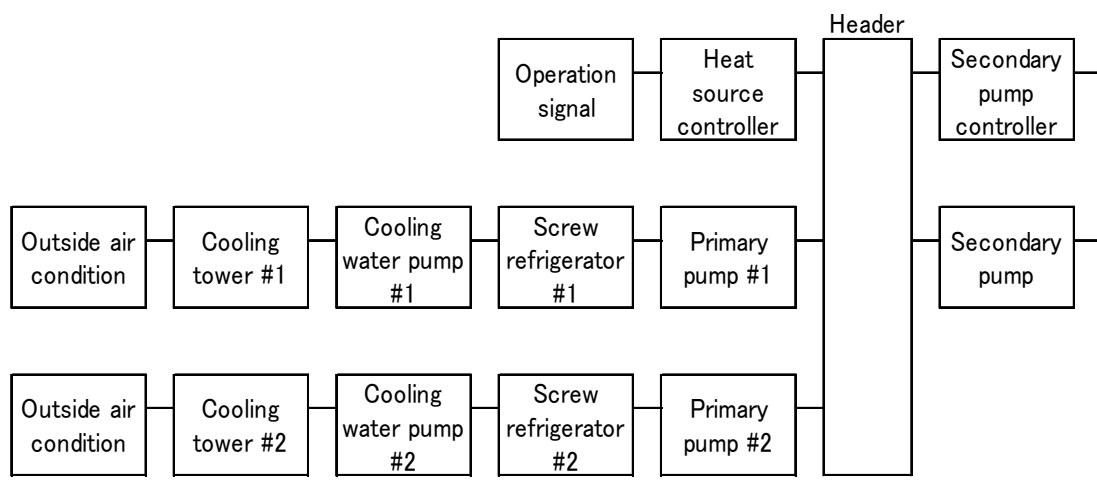


Figure 5.4-4. Primary subsystem of LCEM

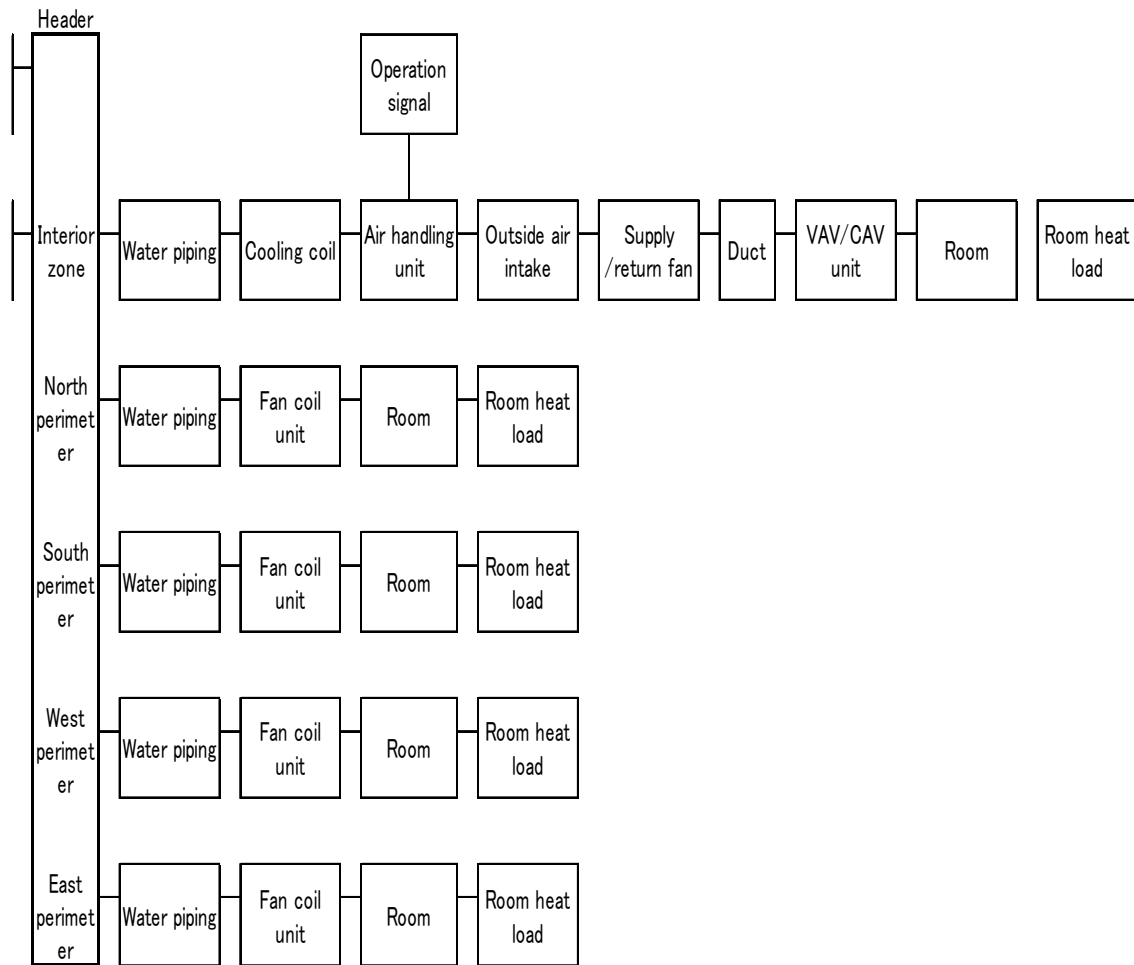


Figure 5.4-5. Secondary subsystem of LCEM

5.5. Energy Performance of Ventilated Double-skin Façade

The energy consumption of the air-conditioning system for three window system has been simulated using LCEM Tool. The result found that by adopting double-skin façade with proper design of air-conditioning system, energy consumption of the air-conditioning system could be reduced. Figure 5.5-1 shows the comparison of annual energy consumptions of 8mm glass single skin façade, 6mm pair glass, and double-skin façade.

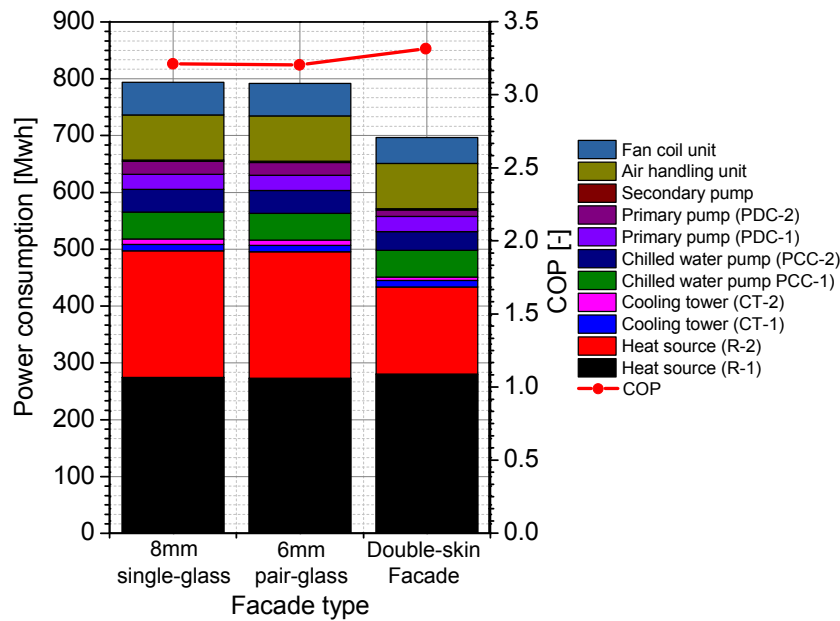


Figure 5.5-1. Annual power consumption

It was confirmed through Figure 5.5-1 that annual total energy consumption of the double-skin façade window system is 12% lower than other window systems (8mm single-glass and 6mm pair glass window types). Some components that contribute to the decreased energy consumption are; heat source (R-2), cooling tower (CT-2), chilled water pump (PCC-2), primary pump (PDC-2), and fan coil unit (FCU).

By dividing the amount of cooling load with the total energy consumption of air conditioning components, the system COP can be determined for all window types. The system COP for both 8mm glass single-skin façade and 6mm pair glass is 3.21, and double-skin façade window system is 3.32. The system COP can be improved by installing double-skin façade obviously.

Compared to other window types, the heat source R-2 of double-skin façade could reduce 31% of annual total energy consumption. About 38% of annual total energy consumption of cooling tower can be saved by the cooling tower CT-2, and

approximately 18% of annual total power consumption of the chilled water pump could be saved by cooling pump PCC-2. Primary pump PDC-2 could save annual total energy consumption about 50% and fan coil unit is about 21%. With the advantages of double-skin façade, those equipments can be changed to lower capacity to meet optimal operational requirements.

However, the energy consumption of heat source R-1 of double-skin façade was slightly higher than the heat source R-1 of other window types. The reason why energy consumption of heat source R-1 of double-skin façade higher is because there was a different capacity between heat source R-1 and heat source R-2 of double-skin façade. Because of the capacity of heat source R-2 is lower than the heat source R-1, the part load ratio of heat source R-2 was increased. Consequently, by using a lower capacity of heat source, the part load ratio will increase.

The energy consumption of single-glass looks like similar to pair glass. Unlike those two window system, the energy consumption of double-skin façade is low and keep in lower level during year. shows monthly power consumption and cooling load of the cases.

There is distinguishing difference between dry season (April-September) and rainy (October-March) season. The highest direct solar radiation occurs around the dry season while the highest diffuse solar radiation occurs at the rainy. Apparently, double-skin façade is useful and effective in reducing energy consumption for both in rainy season and in dry season, all months.

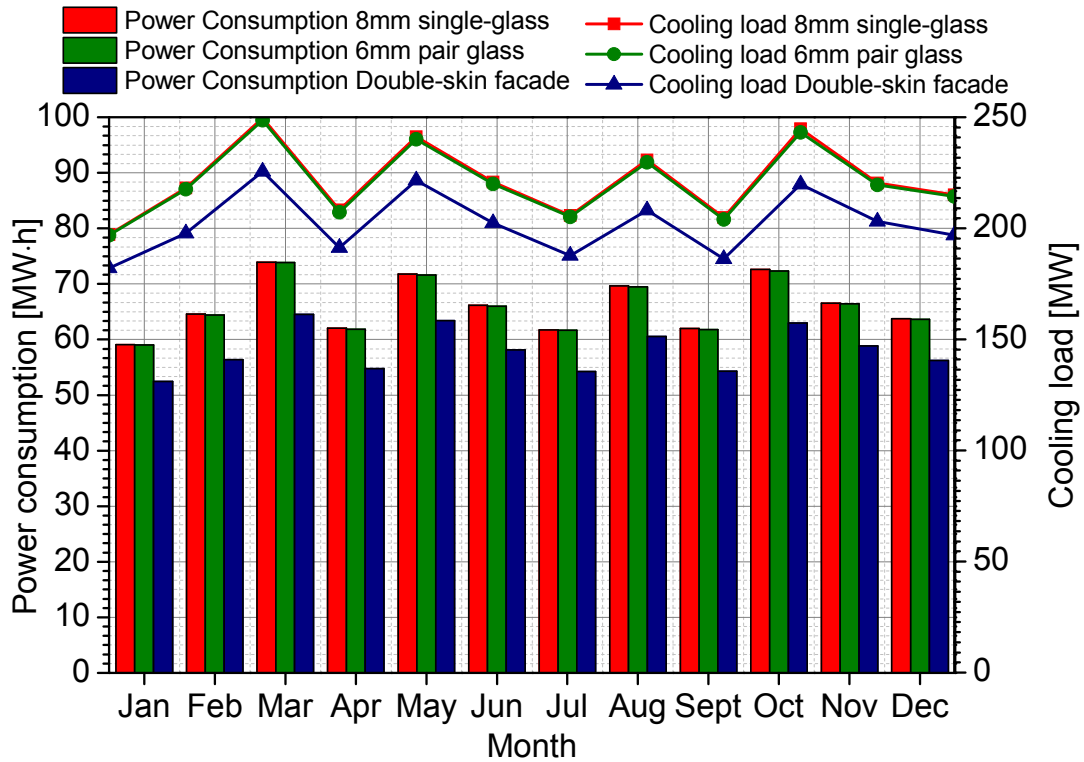


Figure 5.5-2. Monthly power consumption

5.6. Summary

The energy consumption of double-skin façade was presented in comparison to the energy consumption of 8mm singles-glass and 6mm pair glass window. The double-skin façade was assumed to be applied at the east and west façade of the model building located in Makassar, Indonesia.

First, the U-value and the SC of double-skin façade was calculated based on the result from numerical simulation. The calculated U-value and SC of double-skin was inputted to MicroHASP/TES along with, building parameter, weather condition, and operational schedule to calculate heat load of the model building. The result from MicroHASP/TES show that more than 50% of heat load of perimeter zones on a peak load time can be reduced by using double-skin façade at west and east side of the

building. In comparison of room load of double-skin façade to other window systems, the amount of 19% of room load can be reduced if compared to 8mm single-glass window system, and amount of 18% of room load can be reduced if compared to the 6mm pair-glass window system. Totally, about 11% of total load is reduced if compared to 8mm single-glass window system, and 10% of total load can be reduced if compared to the 6mm pair glass window system. Based on the heat load resulted from MicroHASP/TES, the air conditioning system was designed.

Second step is the calculation of energy consumption of the building model. Calculation done by LCEM Tool using the sensible and latent heat load resulted from MicroHASP/TES along with ambient temperature, humidity, and radiation data of Makassar, Indonesia. The result from LCEM Tool shows that annual total energy consumption of the double-skin façade window system is 12% lower than other window systems (8mm single-glass and 6mm pair glass window types). The system COP(Coefficient of Performance) for both 8mm glass single-skin façade and 6mm pair glass is 3.21, and double-skin façade window system is 3.32. Compared to other window types, the heat source R-2 of double-skin façade could reduce 31% of annual total energy consumption. About 38% of annual total energy consumption of cooling tower can be saved by the cooling tower CT-2, and approximately 18% of annual total power consumption of the chilled water pump could be saved by cooling pump PCC-2. Primary pump PDC-2 could save annual total energy consumption about 50% and fan coil unit is about 21%. With the advantages of double-skin façade, those equipments can be changed to lower capacity to meet optimal operational requirements. Consequently, double-skin façade is useful in reducing energy consumption of the air-conditioning system under Indonesia's weather condition.

CHAPTER 6. CONCLUSION

This research was studied the performance on naturally ventilated double-skin façade in hot and humid climate with the case study of Indonesia. The study focused on the solar heat gain and thermal transmittance of various configurations of the outer and inner glasses combination as well as the distance between the outer and inner glasses as the first stage of study. This step was also intended to find-out the applicability of the naturally ventilated double-skin façade in the hot and humid climate region. The second stage was to evaluate the energy-efficient performance of double-skin façade in the hot and humid climate region.

The result of the first stage confirmed that naturally ventilated double-skin façade could be applied in hot-and humid climate region. It was found also that naturally ventilated double-skin façade was effective in minimizing the heat gain compared to the single-skin and pair glass window system. In comparison among double-skin façade cases, selecting a suitable combination of inner and outer glass skin thickness was useful in reducing the solar heat gain. Although there are slight differences in thermal transmittance could be achieved, the distance between the outer and inner glass skins is an important factor in reducing thermal transmittance on a double-skin façade system. Hence, the double-skin façade also exhibited the best performance at reducing the solar heat gain when compared to a single-skin façade, and more than 50% of the heat gain can be reduced by using a double-skin façade.

In addition, during the rainy season the humidity is high. Calculation was performed during operation time of building from 08:00 to 17:00 with indoor setup temperature was 25°C. The result found that there were no possibilities of condensations, which can be occurred during operation time.

Moreover, reflectance, absorption, and transmission of solar radiation in double-skin façade are varying based on the angle incidence of solar radiation. When the angle incidence is lower than 70° , the percentage and absorptance of the solar radiation increased gradually, while the percentage of transmission of solar radiation decreased gradually. The percentage of reflected solar radiation will increase rapidly and percentage of absorbed and transmitted solar radiation will decrease rapidly when the solar incidence angle higher than 70° .

In the second stage, the energy-efficient performance of double-skin façade that was simulated using LCEM-Tool, was compared to the 8mm single glass façade and 6mm pair glass façade. Through this simulation, the energy efficient of double-skin façade was confirmed effective in reducing energy consumption of the air-conditioning in building. The annual total energy consumption of the double-skin façade window system was 12% lower than other window systems (8mm single-glass and 6mm pair glass window types). Moreover, the system COP for both 8mm glass single-skin façade and 6mm pair glass was 3.21, and double-skin façade window system is 3.32. System COP of the air-conditioning system also improved when double-skin façade is installed.

If compared to other window types, the heat source R-2 of double-skin façade could reduce 31% of annual total energy consumption. About 38% of annual total energy consumption of cooling tower can be saved by the cooling tower CT-2, and approximately 18% of annual total power consumption of the chilled water pump could be saved by cooling pump PCC-2. Primary pump PDC-2 could save annual total energy consumption about 50% and fan coil unit is about 21%. With the advantages of double-skin façade, those equipments can be changed to lower capacity to meet optimal

operational requirements. Consequently, double-skin façade is useful in reducing energy consumption of the air-conditioning system under Indonesia's weather condition.

In the future work, it will be necessary to extend the simulation to take into account several glass properties, including glass coatings, to determine the performance of double-skin façades in hot and humid climate.

REFERENCES

- [1] M. McClintock and J. Perry, "The Challenge of 'Green' Buildings in Asia," in *International Conference of Building Envelope Systems and Technologies (ICBEST)*, Bath University, UK, 1997.
- [2] V. Yellamraju, "Evaluation and Design of Double-skin Facades for Office Building in Hot Climate," Master Thesis, Texas A&M University, Texas, 2004.
- [3] D. M. M. Arons, "Properties and Applications of Double-Skin Facades," Master Thesis, Department of Architecture, Massachusetts Institute of Technology, Cambridge, 2000.
- [4] D. Saelens, "Energy Performance of Single Storey Multiple-skin Facades," PhD Thesis, Laboratory for Building Physics, Department of Civil Engineering, Catholic University of Leuven, Belgium, 2002.
- [5] H. Poirazis, "Double Skin Facades for Pffice Buildings. Literature Review," 2004. [Online]. Available: <http://www.dsbo.dk/Portals/0/Dobbelte%20facader%20Lund%20universitet.pdf>. [Accessed 7 12 2011].
- [6] H. Poirazis, "Double skin facades a literature review," 2006. [Online]. Available: http://www.ecbcs.org/docs/Annex_43_Task34-Double_Skin_Facades_A_Literature_Review.pdf. [Accessed 7 12 2011].
- [7] I. F. Solla, "The Steiff factory and the birth of curtain walling," 27 11 2011. [Online]. Available: <http://facadesconfidential.blogspot.jp/2011/11/steiff-factory-and-birth-of-curtain.html>. [Accessed 30 5 2012].
- [8] A. Barkkume, *Innovative Building Skins: Double Glass Wall Ventilated Fcade*, New Jersey: New Jersey School of Architecture, New Jersey Institute of Technology, 2007.
- [9] A. Fissabre and B. Niethammer, "The Invention of Glazed Curtain Wall in 1903 - The Steiff Toy Factory," in *The Third International Congress on Construction History*, Cottbus, 2009.
- [10] M. Wigginton and B. McCarthy, "Environmental Second Skin Systems," 1 June 2000. [Online]. Available: http://www.battlemccarthy.com/external%20site_double%20skin%20website/in

- dex.htm. [Accessed 5 June 2012].
- [11] S.-S. Li, "A Protocol to Determine the Performance of South Facing Double Glass Façade System: A Preliminary Study of Active/Passive Double Glass Façade Systems," MSc Thesis, Virginia Polytechnic Institute and State University, Blacksburg, 2001.
- [12] F. S. Ignacio, "Le Corbusier: a French lesson on 'Murs neutralisants'," 19 April 2012. [Online]. Available: http://facadesconfidential.blogspot.jp/2012_04_01_archive.html. [Accessed 7 July 2012].
- [13] T. M. Boake, K. Harrison and A. Chatham, "The Tectonics of the Double Skin: Green Building or Just more Hi-Tech Hi-Jinx?," [Online]. Available: http://www.architecture.uwaterloo.ca/faculty_projects/terri/ds/tectcase.pdf. [Accessed 5 June 2012].
- [14] W. Streicher, "Best Practice for Double Skin Façades (EIE/04/135/S07.38652). WP 1 Report "State of the Art"," BESTFAÇADE, 2005.
- [15] X. Lancour, A. Deneyer, M. Blasco, G. Flamat and P. Wouters, "Ventilated Double Facades: Classification & illustration of facade concepts," 2004. [Online]. Available: <http://www.bbri.be/activefacades/new/download/Ventilated%20Doubles%20Facades%20-%20Classification%20&%20illustrations.dvf2%20-%20final.pdf>. [Accessed 1 March 2012].
- [16] R. Waldner, G. Flamant, S. Prieus, H. Erhorn-Kluttig, I. Farou, R. Duarte, C. Blomqvist, N. Kiossefidi, D. Geysels, G. Guarracino and B. Moujalled, "BESTFAÇADE: Best Practice for Double Skin Façades," 2007. [Online]. Available: <http://www.bestfacade.com/pdf/downloads/WP5%20Best%20practice%20guide%20lines%20report%20v17final.pdf>. [Accessed 13 2012].
- [17] P. Roelofsen, Ventilated Facades: climate Facade versus Double-skin Facade, European Consulting Engineering Network, 2002.
- [18] R. Waldner, G. Flamant, S. Prieus, H. Erhorn-Kluttig, I. Farou, R. Duarte, C. Blomqvist, N. Kiossefidi, D. Geysels, G. Guarracino and B. Moujalled, "BESTFAÇADE: Best Practice for Double Skin Façades," 2007.
- [19] Best Facade, "Partitioning of the facade," [Online]. Available: http://www.bestfacade.com/textde/01_history_gesamt.htm. [Accessed 5 June 2012].

- [20] X. Lancour, P. Wouters and G. Flamant, "Impact of Double Ventilated Facades in Buildings," in *CIB World Building Congress 2004*, Toronto, 2004.
- [21] E. Djunaedy, J. Hensen and M. Loomans, "Towards a Strategy for Airflow Simulation in Building Design," in *the 8th International Conference on Air Distribution in Rooms-Roomvent 2002*, Copenhagen, 2002.
- [22] M. Barták, T. Dunovská and J. Hensen, "Design support simulation for a double-skin facade," in *1st International Conference on Renewable Energy in Buildings "Sustainable Buildings and Solar Energy 2001"*, Prague, 2001.
- [23] A. Pappas and Z. Zhai, "Numerical investigation on thermal performance and correlations of double skin façade with buoyancy-driven airflow," *Energy and Buildings*, vol. 40, no. 4, p. 466–475, 2008.
- [24] W. Ding, Y. Hasemi and T. Yamada, "Natural ventilation performance of a double-skin façade with a solar chimney," *Energy and Buildings*, vol. 37, no. 4, p. 411–418, 2005.
- [25] H. Manz and T. Frank, "Thermal simulation of buildings with double-skin façades," *Energy and Buildings*, vol. 37, no. 11, p. 1114–1121, 2005.
- [26] A. Chan, T. Chow, K. Fong and Z. Lin, "Investigation on energy performance of double skin façade in Hong Kong," *Energy and Buildings*, vol. 41, no. 11, p. 1135–1142, 2009.
- [27] N. Hamza, "Double versus single skin facades in hot arid areas," *Energy and Buildings*, vol. 40, no. 3, p. 240–248, 2008.
- [28] X.-l. Xu and Z. Yang, "Natural ventilation in the double skin facade with venetian blind," *Energy and Buildings*, vol. 40, no. 8, p. 1498–1504, 2008.
- [29] W. N. Hien, W. Liping, A. N. Chandra, A. R. Pandey and W. Xiaolin, "Effects of double glazed facade on energy consumption, thermal comfort and condensation for a typical office building in Singapore," *Energy and Buildings*, vol. 37, no. 6, p. 563–572, 2005.
- [30] H. Kato, G. Yoon, H. Tanaka, Y. Hatate, M. Yoshida, Y. Torigoe and M. Okumiya, "Effectiveness of reducing heating and cooling load by using double-skin facade coupling the earth-to-air heat exchanger," in *7th International Conference on Sustainable Energy Technology*, Seoul, 2008.
- [31] G. Yoon, H. Kato and M. Okumiya, "Study on the Thermal Performance of Double-skin Facade: Part 1. Proposal of Prediction Technique for Thermal Performance on Cooling Season," *J. Environ. Eng. AIJ*, vol. 77, no. 674, pp.

251-257, 2012.

- [32] B. Todorovic and B. Maric, "The influence of double façades on building," [Online]. Available: <http://afrodita.rcub.bg.ac.rs/~todorom/tutorials/rad31.html>. [Accessed 6 June 2012].
- [33] D. Saelens, J. Carmeliet and H. Hens, "Energy Performance Assessment of Multiple-Skin Facades," in *International Journal of HAVAC&R Research*, 2003.
- [34] A. Pappas, "Energy Performance of a Double-Skin Facade-Analysis for the Museum of Contemporary Art," 2006. [Online]. Available: www.solar2006.org/presentations/tech_sessions/t45-p201.pdf.
- [35] D. Stribling and B. Stigge, "A Critical Review of the Energy Savings and Cost Payback Issues of Double Facades-CIBSE/ASHRAE Conference," 2003. [Online]. Available: www.cibse.org/pdfs/8cstribling.pdf.
- [36] JIS R 3106, Testing method on transmittance, reflectance and emittance of flat glasses and evaluation of solar heat gain coefficient, Japanese Industrial Standard (JIS), 1998.
- [37] H. Kato, "Study on the Thermal Performance of Double-Skin Facade: Examination on the Shade Coefficient and the Overall Heat Transfer Coefficient to Evaluate Cooling Load," Master Thesis, Department of Environmental Engineering and Architectural Design Nagoya University, Nagoya, 2008.
- [38] S. Inoue, S. Tanaka, H. Takeda, T. Iwata, T. Tsuchiya and M. Terao, *Newest Architectural and Environmental Engineering* (in Japanese: 最新建築環境工学), 3rd ed., 2006.
- [39] Y. Nakamura, Y. Matsuo, M. Matsumoto, T. Tsuchiya, H. Tachibana and M. Toshimoto, *Compendium of New Architectural 10, the Physical Environment* (in Japanese: 新建築学大系 10 環境物理), Tokyo: Hikari Inc., 1984.
- [40] K. Watanabe, *Principles of Architectural Planning II* (in Japanese: 建築計画原論 II), Tokyo: Maruzen Co. Ltd., 1965.
- [41] M. Okumiya, "Control of thermal environment in building by architectural method," [Online]. Available: http://www.sangetsu.co.jp/hibizaidan/pdf/hibi_18/okumiya.pdf. [Accessed 6 June 2012].
- [42] M. C. Peel, B. L. Finlayson and T. A. McMahon, "Updated world map of the Koppen-Geiger climate classification," *Hydrol. Earth Syst. Sci.*, Vols. 1633-

1644, 2007.

- [43] Anonimous, "Weather online: Indonesia," 2012. [Online]. Available: <http://www.weatheronline.co.uk/reports/climate/Indonesia.htm>. [Accessed 28 May 2012].
- [44] Anonimous, "Encyclopedia of the nations: Indonesia - Climate," 2012. [Online]. Available: <http://www.nationsencyclopedia.com/Asia-and-Oceania/Indonesia-CLIMATE.html#b>. [Accessed 28 May 2012].
- [45] G. S. D. and P. M. G., "An analog evaluation of methods for controlling solar heat gain through windows," *American Society of Heating, Refrigerating and Air Conditioning, Engineers (ASHRAE)*, vol. 4, no. 2, pp. 41-46, 1962.
- [46] M. W. English, "Solar heat gain in the optometry building: An evaluation of retrofit sun controls," Department of Environment and Resource Studies, Faculty of Environmental Studies, University of Waterloo, 1990.
- [47] Ministry of Energy and Mineral Resources Republic of Indonesia, "The guidelines on energy saving for office building," Jakarta, 2005.

APPENDICES

- Publication:

1. Title: Skin load performance of double-skin façade in Indonesia
Author: Rosady Mulyadi, Gyuyoung Yoon, Masaya Okumiya
Published in: The 11th International Conference on Sustainable Environmental Architecture, Sepuluh Nopember Institute of Technology, Surabaya, Indonesia 14-16th October 2010.
Proceeding page I-21~I-32
2. Title: Study on solar heat gain and thermal transmittance of east- and west-facing double-skin façade in hot and humid climate
Author: Rosady Mulyadi, Gyuyoung Yoon, Masaya Okumiya
Scheduled for publication in AIJ Journal of Technology and Design.
AIJ J. Technol. Des. Vol. 18 No. 40 page 995-1000., Oct. 2012
3. Title: Study on the Energy Performance of Double-skin Façade in Indonesia
Author: Rosady Mulyadi, Gyuyoung Yoon, Masaya Okumiya
Published in Transaction of the Society of Heating, Air-Conditioning and Sanitary Engineers of Japan, No. 183, June, 2012, pp. 9-17

- Numerical simulation source code